International Journal of Fusion Energy

Vol. 3, No. 3 July 1985

Published Quarterly by the Fusion Energy Foundation

International Journal of Fusion Energy (ISSN: 0146-4981) is published quarterly by the Fusion Energy Foundation, P.O. Box 17149, Washington, D.C. 20041-0149. Tel. (703) 689-2490.

Subscription price: $80 per volume (four issues) domestic; $100 per volume foreign. Payment must be in U.S. dollars.

Address all correspondence to IJFE, Fusion Energy Foundation, P.O. Box 17149, Washington, D.C. 20041-0149.

Postmaster: Send address changes to IJFE, Fusion Energy Foundation, P.O. Box 17149, Washington, D.C. 20041-0149.

International Journal of Fusion Energy

Vol. 3, No. 3 **July 1985**

Editorial Policy

The International Journal of Fusion Energy (IJFE) is an independent scientific journal published quarterly by the Fusion Energy Foundation. The IJFE is dedicated to the promotion of fundamental advance in science, with special emphasis on the following areas:

1. The physics of plasmas at high energy densities, and research bearing on the scientific and technological mastery of nuclear fusion processes.

2. Coherent, directed forms of electromagnetic action, including laser and particle beams and superconductivity.

3. The physics of living processes, with applications to fundamental problems of biology and medicine.

In addition to research articles and state-of-the-art reviews, the IJFE welcomes short, informal communications addressing questions of interest to researchers and others in the cited areas. Contributions in other fields will be accepted on the basis of extraordinary scientific interest or manifest relevance to the three specific fields covered by the journal.

IJFE will also run abstracts of relevant, recent published and unpublished work as a regular service to the reader. The editors will be grateful for references to significant new work, not previously covered in the abstracts and other departments of the journal.

International Journal of Fusion Energy

Vol. 3, No. 3 July 1985

Articles

Reports

Gravitational Binding Mass Nonequivalence and the Foundations of Physics

With the Lageos Satellite As a Laboratory

by B.A. Soldano
Department of Physics
Furman University
Greenville, SC 29613

Abstract—Experimental parameters obtained from the Lageos satellite are used to set limits of validity for both general and special relativity. It is usually acknowledged that the theory of general relativity, whose basic premise is the absolute equivalence of inertial and gravitational mass, paradoxically fails to properly account for the gravitational self-energy component of mass. This leads to the need for coordinate specification via pseudotensors, thereby marring the coordinate independence inherent in tensors. We shall demonstrate that a fractional difference between inertial and gravitational mass $(m_G - m_i)/m_G = -5.05 \times 10^{-12}$, restricted solely to the gravitational binding component of mass, eliminates the aforementioned difficulty and provides solutions for a broad array of problems presently confronting physics. For example, the violation of CP invariance encountered in both strange and nonstrange particle physics as well as the problems of "missing" solar neutrinos are shown to arise from a gravitational binding mass nonequivalence omission in the present structure of science.

A purely classical description of the quantum h is presented that originates in the aforementioned binding mass nonequivalence and a related fractional difference between ephemeris and atomic time. Many of the widely disparate, experimental upper limits presently associated with tests of general relativity, such as those related to gravitational red shift and solar, radio wave, "light" bending are shown to actually represent the limit of validity for the theory of general relativity.

Finally, the recent series of two-clock orientation invariance upper-limit tests of special relativity, in reality, represent validity limits of special relativity. The broad variation in these $TH\varepsilon\mu$ limits, ranging from $\leqq 5 \times 10^{-9}$ for the Hall-Brillet two-laser test to an upper limit of $\leqq 1 \times 10^{-20}$ found by the Washington group that is based in the use of a ^{199}Hg–^{201}Hg test pair, is shown to depend upon the nature of the two clocks used in the experiment. Note added in proof explains the Fischbach variable G results.

Introduction: Which Is Primary, Classical or Quantum Physics?

For decades, a conflict has raged in physics over the question of the primacy of classical physics inherent in general relativity and special relativity (see Appendix A), or of quantum mechanics. At present, physics maintains two parallel paths and occasionally attempts to interrelate these two conflicting disciplines.

An earlier version of this paper was presented at the weekly seminar of the 1985 NASA-ASEE Summer Faculty Fellowship Program held at Goddard Space Flight Center, July 5, 1985.

An answer to the question of primacy already exists. We propose to show that classical physics, slightly modified to accommodate a restricted nonequality between inertial and gravitational binding mass, leads to a purely classical explanation of the quantum h. Further, we propose to show that the seeds of a resolution of the above conflict already exist in the framework of both quantum mechanics and general relativity.

In the absence of a resolution of the conflict, each of these two disciplines has generated a series of "black box" problems, for example, the solar neutrino problem and the ΔCP question, to mention two.

In order to obtain accurate enough parameters for resolving a wide array of problems in both general relativity and quantum mechanics, we begin by demonstrating that the Lageos satellite constitutes an extremely sensitive "laboratory" for quantifying some of the parameters required by explanations based on nonequivalence in gravitational binding.

The Lageos Satellite

Lageos, NASA's LASER Geodynamic Satellite, was placed in nearly circular orbit at $\sim 2R_{\oplus}$ semidiameter and $\sim 110°$ inclination to Earth's equator in order to provide a stable benchmark for the determination of nonlinear changes in the accumulated rotation angle of the Earth (UT1) (Smith and Dunn 1981; Yoder et al. 1983). Because of the nearly circular orbit, Lageos's accurately monitored position is most conveniently expressed as the longitude of the ascending node Ω, in Figure 1.

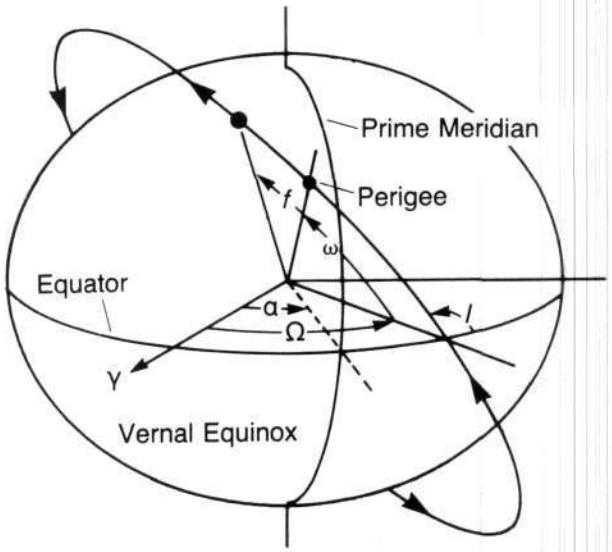

Figure 1. Earth satellite geometrical relationships and definitions: the angle α, which is nearly a linear functions of UT1, measures the Earth's rotation with respect to the vernal equinox, γ. The longitude of the ascending node, Ω, and the inclination, I, determine the orientation of the satellite's orbital plane. The argument of perigee, ω, is measured in the orbital plane from the equator to the equator to the orbit's point of closest approach to the Earth.

Two problems have plagued the program of monitoring UT1 variations and of discriminating sources of UT1 variation arising from $J_{2,\oplus}$ changes from those which do not. First, the satellite has been clearly demonstrated to be experiencing an unexpected acceleration (Smith and Dunn 1981). This acceleration results in a secular decrease in the satellite's semidiameter (initially 1.227×10^9 cm) of 1.1 mm per day. Second, accurate fitting of Ω as a function of time has clearly identified an acceleration, $\ddot{\Omega}$ related to the time derivative of the Earth's second gravitational harmonic coefficient $\dot{J}_{2,\oplus}$ (Yoder et al. 1983; Rubincam 1984; Kaula 1983).

Many explanations have been proposed for these two effects, but to date neither has been successfully modeled. The most widely accepted explanation for the orbital degradation is ion drag (Rubincam 1982; Jastrow and Pearse 1957; Knetchel and Pitts 1964; Rubincam 1980). But this mechanism is subject to serious questions raised by the difficulty of justifying high enough charge concentrations at Lageos's altitude to account for the observed effect, nor does it account for cyclic changes in the semidiameter degradation (Smith and Dunn 1981). Efforts to explain $\ddot{\Omega}$ have centered on the postglacial rebound of the Earth as the origin of $\dot{J}_{2,\oplus}$ (Yoder et al. 1983; Rubincam 1984; Rubincam 1982; Peltier 1983; Lambeck and Nakeboglu 1983).

The thesis proposed in this paper is that both of these problems, heretofore treated as unrelated, are in fact simply different consequences of the same underlying cause, namely, a small but very important nonequivalence in gravitational binding of the Earth (Soldano 1974 to 1985). It is proposed that the Lageos satellite constitutes a remarkably sensitive laboratory for quantification of the limit of validity of the equivalence principle, one of the central tenets of general relativity.

The Nonequivalence Model

Paradoxically, it is in the gravitational energy component of mass that the theory of general relativity has encountered its greatest difficulty (Maddox 1985). The gravitational energy is the only portion of the total energy considered by general relativity that cannot be described by tensors *free* of the coordinates. It requires use of pseudotensors that are *not* free of the coordinate frame. Further, in general relativity this fraction of the energy appears to violate both energy and momentum conservation.

It is therefore significant that the term we use to describe gravitational self-binding energy violates the strict equivalence between inertial and gravitational mass inherent in general relativity. Further, our premise is consistent with the violation of energy and momentum conservation encountered by general relativity at the microscopic level in its description of gravita-

tional energy. That nonequivalence in gravitational binding involves a detailed delineation of one's coordinate reference frame would appear to be an insurmountable handicap. However, since the inertial and gravitational binding components of Sun, Moon, Earth, and a satellite are gravitationally locked together, and continuously undergoing gravitational binding changes, it follows that the system is extraordinarily sensitive to rotationally dependent transfer of differences between inertial and gravitational mass as the system unsuccessfully attempts to achieve gravitational binding equilibrium. These time-dependent nonequivalent binding changes make experiments done in one's reference frame acutely sensitive to such subtle factors as shape, orbital eccentricities, quadrupole moments, and so forth, which give rise to continual changes in the gravitational binding of the systems. Thus one should expect, in a theory based on gravitational binding nonequivalence, a deeper relationship between astronomical factors and microscopic processes in general.

In the model proposed here, a universal fractional difference between inertial and gravitational mass, $(m_G - m_i)/m_G = -5.05 \times 10^{-12}$, is presumed to exist in the gravitational self-binding component *only* (Soldano 1974 to 1985). (For a discussion of the origin of this effect, see Appendix B.) The latter fraction, f_{g_i}, a function of the number of nucleons A, is quantified by the Wheeler relationship (Harrison et al. 1965),

$$f_{g_i} = -1.99 \times 10^{-44} (A)^{2/3}. \tag{1}$$

In general, the proposed violation of the equivalence principle for the total nucleonic energy of a nucleon is given by $m_N c^2 f_{g_i}[(m_G - m_i)/m_G]$. For the earth, $f_{g_\oplus} = -4.67 \times 10^{-10}$.

Certain features will be seen to emerge in the following treatment that are characteristic of this binding nonequivalence model. One feature is the appearance of gravitational and inertial time acausalities associated with nonequivalence mass effects. These effects may be described as arising from a gravitational complementary field and will be quantified by the introduction of a gravitational complementary field length derived from the aforementioned time acausalities.

Our construct for the complementary field length illustrates another feature of this approach; namely, the importance of geometric averaging when the universal difference between inertial and gravitational mass is accounted for in various situations.

Further, the nonequivalence model requires that spin-dependent effects must be referenced to the ecliptic plane. Finally, the importance of the nonequivalence effects will clearly be dependent on the inclination of the satellite orbit.

An important feature of the model is its distinguishing between inertial and noninertial frames of reference.

Calculation of the Acceleration of Lageos's Orbital Precession: $\ddot{\Omega}$

The precessional angular velocity of the Lageos node, $\dot{\Omega}$, is given by the Newtonian dynamic relationship (Kaula 1968), Eq. (2), in terms of eccentricity and other orbital parameters,

$$\dot{\Omega} = \frac{3}{2} \frac{J_{2,\oplus} n_L}{(1 - e^2)^2} \frac{R_\oplus^2}{a_L^2} \cos I \tag{2}$$

the mean orbital motion of Lageos, n_L, and Earth's quadrupole moment $J_{2,\oplus}$,

$$J_{2,\oplus} = \frac{C - A}{m_\oplus R^2_{\oplus,\text{equator}}}, \tag{3}$$

where $(C - A)$ describes the Earth's oblateness as the difference between the moments of inertia about the spin and equatorial axes, respectively. The quadrupole moment, or second spherical harmonic constant, represents an oblateness perturbation of Earth's gravitational potential,

$$U \cong \frac{GM_\oplus}{r_\oplus} [1 + J_{2,\oplus} (\tfrac{1}{2})(3\cos^2 \theta - 1)] . \tag{4}$$

The value of $J_{2,\oplus}$ is well established to be $+1.0826 \times 10^{-3}$ (Soldano 1984). This term possesses a positive signature in contrast with the negative signature of its time derivative, $\dot{J}_{2,\oplus}$, which will figure importantly in the following analysis.

Simply taking the time derivative of Eq. (2) leads at once to the relationship

$$\frac{\ddot{\Omega}}{\dot{\Omega}} = \frac{\dot{J}_{2,\oplus}}{J_{2,\oplus}} . \tag{5}$$

The Lageos ranging data yield a very precise value (Smith and Dunn 1981) for $\dot{\Omega}$ of $+0.343$ deg/day so that Eq. (5) would afford a route to the determination of $\ddot{\Omega}$ if a reliable value of $\dot{J}_{2,\oplus}$ were available.

In previous work (Soldano 1984), the nonequivalence model has been applied to an analysis of very precise gravitational red-shift experiments, to test location position invariance (weak equivalence principle) in general relativity (Turneau et al. 1983), to yield a theoretical value of $\dot{J}_{2,\oplus} = -2.48 \times 10^{-11}$/year.

(See the following section for a brief exposition of this number's origin.) Use of this value, along with the values cited for $\dot{\Omega}$ and $J_{2,\oplus}$ in Eq. (5) yields a prediction of the acceleration of Lageos's node of $\ddot{\Omega} = -7.76 \times 10^{-8}$ arc sec/day^2. The numerous estimates of $\ddot{\Omega}$ available to date range rather widely (Yoder et al. 1983; Rubincam 1984), but the present result is well within the uncertainty of the Rubincam 1984 value of $(-8.1 \pm 1.8) \times 10^{-8}$ arc sec/day^2 required for the best fit of experimental data to

$$\Delta\Omega = \Omega_0 + \dot{\Omega}T + (\tfrac{1}{2})\,\ddot{\Omega}T^2 + [A \sin \hat{\Omega}]_{18.61\text{yr}} \quad (6)$$

In arriving at his value, Rubincam assumed an equilibrium lunar body tide in the last term.

The present result for $\ddot{\Omega}$ not only agrees with the best value available, but, more importantly, it is based on a value of $\dot{J}_{2,\oplus}$ which is very tightly constrained by experiments independent of the Lageos ranging data. It may be the best available value of $\ddot{\Omega}$ at this time.

Of even greater significance, our $\dot{J}_{2,\oplus}$ value, and hence our value of $\ddot{\Omega}$, is totally dependent upon the validity of the nonequivalence model, and the origin of $\ddot{\Omega}$ is therefore explained solely on the basis of nonequivalence perturbations of Lageos's orbital angular momentum without appeal to geodynamic parameters which are far more tenuous than $\ddot{\Omega}$ itself (Yoder et al. 1983; Peltier 1983; Lambeck and Nakeboglu 1983).

Calculation of $\dot{J}_{2,\oplus}$ from the Nonequivalence Model

The severe numerical constraint placed on our value for $\dot{J}_{2,\oplus} = -2.48 \times 10^{-11}$/year is reflected in

$$\dot{J}_{2,\oplus} \sqrt{\left(\frac{1+e_c}{1-e_c}\right)} = J_{2,\oplus} f_{S_\oplus} \frac{m_G - m_i}{m_G} \frac{1}{\sqrt{\left(\frac{a'-c'}{c}\right)_c \left(\frac{b'-c'}{c}\right)_c}}, \quad (7)$$

grav. inertial

where $\dot{J}_{2,\oplus}$ is treated as a gravitational binding nonequivalent perturbation of $J_{2,\oplus}$. In Eq. (7) the assumption is made that the difference $a'-c'$ between the lunar radius directed toward the earth a' and the lunar radius directed toward the pole c' is *gravitational* in origin and the difference $b'-c'$ between the lunar radius directed along the orbital direction b' and the lunar radius directed toward the pole c' is *inertial* in nature. These differences in Eq. (7) are divided by the speed of gravitation $c = 3 \times 10^{10}$ cm/sec. The lunar eccentricity ratio, $\sqrt{(1+e_c)/(1-e_c)}$, is equal to $r_{a,c}/r_{p,c}$, where $r_{a,c}$ and $r_{p,c}$ are the lunar orbital apogee and perigee distances relative to Earth. Whereas the terrestrial oblateness inherent in $\dot{J}_{2,\oplus}$ is defined by the lunar-terrestrial time acausality at lunar perigee, the lunar oblateness inherent in $a'-c'$ and $b'-c'$ is defined by the lunar-terrestrial time acausality at lunar apogee.

That there should exist a lunar relationship in the time dependency of $J_{2,\oplus} = (C-A)/(m_\oplus R^2_{\oplus,\text{eq.}})$ is not surprising since the terrestrial moment of inertia difference $C-A$ is directly coupled to the moon (Cook 1969). What is unique to the present nonequivalence approach is that the time acausalities inherent in nonequivalence enable one to specify extraordinarily minute details relevant to the terrestrial-lunar coupling.

In view of Eqq. (2) and (5), we can rewrite Eq. (6) as

$$\Delta\Omega - \Omega_0 - [A \sin \hat{\Omega}]_{c,18.61\text{yr}} = \frac{3J_{2,\oplus} n_L T \cos I}{2(a_l^2/R_\oplus^2)(1-e_L^2)^2} \times \left[1 + \frac{1}{2} \frac{T f_{S_\oplus} [(m_G - m_i)/m_G]}{\sqrt{\left(\frac{1+e_c}{1-e_c}\right)\left(\frac{a'-c'}{c}\right)_c \left(\frac{b'-c'}{c}\right)_c}}\right]. \quad (8)$$

The bracketed term suggests that this precession is not only sensitive to the eccentricity and oblateness of the Moon, but it can differentiate these effects from the binding mass perturbation of the Earth.

Specifically, the Kaula term $\dot{\Omega}$ (1968), described in Eqq. (2), (6), and (8), is composed in part of $J_{2,\oplus} = (C-A)/(m_\oplus R^2_{\oplus,\text{equator}})$, where the moment of inertia difference $(C-A)$ couples to the orbiting Moon. This coupling is one of the reasons for incorporating the lunar time acausality $\sqrt{[(1+e_c)/(1-e_c)][(a'-c')/c][(b'-c')/c]}$ in the construct for $\dot{J}_{2,\oplus}$, Eq. (7). Moreover, since $(3/2)J_{2,\oplus} = J_\oplus$ in Eq. (8), it follows that the term $2\sqrt{[(1+e_c)/(1-e_c)][(a'-c')/c][b'-c')/c]}$ in Eq. 8 should also have relevance. It is equal to the geometric average of the *average* distance between the centers of mass of the Earth and Moon, and the Earth's Schwarzschild radius, $2L_\oplus$,

$$2\sqrt{(a'-c')(b'-c')} = \sqrt{a_{\oplus-c}\, 2L_\oplus} \quad (9)$$

In view of this, the last (bracketed) term in Eq. (8) can be written

Table 1
Analogues

C_γ	n_L
$\dfrac{m_G - m_i}{m_G}$	$J_{2,\oplus} \approx \dfrac{mR^2_{\text{polar}} - mR^2_{\text{x,equa.}}}{mR^2_{\oplus,\text{equa.}}}$
$\sqrt{(1 + e_c)/(1 - e_c)}\ \sqrt{a_{\oplus-c}\ 2L_\oplus}$	$(1 - e_L^2)^2\ (a_L^2/R_\oplus^2)$

$$\left[1 + \frac{Tc_\gamma f_{g\oplus}\,[(m_G - m_i)/m_G]}{\sqrt{\left(\dfrac{1 + e_c}{1 - e_c}\right)}\ \sqrt{a_{\oplus-c}\ 2L_\oplus}}\right]. \qquad (10)$$

Significantly, each term in Eq. (10) has its counterpart in Kaula's description of $\dot{\Omega}$, Eqq. (2) and (8) (1968). Table 1 presents analogue terms reminiscent of ordinary translation and rotational analogues in classical mechanics.

The Kaula terms describing $\dot{\Omega}$ are based on strict equivalence, whereas the present $\ddot{\Omega}$ terms are consequences of nonequivalence between the inertial and gravitational mass in the gravitational binding component only of the Earth-Moon system. Thus it is argued that the conventional postglacial rebound disturbance of the Earth's interior "does more than one thing." In addition to providing a wide array of geophysical information about the Earth's interior, the effect of gravitational binding nonequivalence resulting from the changing shape of the earth enables one to exploit the extraordinary sensitivity of nonequivalence binding effects that accompany this process.

It is now important to demonstrate that exactly the same model which has yielded $\ddot{\Omega}$ by treating nonequivalence as a perturbation of $\dot{\Omega}$ can also yield a prediction of the orbital decay of Lageos by a similar nonequivalence perturbation of the satellite's angular momentum. It is to this task that we now turn.

Calculation of the Secular Decrease in Lageos's Semidiameter: *da/dt*

The acceleration of Lageos's ascending node was calculated on the premise that nonequivalence effects on $J_{2,\oplus}$ are transmitted to the satellite as a perturbation of its precessional motion. The degradation of Lageos's semidiameter (Smith and Dunn 1981 and Rubincam 1982) can be treated in an analogous manner.

The nonequivalence perturbation in $\dot{\Omega}$ involves a minute fractional ($\sim 10^{-21}$) violation of strict orbital angular momentum conservation for the satellite. When the relevant time interval for the process of annealing out inertial and gravitational binding mass effects is taken into account, the result is a non-Newtonian force which results in the predicted change in the orbital radius.

According to Yoder et al. (1983), Lageos's Ω and Earth's accumulated rotational angle (UT1) exhibit comparable sensitivities to changes in $J_{2,\oplus}$. By application of strict conservation of angular momentum to the Earth-Lageos system, they were able to show a strict proportionality of $\Delta\Omega(J_{2,\oplus})$ to $\Delta\text{UT1}(J_{2,\oplus})$, the value of their ratio being given by

$$\frac{\Delta\Omega(J_2)}{\Delta UTI(J_2)} = \frac{9}{4}\frac{C_{\oplus,\text{pole}}}{M\,R^2}\frac{n_L}{\omega_\oplus}\frac{R_\oplus^2}{a^2}\ \cos I = -0.437. \qquad (11)$$

In Yoder's Newtonian treatment, (1983) this ratio represents a ratio of Lageos's orbital (n_L) angular momentum to the spin ($\omega_\oplus$) angular momentum of the Earth. The nonequivalence perturbation of $\Delta\Omega$, which affects only the numerator, results in a slight deviation from the strict proportionality in Eq. (11). The perturbation factor may be constructed as the product of three terms, required by the nonequivalence model, which act on this ratio:

(1) nonequivalence violation of angular momentum conservation $= f_{g\oplus}\,[(m_G - m_i/m_G] = 2.36 \times 10^{-21}$
(2) time acausality in inertial/gravitational nonequivalence transmission effects $= \sqrt{(a/c)(2L_\oplus/c)} = 1.1 \times 10^{-6}$ sec
(3) normalization by projection of the Earth's angular momentum (in the denominator) onto a normal to the ecliptic plane $= (\hat{u}_n \cdot \hat{\omega}_\oplus) = \cos 23.45° = 0.9174$.

The resulting expression for Lageos's orbital degradation is

$$\frac{1}{a}\frac{da}{dt} = \left[\frac{9\,C_{\text{pole}}\,R_{\oplus}^2}{4\,MR^2\,a^2}\right]\left[\frac{\cos I}{(\hat{u}_n \cdot \hat{\omega}_{\oplus})}\frac{n_L}{\omega_{\oplus}}\right]\frac{\left[f_{g_{\oplus}}\dfrac{m_G - m_i}{m_G}\right]}{\sqrt{\dfrac{a}{c}\dfrac{2L_{\oplus}}{c}}} \qquad (12)$$

where $C_{\text{polar},\oplus}$ is the Earth's polar moment of inertia and I is the inclination of the Lageos orbit. Substitution of $a = 1.227 \times 10^9$ cm, Yoder's value for the Newtonian ratio (-0.437), and the values cited in Table 1 for the nonequivalence correction factors yields, for the predicted orbital degradation,

$$\frac{da}{dt} = -1.08 \times 10^{-1} \text{ cm/day} \qquad (13)$$

in remarkable agreement with the best fit to the long-term orbital tracking data, which is -1.1×10^{-1} cm/day (Yoder et al. 1983 and Rubincam 1982).

Discussion of Elements of the Nonequivalence Model

The validity of this approach becomes clearer when it is noted that the nonequivalence factors in Eq. (12) show a remarkable symmetry with respect to Yoder's corresponding Newtonian terms in Eq. (11), and with respect to the nonequivalence terms in Eqq. (8) and (10). There are some indications that the operations involved in this calculation have far deeper implications and thus promise much broader applications in science. First, the relevant nonequivalence factor, $f_{g_{\oplus}}[(m_G - m_i)/m_G]$, is just that used in the description of the $\dot{J}_{2,\oplus}$ value essential to calculating $\ddot{\Omega}$. Thus, in contrast to previous analyses which appeal to diverse mechanisms for these effects, the present model has accounted for both the acceleration of Lageos's node and the degradation of its orbit on the basis of the same extra-Newtonian term.

The geometric average form of our time acausality factor is also highly suggestive of much deeper and broader significance. From a *gravitational* standpoint, McCrea (1964) has shown that the Schwarzschild radius of a body such as Earth ($2L_{\oplus} = 2Gm_{\oplus}/c^2$) represents that radius at which any attempted addition of proper mass (such as a "falling" Lageos) is equivalent to a change in the body's (Earth's) gravitational binding mass. In other words, at the Schwarzschild radius all of the proper mass of Lageos would be converted quantitatively to gravitational binding energy. This effect gives rise to a minimum gravitational time acausality given by $2L_{\oplus}/c$. Furthermore, the coupled Lageos-Earth system, wherein the local center of inertial mass (Lageos) is situated at distance a from the center of gravitational mass (Earth), involves an additional inertial time acausality, a/c. The geometric average of these two times used above represents the overall coupled minimum acausal time required to anneal out inertial and gravitational binding mass effects which are inescapable if our central nonequivalence premise is correct. This same approach was used in connection with Eq. (10).

If the Schwarzschild radius of the Earth is related to the gravitational component of our gravo-inertial complementary field, then the inertial length is associated with the semidiameter of an object orbiting about the Earth. In both cases involving the Lageos satellite and the Moon, objects which truly orbit the Earth, our gravitational-inertial complementary field is describing a truly inertial frame of reference, one in which there exists no acceleration relative to the fixed stars. On the other hand, if the complementary field consists of the inertia-related distance between the Earth and the Sun and the Earth's Schwarzschild radius, $\sqrt{1\text{A.U.}\ 2L_{\oplus}}$, this represents a *noninertial* system, since the sun is *not* inertially orbiting about the Earth. In this case, the gravitational complementary field will provide information about the acceleration of the earth relative to the fixed stars. Thus it follows that the gravo-inertial complementary field can be used to discriminate between inertial and noninertial frames of reference.

One further aspect of our geometric average form for the time acausality is noteworthy. Clearly our time average is a thinly veiled geometric average of two lengths $\sqrt{a\ 2L_{\oplus}}$, one being a real system length (in this case the inertial length a) and the other based on theory (the gravitational length $2L_{\oplus}$). The similarity of this construct with Debye's electromagnetic complementary field length is evident:

$$L_k = \sqrt{\frac{V}{n_0}\frac{1}{e^2/(\epsilon_0\,kT)}} \qquad (14)$$

where a real length inherent in the volume V is averaged with a theoretically calculated electrical length represented by the term $\epsilon_0 kT/e^2$. Thus our use of the acausality factor both in the calculation of da/dt and in the calculation of $\dot{J}_{2,\oplus}$, used to determine $\ddot{\Omega}$, may be described as the application of a *gravitational binding-inertial* complementary field pervading the system when nonequivalence effects are involved. This result fulfills a remarkable prediction of Bridgman (1961) that gravitational energy would be found to possess a localization length comparable to that encountered in electricity and magnetism.

The one-to-one correspondence between the elements of the present approach and that of the Debye L_k may explain the tantalizing way in which the Lageos orbital data have mimicked the qualitative behavior of a charge moving through a Debye ion atmosphere while never quite quantitatively fitting the ion drag model.

Finally, the presence of a well documented periodicity of 0.1 arc second amplitude in the $\hat{u}_n \cdot \hat{\omega}_\oplus = \cos 23.45°$ term (a phenomenon known as the Chandler wobble), suggests a possible origin of the unexplained cyclic variation in the measured value of da/dt. Furthermore, cyclic variations in the inclination term $\cos I$ in Eq. (12) could also serve as an additional source of variation in (da/dt).

Applications of the da/dt Term to Other Problems in Physics

In Eq. (12) da/dt is the *average* falling velocity of the satellite. If we assume its initial velocity is zero, then there is an instantaneous velocity of Lageos $(da/dt)_{inst} = 2(da/dt)$ which is twice that calculated by Eq. (12). In principle, knowledge of this instantaneous velocity at any particular location should enable one to relate it to the gravitational acceleration g at that point, thereby obtaining an estimate of the gravitational decremental effect at that location. An examination of Eq. (12) suggests that $(da/dt)_{avg}$ is inversely proportional to the cube of a. It follows, therefore, that $(da/dt)_{surface}$ at the Earth's surface (ignoring ion drag, air resistance, and so forth) is 0.905×10^{-5} cm/sec. Converting this average velocity to an instantaneous one, we can write

$$\frac{c}{g_{surface}} 2\left(\frac{da}{dt}\right)_{surface} = \Delta L, \tag{15}$$

where c is the speed of gravitation, $g_{surface}$ is the gravitational acceleration at the Earth's surface, and ΔL is the resultant decremental length, $\Delta L = 5.56$ meters. Dividing ΔL by the distance from the center of mass of the Earth to its surface, $R_\oplus$, we obtain a value of 8.72×10^{-7} for the depressional effect monitored by the "falling" Lageos.

In addition to da/dt being dependent on $1/a^3$ in Eq. (12), it also depends on the orbital inclination I. Therefore, if one wishes to use Eq. (15) to obtain an estimate of the *maximum* depression of the Earth's spheroid, it must be corrected by the ratio $\cos 45°/\cos 109.9°$, since the maximum depression occurs at 45°. The resultant value, $(\Delta L/R_\oplus)(\cos 45°/\cos 109.9°) = 18.1 \times 10^{-7}$, compares favorably with Darwin's $\chi = (17.5 \pm 20.3) \times 10^{-7}$, where χ represents the maximum departure of the earth's spheroid from an ellipsoidal shape (Garland 1965). Thus we can conclude that, via Eqq. (12) and (15), the decremental change in the satellite's semidiameter can provide meaningful information on the earth's gravitational field. This conclusion stands in stark contrast with the widespread belief that all satellite decremental effects must be attributed to ion and air drag. This belief has led to considerable information about the atmosphere, but precious little about the earth's gravitational field. One reason that the present nonequivalence approach has yielded gravitational field information free of complications is that both the shape of Lageos and its orbital semidiameter were originally selected to avoid both ion and air drag. Thus nonequivalence in gravitational binding offers the possibility of using high ranging satellites to sharply define the earth's geoidal surface, thereby improving the accuracy of mobile missile launching.

Relationship of the Term $\sqrt{(a/c)(2\,L_\oplus/c)}$ To Special and General Relativity

Moving the square root term in Eq. (12) from the right to the left side, one can easily demonstrate that the left hand side can be recast into a format that reveals the essential nature of the present approach,

$$\frac{1}{a}\frac{da}{dt}\sqrt{\frac{a}{c}\frac{2L_\oplus}{c}} = \sqrt{\frac{(\tfrac{1}{2})(da/dt)^2}{c^2}\;\frac{2 \times 2L_\oplus}{a}}. \tag{16}$$

special relativity — general relativity light bending

The term $\frac{1}{2}[(da/dt)^2/c^2]$ represents the special relativistic approximation of $\gamma = 1/\sqrt{1-(v/c)^2}$. For this inertial mass, one writes at low velocity (which is certainly the case for da/dt):

$$m = m_0\left[1 + \frac{1}{2}\frac{v^2}{c^2} + \ldots\right] \tag{17}$$

$$\left[\frac{m - m_0}{m_0}\right] \cong \frac{1}{2}\frac{v^2}{c^2}. \tag{18}$$

One further recognizes that the term $2 \times 2L_\oplus/a$ in Eq. (16) is simply the general relativity description of light deflection in our terrestrial reference frame. Light

deflection is an aspect of gravitational binding. It follows therefore that nonequivalence in gravitational binding represents a *geometric average* of two limiting cases, one is that of special relativity, wherein the relativity of velocity is treated, and the second is that of general relativity, wherein the relativity of acceleration is accounted for.

In view of the preceding arguments linking the length $\sqrt{a2L_\oplus}$ to limits of special and general relativity, it is reasonable to expect that this length should be relevant to a limit to the CPT theorem, since the latter is based upon the validity of special relativity and the locality concept. By contrast, nonequivalence requires that *non*local effects accompanying inertial and gravitational mass imbalances will affect *local* interactions.

If CPT invariance is violated, differences in the decay lifetimes and masses for particle–anti-particle pairs such as K^0 and $\overline{K^0}$, should exist.

It has been suggested that if a limit to the validity of the CPT theorem is ultimately found to exist, it could not be any larger than that defined by the following strangeness mass split ratio (Ryder 1975).

$$\frac{K_2^0 - K_1^0}{Kc^2} = 0.707 \times 10^{-14}. \qquad (19)$$

Since both K_2^0 and K_1^0 represent composites of K^0 and $\overline{K^0}$, a mass difference between K^0 and $\overline{K^0}$ could be even less than the $(K_2^0 - K_1^0)$ mass difference.

Our complementary field length and its related time acausalities involve *non*strange parameters and are related to a limit to the validity of special and general relativity, Eq. (16), as well. It follows therefore that the Lageos time acausality defined by the term $\sqrt{(a/c)(2L_\oplus/c)}$ should also be related to any potential limit to the validity of the CPT theorem. Smith (1981) and Yoder et al. (1983) have isolated a series of Lageos nodal rotational periods that arise from tidal perturbations. The sources of these tidal effects are identified by letters such as M_2, N_2, . . . K_2 . . ., the letters signifying the nature of the perturbations. For example, the principal lunar and solar tidal components are designated M_2,O_1 and S_2,P_1, respectively. Tidal components due to lunar and solar flattening are named M_0 and S_0. Significantly, only one of nine components arises from the declinations of the Sun and the Moon. In this regard we have already emphasized that the orientation of the spin axis of celestial bodies relative to a unit normal to the ecliptic plane constitutes one of the elements of a nonequivalence description.

Yoder (1983) identifies a Lageos nodal rotation period of 1045.6 days with the K_1 solar-lunar tidal declination mode. It follows that the Lageos complementary field time $\sqrt{(a/c)(2L_\oplus/c)}$ can be interpreted as a CPT violating perturbation of the Lageos 1045.6 day rotation period. It is significant that the Lageos time ratio,

$$\frac{\left[\sqrt{\frac{a}{c}\frac{2L_\oplus}{c}}\right]}{[P_L = 1045.6 \text{ days}]} \cong 1 \times 10^{-14} \qquad (20)$$

arising from the aforementioned *nonstrange* Lageos parameters, is comparable in magnitude to that set by the highly investigated $K_2^0 - K_1^0$ strangeness system. This suggests that not only is our Lageos time ratio potentially related to the validity limit of the CPT theorem, but its comparability in magnitude to the strangeness ratio obtained from the $K_2^0 - K_1^0$ mass split indicates that the Lageos satellite may well be providing a fertile "real" (as opposed to the usual "strangeness") laboratory for studying the limits to the structure of science. That this is the case has been the central thesis of this work.

The Relationship of $\sqrt{a_L 2L_\oplus}$ to the Conventional Ion Drag Model

From Eqq. (12) and (13) it follows that the gravitational complementary field that originates from binding nonequivalence accounts for at least 95% of the orbital degradation of Lageos. This means that neutral atom effects, often referred to as aerodynamic resistance, account for no more than 5% of the entire orbital degradation. The central question, therefore, that one would expect to be raised, concerns the absence of ion drag in our model. A voluminous body of literature (Chapra 1961) has evolved over the last thirty years that attributes satellite orbital degradation to the effects of electric ion drag. To be sure, the electric drag theories involve extreme complexities associated with plasma behavior in dynamic systems. Nevertheless, experiment combined with theory has led to the identification of certain relevant electrical scaling factors that seem to account in part for satellite orbital degradation. What follows is a brief outline of the generally accepted theory of Jastrow and Pearse (1957) and a demonstration that the gravitational complementary field presented here already *implicitly* contains many of this theory's elements.

The Jastrow-Pearse theory assumes that a spherically symmetric charge distribution surrounds a spherical satellite of radius R. Further, a negative potential ϕ exists on the surface of the satellite due to chance encounters with fast moving electrons. Finally, the effective collisional radius of the satellite is in-

creased due to the existence of an ion sheath that arises from electrical induction. Knetchel and Pitts (1964) have *experimentally* confirmed the existence of these three electrical scaling factors inherent in the Jastrow-Pearse theory:

$$\frac{D_0 - D_{e^-}}{D_0} = 1 - \frac{e\phi}{E_k}\left[1 - \exp\left\{\frac{-3.63(-e^-\phi/kT_{e^-})^{1/2}}{-(q^+\phi/E_k)\,(R/\lambda_{D.H.})}\right\}\right] \quad (21)$$

The ratio $q^+\phi/E_k$ is that of the satellite's potential acting on the positive charge of the hydrogen ions in free space divided by the kinetic energy of these hydrogen ions. The ratio $R/\lambda_{D.H.}$ is the radius of the satellite divided by the Debye-Hückel complementary field length $\lambda_{D.H.} = \sqrt{[\varepsilon_0 kT/(N/V)(e^-)^2]}$, where (N/V) is the number density of the ambient ions at a temperature T. The scaling factor $e^-\phi/kT_{e^-}$ represents the ratio of the electron energy due to the satellite's surface potential ϕ relative to the electron's average temperature T_{e^-}. Physically, this ratio determines the penetration depth of the average electron into the induced sheath surrounding the satellite. D_0 represents the drag due to *non*electrical effects and D_{e^-} that due to charge factors. In essence, electric charge tends to increase the effective collisional radius of the satellite thereby increasing the number of ambient ions affected by the satellite. The machine solution of the Jastrow-Pearse equation requires the introduction of the empirical numeric -3.63 into Eq. (21). Knetchel and Pitts' terrestrially based experiments confirmed that the size of D_{e^-} increases with an increase in the scaling factor $\phi q^+/E_k$. Further, they found that electrical drag effects were greater for a scaling ratio $R/\lambda_{D.H.} = 7.5$ than for one with $R/\lambda_{D.H.} = 10$.

Having briefly examined the nature of the scaling elements inherent in the Jastrow-Pearse theory, we now turn to its application by Rubincam (1982, 1980) in his explanation of the Lageos orbital degradation. In spite of the fact that Lageos was inserted into an orbit high enough to avoid any significant concentration of electrical ions, Rubincam claimed, on the basis of a detailed analysis of over ten alternative mechanisms, that the only remaining viable explanation for at least 60% of Lageos's orbital degradation must involve electric ion drag.

Specifically, his explanation required that the value of the electrical drag scaling factor $\phi e^+/E_{\text{kinetic}} = 5.14$, based in part on the assumption of a satellite surface potential of 1 volt. Further, he required that for a Lageos radius $R_L = 30$ cm, the second scaling factor $R_L/\lambda_{D.H.} = 7.5$, in order, as Knetchel had previously shown, that noncontacting electric ion effects be factored into the overall ion drag mechanism.

Clearly, two of the three Jastrow-Pearse scaling factors were employed by Rubincam to explain ~60% of the Lageos orbital degradation.

We will now show that our gravitational complementary field not only implicitly accounts for the presence of these two electrical scaling factors, but successfully accounts for their magnitudes as well.

Chapra (1961), in reviewing the voluminous literature associated with electric ion drag, noted that an additional dispersion length beyond the Debye-Hückel $\lambda_{D.H.}$ could well be involved in an electric ion drag model. He suggested that the de Broglie wavelength of the electron $(\hbar/m_{e^-}c)$ might well be one of these dispersion lengths. The fact that the major constituent of the upper atmosphere is hydrogen would suggest to us that the related de Broglie wavelength $(\hbar/m_{p^+}c)$ of the proton is also involved.

The strongest argument, however, for both wavelengths being involved in any complete explanation of ion drag is based in part on a comment by Wyatt (1960), who suggested that the fact that the speed of light is much larger than any satellite or electron velocity would automatically ensure that electric inductive effects dominate any electric ion drag mechanism. This electric inductive mechanism should also reflect the large mass disparity between the proton and the electron. In Eq. (22) the Lageos gravitational complementary field length $\sqrt{a_L 2L_\oplus}$ not only includes two of the previously discussed ion drag Jastrow-Pearse scaling elements, but the magnitudes $\lambda_{D.H.} = R_L/7.5$ and $\phi q^+/E_{\text{kinetic}} = 4.9$, as required by the equation, are comparable to those used in the Rubincam application of the Knetchel-Pitts results:

$$\left(\frac{\hbar}{m_{e^-}c}\right)\left(\frac{\phi e^+}{E_k} = 5.14\right)\lambda_{D.H.,7.5} = \left(\frac{\hbar}{m_{p^+}c}\right)\sqrt{a_L 2L_\oplus} \quad (22)$$

How is it that the gravitational complementary field based on nonequivalence automatically contains many of the relevant electric ion drag scaling factors? The explanation lies in the likelihood that nonequivalence in gravitational binding gives rise to an *electric vacuum polarization* such that anyone using the conventional electric ion drag model will experience a partial degree of success in accounting for any orbital degradation remaining when the effect of any ambient ions has been accounted for. In a truly unified field theory one should expect that the gravitational field should account for electrical effects as well.

How Nonequivalence in Gravitational Binding Establishes Validity Limits to Special and General Relativity

At this juncture the Lageos experiment can be considered a test of the central premise of general relativity, namely the equivalence principle, which states that without exception the inertial mass of any object is precisely equal to its gravitational mass. Clearly, our thesis requires the contrary. Is there any other direct test of general relativity that confirms the present interpretation?

Other Tests of General Relativity

It is the assumed exact equivalence between inertial and gravitational mass (at present experimentally confirmed to about 1 part in 10^{12}) that permitted Einstein to eliminate mass as a fundamental undefinable and thereby reduce physical description to four dimensional geometry. It is therefore fundamental to show that the aforementioned limit to the equivalence principle is not unique to Lageos but has already been found, even though unrecognized, by a series of other experiments.

In particular we focus on the solar-normalized, gravitational red-shift test of general relativity performed by Turneaure et al. (1983).

Advances in stable clocks have made possible a new type of red-shift experiment that provides a direct test of local position invariance (LPI) or independence. Any violation of the equivalence principle would result in the need for local positional specification. As already noted, general relativity cannot free itself from a coordinate dependency (Maddox 1985; Bell and Katz 1985; Penrose 1982). Further, the discussion of $J_{2,\oplus}$ above [Eq. (7)] represents a prime example of local positional *non*invariance. If LPI is violated, then not only can the proper ticking rate of an atomic clock vary with position, but the variation must depend on structure and composition of the clock, unless all clocks vary with position in the same way, in which case no operational way would exist to detect such a positional violation (Will 1981). Turneaure performed a null red-shift experiment by comparing the rates of two hydrogen maser clocks and a bank of SCSO clocks. For the hydrogen clocks one defines a general-relativity-violating location frequency effect α^H, in addition to the standard red shift, as

$$\tau = \tau_0^H\left[1 - \alpha^H\left(\frac{\Delta U}{c^2}\right)\right], \qquad (23)$$

where $\Delta U_\odot$ is the change in the Sun's gravitational potential during the period of the experiment. A similar expression can be written for the SCSO clocks with the LPI-violating effect specified by α^{SCSO}.

Experimentally comparing the two structurally different clocks located near each other, we obtain

$$\left(\frac{\tau^H}{\tau^{SCSO}}\right) = \left(\frac{\tau^H}{\tau^{SCSO}}\right)_0\left[1 - (\alpha^H - \alpha^{SCSO})\left(\frac{\Delta U_\odot}{c^2}\right)\right], \qquad (24)$$

where $(\tau^H/\tau^{SCSO})_0$ is a constant-period ratio between the two clocks at a chosen starting location. If LPI is violated, then $(\alpha^H - \alpha^{SCSO}) \neq 0$ as required by the equivalence principle. Turneaure et al. found that $(\alpha^H - \alpha^{SCSO}) \leqq 0.02$. During the 10-day duration of the experiment they found that the solar gravitational potential $U_\odot$ changed sinusoidally, due to the Earth's spin, with a 24-hour period empirically quantified by the term $-3.2 \times 10^{-13}\cos[2\pi(t - t_0)]$. Further, $U_\odot$ also changed linearly with time $+2.8 \times 10^{-12}$/day because the Earth was 90° from its orbital perihelion at the time of the experiment. The two effects are empirically summarized in

$$\frac{\Delta U_\odot}{c^2} = -3.2 \times 10^{-13}\cos[2\pi(t - t_0)] + \frac{2.8 \times 10^{-12}}{\text{day}}(t - t_0), \qquad (25)$$

where the first term, cyclic in time, reflects the effect of the Earth's spin on $U_\odot$ and the second, which is linear in time, accounts for the effect of the Earth's orbital motion about the Sun (Turneaure et al. 1983). If any gravitational nonequivalence exists between the two sets of clocks, the signal set up between them possesses a magnitude equal to the *product* of the location difference $\alpha^H - \alpha^S$ between the two sets of clocks and $\Delta U_\odot/c^2$. If, on the other hand, the equivalence principle holds, then $\alpha^H - \alpha^S = 0$. Based on the limit of detectability of any frequency difference developing between the two banks of clocks, they concluded that $\alpha^H - \alpha^S \leqq 0.02$. This means that in principle an effect of a size equal to $(\alpha^H - \alpha^S)(\Delta U_\odot/c^2)$ could conceivably exist.

There are theoretical reasons based on nonequivalence to believe that the general relativity gravitational red-shift experiments *normalized to the Sun* should encounter an LPI violation at $\Delta\Theta_\odot/(41.°84)_\oplus = 0.02045$. In a later section we examine the nature and the consequences of these two important angles. For now, simply multiply $\Delta U/c^2$, as described by the two-parameter empirical relationship of Turneaure, Eq. (25), by the factor $\Delta\Theta_\odot/(41.°84)_\oplus = 0.02045$, to obtain

$$\frac{\Delta\Theta_\odot}{(41.84°)_\oplus}\frac{\Delta U_\odot}{c^2} = +J_{2,\oplus}\,\Delta t_\oplus\cos[2\pi(t - t_0)] - J_{2,\oplus}(t - t_0)\cos(23.45° - 1.54°), \qquad (26)$$

a detailed description of the role played by gravitational binding nonequivalence in Turneaure's gravitational red-shift experiment normalized to the Sun. Numerically, it is consistent with the product of 0.02045, and the empirical description of $(\Delta U_\odot/c^2)$ given by Turneaure, Eq. (25).

In Eq. (26) not only has all empiricism been removed from the Turneaure description of $(\Delta U_\odot/c^2)$, but far more significantly, a real effect is describable, one that represents the product $[\Delta\Theta_\odot/(41.9°)_\odot](\Delta U_\odot/c^2)$. Essentially, Eq. (26) suggests that nonequivalence in gravitational binding involves the *difference* between a cyclic spin-dominated orbital term $\dot{J}_{2,\oplus}\,\Delta t_\oplus \cos[2\pi(t-t_0)]$, and a terrestrial orbital-dominated spin term, one linear in time, $\dot{J}_{2,\oplus}\,(t-t_0)\cos(23.45°-1.54°)$. The reasons for the time rate of change of the Earth's quadrupole $\dot{J}_{2,\oplus}$ playing a dominant role in accounting for the ΔLPI violation are these: (1) In the present approach $\dot{J}_{2,\oplus}$ contains a detailed description in Eq. (7) of the effects of mass nonequivalence in gravitational binding inherent in the term $\Delta\Theta_{\odot,\oplus}$ which specifies the reasons for the ΔLPI violation. (2) The relationship of $\dot{J}_{2,\oplus}$ to the change in oblateness of the earth makes it highly sensitive to terrestrial spin effects, which will become clearer from our description of $\Delta t_\oplus$. (3) The precise value of $\dot{J}_{2,\oplus} = -2.48\times10^{-11}$/year, given by Eq. (7) and approximated by Rubincam's 1982 estimate $(-2.6\times10^{-11}$/year), is required for Eq. (26) to hold exactly. The Yoder estimate of -3×10^{-11}/year would not lead to exact agreement. In fact, Eq. (26) serves as a very sensitive measure of $\dot{J}_{2,\oplus}$. (4) Our description of $\dot{J}_{2,\oplus}$ in Eq. (7) contains the lunar terms necessary in the description of what is at least a three body problem.

Since LPI violations are highly sensitive to multipoint alignments, the time $\Delta t_{\odot,\oplus}$ in Eq. (26) represents the minimum excess, terrestrial spin lag-time required to effect a three-body conjunction of the Sun, Moon, and Earth, a prerequisite of a solar normalized system. The actual LPI violation is described by our construct of $\dot{J}_{2,\oplus}$ in Eq. (7). Since the Earth is in absolute motion about the Sun, the daily spin period difference between the solar normalized day, P_{syn}, and the sidereal day, P_{sid}, is $(P_{syn}-P_{sid})_\odot = 236.55$ seconds. For the three-body conjunction, the above time difference is multiplied by the lunar synodic orbital period, $P_c = 29.53$ days. The exact value for $\Delta t_\oplus = 2.16$ hours, required by Eq. (26), is given by

$$\Delta t_\oplus = \left(\frac{P_{syn}-P_{sid}}{\text{day}}\right)_\oplus \left(\frac{P_c}{3\text{ pt. align.}}\right)\left(\frac{1+e_c}{1-e_c}\right), \quad (27)$$

where $e_c = 0.0549$, the lunar eccentricity correction, is introduced in Eq. (7). It is of interest to note that the product $P_c[(1+e_c)/(1-e_c)]$ is comparable to the lunar evection period of 31.81 days. It has been known for over 200 years that the lunar orbit deviates from the orbit required by Kepler's laws by a distance of 2.5 lunar diameters within a period of 31.81 days, due to the Sun's perturbing of the lunar orbit (Kovalevsky 1963).

It is clear from Eq. (7) that $\dot{J}_{2,\oplus}$ represents a terrestrial-lunar *rotational* monitor of gravitational binding nonequivalence. It follows therefore that coupling $\dot{J}_{2,\oplus}$ with the spin of the Earth should provide a general basis for determining the limit to the validity of various elements of special and general relativity. Specifically, the difference between the synodic and sidereal mean solar day $[(P_{syn}-P_{sid})/\text{day}]_\oplus = 236.55$ secs/day represents that fraction of the earth's spin that rises from the *absolute motion* of the Earth about the Sun in contradistinction to the relativity of velocity and acceleration inherent in special and general relativity, respectively. It follows, therefore, that the product $\dot{J}_{2,\oplus}\,(P_{syn}-P_{sid})/\text{day}$ should play a fundamental role in determining the limits of validity of various orientation invariance elements inherent in special and general relativity; specifically those relative to the Sun and the fixed stars. The magnitude of the specific violation is determined by the product of $\dot{J}_{2,\oplus}$ $[(P_{syn}-P_{sid})/\text{day}]_\oplus$ and the *minimum* time acausality associated with the specific test. In general, the equilibrium minimum times associated with the macroscopic gravitational red-shift tests are considerably larger than those encountered in atomic processes such as spin flip.

Returning to Eq. (25), Will suggests that the linearity in time in the second term arises because the earth was 90° from perihelion when the experiment was initiated. This is not the case when the empirical term in Eq. (25) is multiplied by 0.02045. The feature in the resultant term, Eq. (26), that reveals the role of nonequivalence is the presence of the cosine of the angles that reflect the tilt of the Earth's and Moon's spin axes relative to a unit vector normal to the ecliptic plane. The presence of this cosine term introduces a measure of symmetry into the two-term expression.

All the detailed richness inherent in our calculation of $\dot{J}_{2,\oplus}$, that is Eqq. (7) and (8), becomes a part of the richness of detail that characterizes gravitational binding nonequivalence. We conclude that Eq. (26) is a creation of nonequivalence in gravitational binding in general and in particular one that arises from solar normalized gravitational red-shift experiments. As it stands, Eq. (26) represents a detected *difference* between a terrestrial *fixed* orbital time, *variable* spin effect [first term, Eq. (26)], and a *variable* orbital time, *fixed* spin effect [second term, Eq. (26)].

For a more complete insight into the terms of Eq.

(26), a detailed analysis of $\Delta\Theta_\odot$ and the terrestrial LPI spin lag angle $(41.^\circ84)_\oplus$ follows.

Examination of $\Delta\Theta_\odot/(41.^\circ84)_\oplus$

The ratio $\Delta\Theta_\odot/(41.^\circ84)_\oplus = 0.02045$ is proposed to fix the magnitude of the validity limit of Turneaure's gravitational red-shift experiment when *normalized to the Sun*. This normalization is in sharp contrast to that inherent in the Rebka-Pound (1960) experiment, which was a gravitational red-shift test of general relativity *normalized to the earth*. In a theory based on nonequivalence, the size of any LPI violation is strongly dependent on the normalization frame since the gravitational binding fraction violating equivalence varies widely with reference frame. It is this pronounced normalization LPI violation dependency that is one of the effects that distinguishes nonequivalence gravitational energy results from those expected from more conventional theories. Aside from the obvious numerical comparability of our theoretical ratio with the upper limit of the Turneaure experiment, that is, $\alpha^H - \alpha^{SCSO} = \Delta\Theta_\odot/(41.^\circ84)_\oplus$, there is reason to believe that a delineation of the nature of these two phase shifts, as well as an examination of the consequences of multiplying Eq. (25) by $\Delta\Theta_\odot/(41.^\circ84)_\oplus$, will clearly demonstrate the richness of the connection between local astronomical motions and local microscopic phenomena. The solar phase lag angle $\Delta\Theta_\odot$,

$$\Delta\Theta_\odot = \frac{H_\odot m_N f_{g\odot}\,[(m_G - m_i)/m_G]}{(\Delta m/\Delta t)_\odot}\,(\hat{u}_n \cdot \vec{\omega}_\odot)$$

$$= 0.01495 \text{ radian}, \qquad (28)$$

represents an advection or lag angle characteristic of the Sun that is required by nonequivalence in gravitational binding. Here $H_\odot$ is the solar nucleon number, $f_{g\odot} = -2.2\times10^{-6}$ is the Sun's gravitational packing fraction, and $|\vec{\omega}_\odot| = 2.86\times10^{-6}$ radian/second is the Sun's surface angular velocity. Note that the vector nature of gravitational binding nonequivalence $f_{g\odot}(m_G - m_i)/m_G$ is reflected by a unit vector $\hat{u}_n$ normal to the ecliptic plane. We have already encountered this requirement in our analysis of the Lageos experiment. The mass current in the denominator $(\Delta m/\Delta t)_\odot$ is simply the luminosity of the Sun divided by c^2. Since radiant energy is *unbound* it obeys *strict equivalence*. Therefore, the ratio in Eq. (28) represents, in angular units, the extent of the violation of equivalence. It can be easily shown that Eq. (28) is strictly consistent with the Kelvin-Heaviside concept of relating the Sun's gravitational self-energy to its luminosity. Clearly, the phase lag angle $\Delta\Theta_\odot$ represents a quantification of nonequivalence effects that are normalized to the Sun. Further, the mass current $(\Delta m/\Delta t)_\odot$ not only satisfies strict equivalence, but it characterizes the rate of this mass change for *our solar, local center of gravitational mass*.

On the other hand, the phase lag angle $(41.^\circ84)_\oplus$, Eq. (29), in contrast to the nonequivalence inherent in $\Delta\Theta_\odot$, involves quantities strictly *obeying the equivalence principle*. The need for this angle arises because a violation of local positional invariance (LPI) requires an angular specification of the *terrestrial* spin frame lag factors that will be involved in multipoint alignments. For example, a synodic month involves the alignment or conjunction of three bodies or three points. The lunar transit involves the alignment of two bodies or two points. Finally, we have single point interactions. Each of these three categories of alignment involves differing amounts of rest frame spin lag time. The terrestrial phase lag angle $(41.^\circ84)_\oplus$ used in Eq. (26) to quantify the size of the LPI violation and detailed in Eq. (29), represents the product of the Earth's spin angular velocity $\omega_\oplus$ acting through three specific spin phase lag periods that quantify three-point, two-point and one-point gravitational alignment categories. In the three-point category, as it relates to the spin of the Earth, we have

$$(41.^\circ84)_\oplus = \omega_\oplus \left[\left(\frac{P_{syn} - P_{sid}}{\text{m.s. day}} \right) \left(\frac{(P_{syn})_c}{\text{3 pt. align.}} \right) + \left(\frac{50.47 \text{ min}}{\text{2 pt. align.}} \right) + \left(\frac{0 \text{ time}}{\text{1 pt. align.}} \right) \right], \qquad (29)$$

where the terrestrial spin lag, $(P_{syn} - P_{sid})_\oplus$/mean solar day = 236.55 secs/mean solar day, arises from the fact that the Earth is in absolute orbital motion about the Sun. The time $(P_{syn})_c = 29.5305882$ mean solar days represents the lunar synodic month, a period characterizing the gravitational alignment or conjunction of three bodies (the Sun, Earth, and Moon) or *three points*. Secondly, since the Earth is orbiting the Sun and the gravitationally-locked Moon is orbiting both the Earth and the Sun, it takes an *additional* 50.47 minutes per mean solar day for a specific point on the Earth to align with one on the Moon; a *two body* or two point alignment. Finally, we have *zero* lag time for a single point.

Relationship of the Phase Lag Angle $(41.^\circ84)_\oplus$ to the Weinberg and Cabbibo Angles

There exists some reason to believe that both the Weinberg (1980), Cabibbo (1975), and Blin-Stoyle (1970) angles are related to the phase lag angle $(41.^\circ84)_\oplus$. First, they both arise from consideration of weak in-

teractions whose singular characteristic is that they are point interactions with zero extension. Thus these point interactions and these "black box" angles should be related to the $(41.°84)_{\oplus}$ angle. According to Eq. (29), there are three different categories of point alignments. Further, there are three different ways of combining the three categories. If we assume that the Cabibbo angle involves one pair of the three categories, then one-third of the $(41.°84)_{\oplus}$ phase angle should correspond to the phase lag angle of Cabibbo. The resultant angle 13.°95 agrees quite well with the experimental estimate of 13.°94 for the Cabibbo angle. If the Weinberg angle involves two pairs of the three categories represented in Eq. (29), then the resultant phase lag angle should be 27.°89, an angle that agrees favorably with the various estimates of the Weinberg angle, whose value ranges depend on the type of experiment employed in its measurement, as well as on the value assumed for Higgs' parameter.

Returning to our specific phase angle $(41.°84)_{\oplus}$ for the Earth, it should be reiterated that the two phase lag-times involved in Eq. (29) arise from strict equivalence. It follows, therefore, that the resulting angle $(41.°84)_{\oplus}$ represents the terrestrial spin lag angle to which angular lag effects due to nonequivalence are to be normalized when one is conducting a gravitational red-shift LPI experiment. To obtain the analogous phase lag angle for the Moon, we simply substitute the *sidereal* spin angular velocity $\omega_{\leftmoon}$ of the Moon for $\omega_{\oplus}$ in Eq. (29) to arrive at the resultant lunar phase lag angle of 1.°54.

LPI Gravitational Red-Shift Test Normalized to Earth

We have gone into considerable detail to delineate the locational parameters involved in the redistribution of the solar nonequivalence binding mass current, $H_{\oplus} m_N f_{S_{\odot}} [(m_G - m_i)/m_G] (\hat{u}_n \cdot \vec{\omega}_{\odot})$, throughout our local Earth-Moon system. Nonequivalence in binding mass gives rise to vorticity effects throughout the solar system and beyond. This is the reason why such factors as orbital eccentricities and shape terms become relevant in the description of an LPI violation.

Having proposed an explanation for an LPI violation that may be as large as 2%, based on gravitational red-shift results, we appear to be faced with a fundamental inconsistency since the Rebka-Pound (1960) gravitational red-shift results validate general relativity to ~1%. Further, the rocket experiment of Vessot et al. (1980) to measure gravitational red shift appears to validate general relativity to $(2.5 \pm 70) \times 10^{-6}$. The conflict between these more stringent *experimental* limits on the validity of general relativity and those *required* by nonequivalence in gravitational binding is in point of fact only apparent. If one accepts general relativity, it doesn't make any difference what reference frame one uses for a gravitational red-shift experiment. Experimental accuracy may suffer by the choice of normalization point, but the limits of validity should be independent of the normalization reference frame; hence all of these tests must produce identically null results within the experimental limits of precision.

The above is absolutely not the case in a theory based on an LPI violation arising from gravitational binding nonequivalence. It makes a great deal of difference whether one performs a test of LPI that is normalized to the Sun, such as that performed by Turneaure, or whether one normalizes to the Earth, as done by Rebka and Pound. We can easily estimate the size of the violation of general relativity that should be anticipated for a Rebka-Pound experiment. It is given by

$$\frac{\Delta\Theta_{\oplus}}{(41.°84)_{\oplus}} = \frac{H_{\oplus} m_N f_{S_{\oplus}} [(m_G - m_i)/m_G]}{(\Delta m/\Delta t)_{\odot} (41.°84)_{\oplus}} (\hat{u}_n \cdot \vec{\omega}_{\oplus}) = 1.2 \times 10^{-11}, \quad (30)$$

where the gravitational packing fraction for the earth $f_{S_{\oplus}} = -4.67 \times 10^{-10}$, $\omega_{\oplus} = 7.292 \times 10^{-5}$ rad/sec, $(\hat{u}_n \cdot \hat{\omega}_{\oplus}) = \cos 23.°45$, and $(\Delta m/\Delta t)_{\odot}$, as before, represents the solar mass current of our Sun acting *as the local gravitational center of mass*. Clearly, gravitational binding nonequivalence effects due to the Earth are minute when compared with those of the Sun.

Since the terrestrial validity limit $(\Delta\Theta_{\oplus}/(41.°84)_{\oplus} = 1.2 \times 10^{-11}$ is minute, a direct LPI test is not practical. However, if we make the reasonable assumption that a *terrestrial* gravitational red-shift LPI test involving two sets of different clocks can be described in a manner similar to that of Eq. (26), $j_{2,\oplus}$ will again be involved. Further, the absolute motion of the Earth inherent in $(P_{syn} - P_{sid})/day = 236.55$ secs/day, in contrast to the relativity of velocity inherent in special relativity, will again be a multiple of $j_{2,\oplus}$. The only difference between the Earth-normalized results and those normalized to the Sun involves the nature of the gravitational complementary field. Clearly, the Schwarzschild radius $2L_{\oplus}$ should again represent the gravitational component of the complementary field. For the inertial component of the field, we will now use the astronomical unit, since it represents the fact that the Earth is inertially orbiting about the Sun.

As before, the resultant effect is slightly modified by the lunar eccentricity ratio. Combining these terms, we arrive at the following description of the *terrestrial* normalized violation of LPI

$$\frac{\Delta\Theta_{\oplus}}{(41.84^{\circ})_{\oplus}}\frac{\Delta U_{\oplus}}{c^2} = \dot{J}_{2,\oplus}\sqrt{\left(\frac{1\,\mathrm{AU}}{c}\right)\left(\frac{2L_{\oplus}}{c}\right)\left(\frac{1+e_c}{1-e_c}\right)}\cos[2\pi(t-t_0)], \quad (31)$$

based in part on the assumption that the ratio of the Earth's gravitational potential relative to that of the Sun $(\Delta U_{\oplus}/\Delta U_{\odot}) = 0.0709$. In spite of the enormous disparity in magnitude between the solar normalized LPI violation compared with that normalized to the Earth, the agreement inherent in Eq. (31) is quite precise.

Finally, we now address the gravitational red-shift tour-de-force, the Vessot et al. rocket experiment, with its stringent general relativity experimental validity limit of $(2 \pm 70) \times 10^{-6}$. If we make the reasonable assumption that the rocket red-shift results involve simultaneous normalization to both the Sun and the Earth, then it follows that a geometric average of the solar normalized general relativity validity limit of 0.02045, and its terrestrial, normalized counterpart, 10^{-11}, should provide a reasonable estimate of the validity limits to general relativity based on this rocket gravitational red-shift experiment,

$$\sqrt{\frac{\Delta\Theta_{\oplus}}{(41.^{\circ}84)_{\oplus}}\frac{\Delta\Theta_{\odot}}{(41.^{\circ}84)_{\oplus}}} = 0.49 \times 10^{-6}. \quad (32)$$

The close agreement of our predicted limit in Eq. (32) and the experimental general relativity validity limits set by the rocket experiment not only attest to the high-order experimental accuracy of the rocket experiment, but reaffirm the fundamental importance of normalization site in any gravitational red-shift test.

The present comparative state of experiment and nonequivalence validity limits of gravitational red-shift tests are summarized in Table 2, where we note (see first line) that experiments directly testing our central premise $(m_G - m_i)/m_G = -5.05 \times 10^{-12}$ agree with our result within two standard deviations.

It is pertinent to emphasize at this point that we have arrived at *each* of the three gravitational red-shift validity limits to general relativity by *two* independent methods. In one of them we have made use of the ratio $\Delta\Theta_i/(41.^{\circ}84)_{\oplus}$, and in the other we have highlighted the role of the product $\dot{J}_{2,\oplus}[(P_{\mathrm{syn}} - P_{\mathrm{sid}})/\mathrm{day}]_{\oplus}$ in describing the details of the gravitational red-shift validity limiting processes.

The Role of Nonequivalence in Setting an Orientation Validity Limit to Local Lorentz Invariance

Recently, widespread attention has been focused on the claim of Prestage et al. (1985) and Ballinger et al. (1985), that their microscopic atomic clock experiment has set a new limit on the orientation independence of clocks $\leqq 10^{-18}$, thereby providing a new validity limit for local Lorentz invariance (LLI). Will has clearly outlined the distinction between LPI limits set by null gravitational red-shift experiments conducted with two different sets of *macroscopic* clocks (see above) and LLI limits based on a frequency of a nuclear spin flip ($|\Delta m_i| = 1$) transition in $^9Be^+$ compared to the frequency of a hydrogen maser transition ($|\Delta F| = 1$, $\Delta m_F = 0$). Comparing the "ticks" of these two atomic microscopic clocks, Prestage et al. concluded that their relative rates were independent of orientation to at least one part in 10^{18}. They further claimed that this result represents a new, more stringent limit to the validity of LLI. Their orientation independence and our gravitational red-shift normalization dependency appear to be in conflict. We shall now show that the two sets of conclusions are consistent.

Although the authors point out that their magnetic field alignment was so directed as to be insensitive to any shifts in the $^9Be^+$ transition caused by the earth's gravitational field, they go on to claim that their orientation independence limit $\leqq 10^{-18}$ is valid for any dependence of clock tick rates relative to the Sun or the fixed stars. The method used by Prestage et al. implicitly assumes the validity of the $TH\varepsilon\mu$ formalism (Will 1981). One of the limits of this formalism is based on its assumption that gravitational fields are quasi-static because the evolution of gravitational fields occurs on a much longer time scale than the atomic time scales used in the Prestage experiment. For example, note the time involved in Eq. (27). However, in all of our gravitational red-shift experiments, the time dependency of the Earth's gravitational quadrupole moment, $\dot{J}_{2,\oplus}$, is playing a critical role, and there indeed exists no $TH\varepsilon\mu$ limit on its time relevance. It therefore follows that our $\dot{J}_{2,\oplus}$, with its built-in statement on terrestrial nonequivalence, Eq. (7), should enable us to also fix a limit to the validity of LLI invariance. The Prestage experiment employs the Ramsey technique whereby the "clock" transition is driven by a synthesizer using a separated oscillatory field with 0.5 second coherent Rabi pulses followed by a 19 second free precession period. Prestage demonstrated that any shift of the $^9Be^+$ frequency relative to the H^- maser transition is clearly dependent on the spin of the Earth.

As previously noted, the absolute motion of the spinning Earth would again require the use of the terrestrial spin dependent time difference between the synodic and sidereal day, that is, $[(P_{\mathrm{syn}} - P_{\mathrm{sid}})/\mathrm{day}]_{\oplus}$. For processes that compare the Earth with the Sun, the minimum time acausality due to nonequivalence is that required to send a one-way signal from the

Earth to the Sun, $t_{\oplus-\odot} = 499.6\ldots$ seconds.

Barring the existence of an additional linear term, our approach would suggest that the limit to local Lorentz invariance is approximated by

$$\dot{J}_{2,\oplus}\left(\frac{P_{syn} - P_{sid}}{\text{m.s. day}}\right)_{\oplus} t_{\oplus-\odot} = 1.075 \times 10^{-18}. \quad (33)$$

Our limit is within 10% of the stringent limits set by Prestage et al. For a complete explanation of the even lower $TH\varepsilon\mu$ orientation Lorentz validity limit (1×10^{-20}) set by the Washington group, as well as the much larger Hall-Brillet $TH\varepsilon\mu$ limit of 5×10^{-9}, see Appendix A.

We can, moreover, use our general approach involving the product of $\dot{J}_{2,\oplus}$ $[(P_{syn} - P_{sid})/\text{day}_{\oplus}]$ to quantitatively differentiate between the validity limit of local Lorentz orientation invariance relative to that of the Sun and that of the fixed stars. As previously noted, the complementary field length $\sqrt{(1\text{A.U.})(2L_{\oplus})}$ used in our terrestrial gravitational red-shift analysis describes a *noninertial* frame of reference since, as written, it implies that the Sun is orbiting about the Earth, that is, $2L_{\oplus}$ (Sciama 1959). A noninertial frame is one that accelerates relative to the fixed stars. It follows therefore that

$$\dot{J}_{2,\oplus}\left(\frac{P_{syn} - P_{sid}}{\text{m.s. day}}\right)_{\oplus} \frac{\sqrt{(1\text{AU})(2L_{\oplus})}}{c} = 7.83 \times 10^{-25}. \quad (34)$$

could well represent the limit of validity of local Lorentz orientation invariance relative to the fixed stars. It is interesting to note that the most accurate experiment to address this question to date, the Hughes-Drever experiment, has set a validity limit of $\leqq 4.5 \times 10^{-23}$ (1961).

Clearly, our nonequivalence approach involving $\dot{J}_{2,\oplus}$ is able to handle both macroscopic and microscopic experiments with complete generality. This serves to reinforce the validity of our central premise in this section, namely, that the gravitational normalization red-shift dependency of macroscopic clocks is fundamentally due to a gravitational binding nonequivalence between inertial and gravitational mass.

The Validity Limit of the CPT Theorem

If our relationship, Eq. (33), is defining the limit of validity of LLI, it follows that we are now in a position to resolve the question of a validity limit of the CPT theorem (Ford 1968).

Earlier, in Eq. (20) we had noted that the validity of the CPT theorem rests on the dual assumption of Lorentz invariance and locality. Clearly, the Lageos time ratio,

$$\frac{\left[\sqrt{\frac{a_L}{c}\frac{2L_{\oplus}}{c}}\right]}{[P_{\odot-c} = 1045.6\text{ days}]} = 1.22 \times 10^{-14} \quad (35)$$

must be defining the limit of validity of the locality assumption. This conclusion in part follows from the fact that the Lageos nodal rotational period, $P_{\odot-c}$ in Eqq. (20) and (35) arises from nonlocal, gravitational binding nonequivalence, tidal effects of the Sun and the Moon. If Eq. (33) defines the limit of validity of LLI and Eqq. (20) and (35) define the validity limit of locality, then these limits to the two key assumptions of the CPT theorem should be related to each other via quantities that explicitly involve the Sun and the Moon. That this is so is quantitatively shown in

$$\frac{\left[\sqrt{\frac{a_L}{c}\frac{2L_{\oplus}}{c}}\right]}{[P_{\odot-c} = 1045.6\text{ days}]}\left(\frac{m_{\oplus}^2}{m_{\odot}\, m_c}\right) = [\dot{J}_{2,\oplus}\left(\frac{P_{syn} - P_{sid}}{\text{m.s.day}}\right)_{\oplus} t_{\oplus-\odot}]\left[\frac{\sqrt{a_L\, a_i}}{a_{\oplus-c}}\right], \quad (36)$$

where $m_{\oplus}$ $m_{\odot}$, and m_i are the terrestrial, solar and lunar masses, respectively. The term $a_{\oplus-c} = 3.84 \times 10^{10}$ cm is the *average* lunar-terrestrial separation and a_i = (1 AU − 0.39 AU); with 0.39 AU the semimajor orbital axis of Mercury and 1 AU that of the Earth. For the Lageos tidal period of 280.7 days (Yoder 1983), a_i = (9.54 AU − 1 AU); 9.54 AU being the semimajor orbital axis of Saturn. It can be shown that the remaining Lageos tidal periods can be associated with the semimajor orbital axis of Mars, Jupiter, and Saturn. Eq. (36) suggests that nonequivalence in gravitational binding points to a gravitational resonance interaction between the Sun and the planets that can be monitored by the Earth-Moon system.

Relevance of Phase Lag Angles to the ΔCP, $K^0_{\pi^+\pi^-}$ Decay

That the phase lag angles of all three bodies (Sun, Moon, and Earth) are relevant to other gravitational binding nonequivalence applications is suggested in the observation that their sum,

$$(41.^{\circ}84)_{\oplus} + (1.^{\circ}54)_{c} + (\Delta\Theta_{\odot} = 0.^{\circ}8594) = 44.^{\circ}23 \quad (37)$$

is equal within experimental precision, to the world

average value $(44.^{\circ}7 \pm 1.^{\circ}2)$ for the phase lag angle required to describe the imaginary component of the CP violating amplitude ratio $Am_{K_2\to\pi^+\pi^-}/Am_{K_1\to\pi^+\pi^-}$ (Cronin 1981; Fitch 1981; Adair and Fowler 1963). Before examining the second order details that involve lunar and terrestrial eccentricity effects, it is worth noting that the solar ratio $(\Delta\Theta_\odot/2\pi) = 2.38\times10^{-3}$ (where 2π represents mass current rotational invariance) approximates the *real* portion of the experimental amplitude ratio $|\eta_{+-}| = Am_{K_2\to\pi^+\pi^-}/Am_{K_1\to\pi^+\pi^-} = (2.27\pm0.02)\times10^{-3}$ as well.

To complete our estimate of the real component of the $Am_{K_2\to\pi^+\pi^-}/Am_{K_1\to\pi^+\pi^-}$ decay, ΔCP amplitude, we must account for the lunar and terrestrial contributions to the major solar term $\Delta\Theta_\odot/2\pi$. For the Moon, the term is simply $(1+e_c)$, where $e_c = 0.0549$ is the lunar orbital eccentricity. Gravitational binding nonequivalence effects are particularly sensitive to gravitational binding changes implicit in eccentricities. In order to make a direct connection of $(1+e_c)$ with particle physics in general and $Am_{K_2\to\pi^+\pi^-}$ decay in particular, we recall that (1) the factor 2π in $\Delta\Theta_\odot/2\pi$ implies that mass effects involved in $K_2^0\to\pi^+\pi^-$ decay are independent of rotation. The term $\Delta\Theta_\odot$ defines how much mass current rotational independence is violated by gravitational binding nonequivalence, since (2) Sternglass has suggested that the $\pi^+\pi^-$ mesons represent positron-electron rotational states, (3) the ΔCP decay of $K_2^0\to\pi^+\pi^-$ normally involves weak interactions. However, we shall show that taking proper account of both strong and gravitational interactions is comparable to introducing weak interactions. That these three ideas are directly interrelated is quantified by

$$\sqrt{(f_{\pi,q}^2 = 0.082)(Gm_e^2/2\hbar c)}\,(1 + e_c) = \mu_{\beta^+\beta^-}^2, \qquad (38)$$

where

$$\mu_{\beta^+\beta^-}^2 = [(G_F/\hbar c)(m_e c/\hbar)^2]^2, \qquad (39)$$

and

$$f_{\pi,q}^2 = 0.082 = \left(\frac{1m_\pi}{2m_N}q\right)^2\frac{1}{\hbar c} \qquad (39a)$$

is the $\pi+$-meson strong coupling constant with q being the nucleonic binding charge. The term $Gm_e^2/2\hbar c$ defines the gravitational positron-electron pair coupling to a graviton. $G_F = 1.41\times10^{-49}$ is the weak interaction electronic Fermi coupling constant and $\hbar/m_e c$ is the Compton wavelength of the electron. The term $1+e_c$ in Eq. (38) operates on the strong charge described by Eq. (39a). Interestingly, our geometric average of strong and gravitational coupling constants, Eq. (38), again involves both an inertial term represented by $f_{\pi,q}^2 = 0.082$ and a gravitational term $Gm_e^2/2\hbar c$. This is an averaging pattern characteristic of nonequivalence in gravitational binding. Eq. (38) implies that the strong force can alter positron-electron pairs. Further, spherical symmetry is violated as reflected in e_c.

The terrestrial factors that, in conjunction with $\Delta\Theta_\odot$ and $1+e_c$, destroy rotational invariance in $K_2^0\to\pi^+\pi^-$ decay are composed of (1) the orbital eccentricity of the earth $(e_\oplus = 0.016722)$ and (2) the eccentricity in the ellipsoidal shape of the Earth, $(\sqrt{a^2 - c^2}/a)_\oplus = 0.08182$, where a is the Earth's equatorial radius and c is its polar radius. In point of fact, our lunar term possesses a shape eccentricity, but we have ignored it because it is negligible in size compared to the lunar orbital eccentricity e_c. Combining the two terrestrial eccentricities $[1-(e_\oplus+\sqrt{a^2-c^2}/a)]_\oplus$, we can write a complete equation for the ΔCP violating amplitude η_{+-} (both real and imaginary),

$$\frac{AmK_2^0\to\pi^+\pi^-}{AmK_1^0\to\pi^+\pi^-} = \left[1 - \left(e_\oplus + \frac{\sqrt{a^2-c^2}}{a}\right)\right]_\oplus \times \left[1 + e_c\left(\frac{\Delta\Theta_\odot}{2\pi}\right)\right] \times e^{i[(41.^{\circ}84)_\oplus + (1.^{\circ}54)_c + \Delta\Theta]}. \qquad (40)$$

Clearly, Eq. (40) agrees with the best world average of both the real and imaginary terms. The remaining problem is to show how the terrestrial term $[1-(e_\oplus+\sqrt{a^2-c^2}/a)]_\oplus$, one required by gravitational binding nonequivalence, is related to strange particle physics.

We have a clue in the fact that a mass effect is clearly involved in the generation of the ΔCP. We can be even more specific because the mass shift should involve the transformation of $\overline{K^0} = 497.67$ MeV with strangeness $S = -1$ to $K^0 = 497.67$ MeV with $S = +1$. Further, the mass shift should also involve the mass shifts related to the corresponding charged states; that is, $(\overline{K^0} - K^-) = 4$ MeV going to $(K^0 - K^+) = 4$ MeV. The total mass shift is 2×497.67 MeV + 8 MeV = 1003.34 MeV. Clearly, nonequivalence involves nucleonic effects and the lowest mass hyperon for strange particles is the $\Lambda^0 = 1115.6$ MeV state, which also possesses strangeness $S = -1$. Further, for *strong* interactions (as was the case in our lunar discussion, that is, $e_c\times q$) virtual processes connecting Λ^0 to both the nucleon and K particles exist; that is, $\Lambda^0 \rightleftarrows \overline{K^0} + n$; $\Lambda^0 \rightleftarrows \overline{K^0} + p^+$. It follows, therefore, with an accuracy of 0.1%, that the following mass relationship obtains,

$$m_{\Lambda^0}\left[1 - \left(e_{\oplus} + \frac{\sqrt{a^2 - c^2}}{a}\right)\right]_{\oplus}$$
$$= [m_{(\overline{K}^0 \to K^0)}] + [m_{(\overline{K}^0 - K^-)} \to m_{(K^0 - K^+)}], \quad (41)$$

suggesting that it is a $\Delta S = 2$ change with the attendant mass shifts for both $\overline{K}^0$ and K^- that gives rise to the ΔCP change in the mass matrix. Our $\Delta S = 2$ change in S, Eq. (41), should not be confused with the super weak model that is introduced solely to account empirically for ΔCP; nonequivalence in gravitational binding, which underlies Eq. (40), is involved throughout the structure of science. At the astronomical level, our two eccentricities, that is, $e_{\oplus}$ and $\sqrt{a^2 - c^2}/a$ appear to be operating in a manner analogous to the third component of isotopic spin T_3 and charge Q, as described by the strangeness, baryon number B relationship (Cronin 1981; Fitch 1981; Adair and Fowler 1963),

$$S = 2(Q - T_3) - B. \quad (41a)$$

Solar Light Deflection and Nonequivalence

We now demonstrate that the nonequivalence solar phase lag angle $\Delta\Theta_{\odot}$ is applicable to more than the Turneaure gravitational red-shift result and the ΔCP problem. If we simply consider that $\Delta\Theta_{\odot}$ perturbs the system angle $\pi/2$ used to quantify the solar light deflection in general relativity, we are led to predict that a general relativity validity limit of 0.95% faces any future light bending test:

$$\frac{\Delta}{\text{radian}} = 2\frac{2L_{\odot}}{r_{\odot}}\left[1 - \frac{\Delta\Theta_{\odot}}{(\pi/2)}\right]. \quad (42)$$

It is interesting to note that the highly accurate electromagnetic radio wave tests (Will 1983) of the "light" deflection by the Sun have for almost a decade given results that deviate by 1% from those predicted by general relativity. We firmly believe that the 1% deviation in their results arises from gravitational binding nonequivalence.

The Question of the 'Missing' Solar Neutrinos

Our final example attesting to the power of $\Delta\Theta_{\odot}$, the solar nonequivalence lag angle, has to do with the question of missing solar neutrinos. According to conventional theory, the Sun is emitting only ~⅓ of the neutrinos expected on the basis of the solar model and particle fusion physics (Zatsepin 1982). The best conventional explanation, namely, neutrino oscillations between two states has recently been eliminated as a viable explanation for the missing factor of ⅔.

If we recall: (1) that nonequivalence in gravitational binding leads to a violation of our *present* formulation of spin, angular momentum, and energy conservation at the microscopic level, a situation shared with general relativity whenever gravitational energy is involved; and (2) that neutrinos serve to restore the conservation of spin, angular momentum and energy at the microscopic particle level, then to the extent that nonequivalence affects the fusion process in the Sun, to that same extent conservation restoring neutrinos should be absent. We can easily estimate the number of missing neutrinos expected from our Sun as follows.

If strict equivalence obtains, it has been estimated (Kuchaeviacz, 1976) that ~0.58 MeV of the 26.72 MeV of energy released during the fusion of four protons ($4p^+ \to He^{++} + 26.72$ MeV) should be in the form of neutrinos. Since $\Delta\Theta_{\odot}$ is both an angle and a nonequivalence fraction normalized to the luminosity of the Sun, that is, $(\Delta m/\Delta t)_{\odot}$, while acting as a local center of gravitational mass, then multiplying the total fusion energy by $\Delta\Theta_{\odot}$ defines the conservation violating energy requiring no neutrino restoration. Thus the ratio of this nonequivalence energy relative to the neutrino energy required by strict equivalence,

$$\frac{\Delta\Theta_{\odot}\ (26.72\ \text{MeV})}{(0.58\ \text{MeV})_{\nu_e}} = 0.69 \quad (43)$$

is a measure of the fraction of neutrino flux from the Sun that *should* be missing due to nonequivalence in gravitational binding. It follows, therefore, that one should detect experimentally only a fraction $f = 0.31 = 1/3.3$ of neutrinos expected on a basis of the standard solar model. Significantly, this value is in precise agreement with the latest estimates of Davis (1978) and Bahcall et al. (1980).

We conclude this section with a comparison of the validity limits set by gravitational binding nonequivalence with the experimental test limits presently being attributed to experimental limitations (Table 2).

Relationship of Nonequivalence to Planck's Constant

Our general thesis is founded on the premise that nonequivalence in gravitational binding plays a fundamental role in science in general and in the question of energy fluctuations in particular.

Table 2. Comparison of present experimental limits of validity of general relativity with those required by nonequality between inertial and gravitational self-binding mass.

(a)	(b)	(c)	(c′)	(d)		(e)
1	SE/GRM	0	$\sim 7\times10^{-12}$‡	5.05×10^{-12}	=	$[(m_i-m_G)/m_G]$
2	WE	0	$\sim 1\times10^{-12}$‡	4.21×10^{-15}	≧	$f_{gk}[(m_i-m_G)/m_G]$
3	WE	0	~0.02§	0.02045	=	$\Delta\Theta_\odot/(41.^\circ84)_\oplus$
4	WE	0	~0.01‡	1.2×10^{-11}	=	$\Delta\Theta_\oplus/(41.^\circ84)_\oplus$
5	WE	0	$(2.5\pm70)\times10^{-6}$‡	0.49×10^{-6}	=	$\sqrt{(\Delta\Theta_\odot\Delta\Theta_\oplus)/(41.^\circ84)^2_\oplus}$
6	WE &	0	$\sim 1\times10^{-3}$‡	0.74×10^{-3}	=	$(\Delta T/T)_\odot$
6′	TRI	0	$\sim 10^{-4}$	4.2×10^{-13}	=	$(\Delta T/T)_\oplus$
7	SE/GRM	0	~0.01‡	0.009549	=	$[1-(\Delta\Theta_\odot)/(\pi/2)]$
8	SE/GRM	0		0.02045	=	$\Delta\Theta_\odot/(41.^\circ84)_\oplus$

Table columns are:
(a) experiments 1-8, described below;
(b) principle tested [strong or weak equivalence (SE or WE), metric of general relativity (GRM), time reversal invariance (TRI)];
(c) fractional theoretical and (c′) experimental deviations from values predicted by general relativity;
(d) fractional derivation from general relativity result required by nonequivalence theory;*
(e) description of the nonequivalence corrections in column (d).
Rows give the experiments:
(1) Nordtvedt test of lunar motion relative to Sun and Earth;
(2) Dicke-Braginski-Eotvos type;
(3) solar red shift (location dependence);‡§
(4) Rebka-Pound terrestrial gravitational red shift;
(5) Vessot rocket, gravitational red shift (normalized to both Sun and Earth because of altitude);
(6) Shapiro time delay test, in reality a solar normalized test of time reversal invariance $(\Delta T/T)_\odot$;
(7) quasar "light" deflection by Sun;
(8) advance of Earth's perihelion.
Some terms in (e) are related by

$$\Delta\Theta_k = M_k[f_{g_k}(m_G-m_i)/m_G](\hat{u}\cdot\vec{\omega}_{k,\text{surface}})/(\Delta m/\Delta t)_\odot,$$

where $(\Delta m/\Delta t)_\odot c^2$ is the luminosity of the Sun, k is for $\text{Sun}_\odot$ or $\text{Earth}_\oplus$, f_{g_k} is the appropriate gravitational packing fraction, and $\hat{u}_n$ is a unit vector normal to the ecliptic plane. For $(41.^\circ84)_\oplus$, see text.
*Soldano, 1984.
‡Will, 1983.
§Turneaure, et al., 1983.

This follows from the fact that the universal difference $(m_G-m_i)/m_G = -5.05\times10^{-12}$ introduces a fundamental uncertainty in the description of gravitational binding energy. For example, the uncertainty of the Earth's gravitational self-binding energy per nucleon is given by

$$\Delta E_\oplus = \frac{-3}{5}\frac{GM_\oplus^2}{R_\oplus}\left(\frac{m_G-m_i}{m_G}\right)\left(\frac{1}{H_\oplus}\right) = 1.96\times10^{-12}\text{eV}, \quad (44)$$

where $m_\oplus$ is the mass of the Earth, $H_\oplus = 3.6\times10^{51}$ is the number of terrestrial nucleons, $R_\oplus$ is the radius of the Earth and the factor 3/5 arises from the assumption of constant density during the gravitational charging process. This uncertainty in energy per nucleon $\Delta E_\oplus$ can be spread over two categories, namely, positive and negative energy. Further, associated with $\Delta E_\oplus$ there exists a minimum time acausality $t_{\oplus\sim\odot} = (L_{\oplus-\odot})/c$, which represents the minimum time (~498.6 sec) necessary to send a signal from the inertially orbiting Earth to our local center of gravitational mass, the

Sun. We can, therefore, combine the aforementioned elements into an overall nucleonic fluctuation

$$F_N = \frac{\Delta E^2_{\oplus}\,(t_{\oplus-\odot})^2}{(2/\text{nucleon})\,(m_N/\text{nucleon})} \tag{45}$$

of energy flowing through a cross sectional area as the Earth's gravitational energy per nucleonic mass m_N goes toward equilibrium with that of the Sun.

Associated with the gravitational energy fluctuation due to nonequivalence, there exists a related fractional difference between ephemeris time and atomic or electronic time,

$$\dot{\xi}_{\oplus,e-} = \frac{dt_{\text{ephemeris}} - dt_{\text{atomic}}}{(t - t_0)dt_{\text{atomic}}} = \frac{0.1090 \times 10^{-11}}{\text{year}}. \tag{46}$$

The recent experimental investigations of Heilings et al. (1983) have shown that if there exists any difference between ephemeris and atomic time it must be $\leqq (0.1 \pm 0.8) \times 10^{-11}$/year. Our postulation of a precise value for $\dot{\xi}_{\oplus,e-}$ arises from the fact that the fine structure constant itself can be shown to represent the ratio of a nonequivalence binding fluctuation, $\dot{\eta}_{\oplus,\gamma} = 5.0 \times 10^{-14}$/year, in the Earth's aberration constant, 20.″496, and the aforementioned $\dot{\xi}_{\oplus,e-}$ of Eq. (46). The ratio for α is

$$\alpha = \frac{1 \text{ rad}}{2\pi}\,\frac{\dot{\eta}_{\oplus,\gamma}}{\dot{\xi}_{\oplus,e-}}. \tag{47}$$

The term $\dot{\eta}_{\oplus,\gamma}$ is

$$\dot{\eta}_{\oplus,\gamma} = \frac{f_{g\oplus}\,[(m_G - m_i)/m_G]\,(\hat{u}_n \cdot \vec{\omega}_{\oplus})}{\left[\left(\frac{2\pi}{P_{\oplus,\text{orbit}}}\right)\left(\frac{1}{c_\gamma}\right)\left(\frac{[2.06\times10^5][1\text{AU}]}{\sqrt{1-e^2_{\oplus}}}\right) = 20.''496\right]}, \tag{48}$$

where $\dot{\eta}_{\oplus,\gamma}$ represents a minute deviation, $\sim 10^{-21}$, from the assumed independence between the velocity of light c and the orbital angular velocity of our terrestrial reference frame, an assumption that underlies the derivation of the aberration angle 20.″496.

The above description of α, Eq. (47), fixes the value of $\dot{\xi}_{\oplus,e-}$ precisely at 0.1090×10^{-11}/year.

Our thesis further requires that associated with the behavior of the electron, the origin of atomic time, there must exist a related time fluctuation $\dot{\xi}_{\oplus,e-}$ whenever a connection with ephemeris time is required, as is the case in our description of $\Delta E_{\oplus}$, Eq. (44). Additionally there are two kinds of electrons $(+,-)$. It follows, therefore, that associated with the electron and positron we can arrive at a fluctuation analogous to that given in Eq. (45),

$$F_{e^\pm} = \frac{e^+\,e^-}{(2/\text{electron})(m_{e^-}/\text{electron})}\left[\dot{\xi}_{\oplus,e-}\left(\frac{R_\oplus}{c}\right)\right]^2 \tag{49}$$

In this equation m_e is the mass of the electron and $R_\oplus/c$ represents the minimum time acausality inherent in any measurement that involves the equilibrium of all of the Earth's gravitational energy and the charge being considered. We note that all of the terms in Eq. (49) are *inertial* in nature. Further, all the terms, including the charge of the electron, are *classical nonquantum*. It should be reiterated that all the terms in $\Delta E_\oplus$, Eqq. (44) and (45) are also classical.

Our previous analysis of the gravitational complementary field had led to the expectation that any complete description of a system involving gravitational binding nonequivalence in mass requires the geometric average of a *gravitational* and an *inertial* component. On a strictly dimensional basis, the geometric average of our two classical fluctuations represented by Eqq. (45) and (49), is dimensionally, action, h.

If we take the geometric average of these two kinds of fluctuations, we obtain

$$1.065\,h = \sqrt{\left(\frac{(\Delta E_\oplus t_{\oplus-\odot})^2}{2m_N}\right)\left(\frac{e^+e^-}{2m_e}\right)\left(\dot{\xi}_{\oplus,e-}\,\frac{R_\oplus}{c}\right)^2}, \tag{50}$$

gravitational inertial

which suggests that a unit of action only 6.5% larger than the quantum $h = 6.672 \times 10^{-27}$ erg-sec, can be obtained from two *purely classical* fluctuations. Further, the product of the two terms remains independent of $R_\oplus$, since any change of R in the gravitational energy term $\Delta E^2{}_\oplus$ is matched by an equivalent change in R in the term $\dot{\xi}_{\oplus,e-}\,(R_\oplus/c)$. Thus our classical geometric average not only agrees with the value of the quantum h, but it reflects the positional independence required of Planck's constant. Eq. (50) further suggests that the quantum of action h may well originate from the invariance in the charge of the electron and not the inverse, as suggested by quantum, magnetic monopole arguments.

There is additional quantum justification for the *geometric* averaging inherent in our classical construct for h, Eq. (50). First, wave mechanics requires that $\hbar$ be multiplied by $\sqrt{l(l+1)}$ instead of l, as required by the Bohr theory. Further, not only must the orbital angular momentum number, l, be treated in this fashion, but the identical geometric averaging is required for spin, that is, $\sqrt{s(s+1)}$. Since our construct for h involves two terms, Eqq. (45) and (49), it is tempting to identify our two groups with the quantum l and s.

Dirac's quantum mechanics identifies intrinsic spin with special relativity, so that, clearly, intrinsic spin has nothing to do with a mechanical spin of an electron. Significantly, the term in Eq. (45) containing nonequivalence, $(m_G - m_i)/m_G$, is related to the limit of validity of special relativity. Further, there is considerable evidence that $(m_G - m_i)/m_G$ itself acts like a vorticity or spin. Thus, we identify the term $\Delta E_\oplus$ in Eq. (45) with spin s.

On the other hand, the inertial term involving both the charge of the electron and the fractional time connection term $\dot{\xi}_{\oplus,e^-}$ in Eq. (49) clearly involves terms deeply related to orbital angular momentum or l, since ephemeris time itself is based upon the orbital period of the Earth.

Finally, it is natural to assume that the factor of 1.065 in Eq. (50) arises from uncertainties in the values under the geometric average. However, our entire dissertation is committed to a universal nonequivalence in gravitational binding given by $(m_G - m_i)/m_G = -5.05 \times 10^{-12}$, and our classical description of the fine structure constant α firmly fixes the value of $\dot{\xi}_{\oplus,e^-}$. Since the value of the electron's charge is also firmly fixed, there appears to be little room, as seen from our vantage point, for attributing the factor 1.065 to uncertainties in terms used in our geometric average. Further, there is a suggestion that the factor 1.065 in Eq. (50) is also amenable to classical derivation.

Empirically, one can arrive at a term involving atomic and ephemeris processes numerically equal to 1.065 as follows. One obtains the numerical value required by taking the difference between the series

$$\sum_{p=1}^{\infty} \frac{1}{p^4} \tag{50a}$$

which has played an important role in connecting quantum theory with classical physics, and the numeric 0.017202095, which is the classical Gaussian gravitational constant. The result is written

$$\Delta K = \left[\sum_{p=1}^{\infty} \frac{1}{p^4} - 0.017202095 \right] = 1.0651 \ . \tag{51}$$

To arrive at an explanation of Eq. (51), we make the assumption that the division of h by 2π in Eq. (50) links our classical construct for h with quantum spin $1\hbar$. The equivalent $(2\pi)^2$ under the square root, Eq. (50), logically operates on the spins, term $\Delta E^2 t^2_{\oplus-\odot}/2m_N(2\pi)^2$, Eq. (45). It follows therefore that the numeric 1.065 in Eq. (51) must represent an enlarged statement on the term $[\dot{\xi}_{\oplus,e^-}(R_\oplus/c)]^2$ in Eq. (50).

To demonstrate this point, we begin by turning to the Stefan-Boltzmann constant σ Eq. (52),

$$\sigma = (12\pi) \left[\sum_{p=1}^{\infty} \frac{1}{p^4} \left(\frac{k_B}{h} \right)^4 \right] \left(\frac{h}{c^2} \right) , \tag{52}$$

which arises from the union of the microscopic quantum h, with the macroscopic blackbody theory. Clearly, the series given by Eq. (50a) is acting as a multiple of h, in Eq. (52), which is the characteristic required by Eqq. (50) and (51). Further, the term (k/h) is proportional to ν/T. Not only does the atomicity ratio k/h represent an uncertainty at the classical level (k), but it involves the uncertainty inherent in h. Further, the relationship of this ratio of uncertainties (k/h) to the ratio of vibration frequency and temperature (ν/T), clearly suggests that the series given by Eq. (50a) represents a continuum statement on vibrational atomicity, a process which underlies the proposed fractional difference between atomic and ephemeris time $\dot{\xi}_{\oplus,e^-}$.

A clue to the origin of the remaining term 0.01720 in Eq. (51) lies in the origin of the ephemeris concept in general and in the term $\dot{\xi}_{\oplus,e^-}(R_\oplus/c)$ in Eq. (50) in particular. Ephemeris time is based upon the orbital period of the Earth about the Sun. Clearly, we can recover the angular numeric required in Eq. (51) by multiplying the mean orbital motion of the Earth ($n_{\oplus,\text{avg}} = 2\pi/365.2563835$ days) by its *minimum* synodic spin period (1 day) giving us $n_{\oplus,\text{avg}} P_{\oplus,\text{min}} = 0.01720$. This minimum rotational period of one day stands in sharp contrast with the minimum radial time acausality $R_\oplus/c$, in the term $\dot{\xi}_{\oplus,e^-}(R_\oplus/c)$ required for the gravitational equilibrium of the Earth. Thus the numeric $1.065 = \Delta K$ required by Eq. (50) can be written as

$$\begin{aligned} \Delta K &= \left[\sum_{p=1}^{\infty} \frac{1}{p^4} - n_{\oplus,\text{avg.}} P_{\oplus,\text{spin min.}} \right] \\ &= 1.0650 \ . \end{aligned} \tag{53}$$

By rewriting Eq. (53) as

$$\Delta K = n_{\oplus,\text{avg.}} \left[\sum_{p=1}^{\infty} \frac{1}{p^4} \frac{365.2563 \text{ days}}{2\pi} - 1 \text{ day} \right] , \tag{54}$$

we can further highlight the atomic nature of the first term in the bracket by identifying the numeric p with the number of electronic vibrations (raised as in many electronic scattering processes to the fourth power). The terrestrial mean orbital angular velocity $n_{\oplus,\text{avg}}$ constitutes the basis of ephemeris time. Eq. (53) represents an enlarged statement analogous to 2π that is relevant to differences between atomic and ephemeris time processes inherent in the term $\dot{\xi}_{\oplus,e^-}(R_\oplus/c)$. If this be so, we can complete our purely *classical* derivation of the quantum spin concept:

$$1\,\hbar = \sqrt{\left(\frac{(\Delta E_{\oplus} t_{\oplus-\odot})^2}{2m_N(2\pi)^2}\right)\left(\frac{e^+e^-}{2m_e}\right)\left(\frac{[\dot{\xi}_{\oplus,e^-}(R_{\oplus}/c)]^2}{(\Delta K)^2}\right)} \quad . \quad (55)$$

The angle represented by Eq. (53) points to a potential restriction on the universal assumption of spherical symmetry.

We now discuss the relevance of our classical construction for h to the theoretical foundations of quantum mechanics. Bohm (1957) concludes that quantum theory, in particular the indeterminancy principle, abandons the following three classical concepts: (1) causality, (2) continuity of motion, and (3) the objective reality of individual micro-objects.

Clearly, nonequivalence in gravitational binding mass introduces a fundamental acausality into physics. Furthermore, since all motion is time-dependent, the fractional difference between ephemeris and atomic time (Eq. 55) introduces an ambiguity in the description of motion which mars the concept of continuity. Finally, we note that our construct for h (Eq. 55) contains both the mass of the nucleon and that of the electron under a square root sign. This geometric average can be interpreted as representing the transformation of the mass of the nucleon into that of an electron. Thus the two masses represent only two end states of a continuum of masses. Clearly, the latter interpretation is consistent with the necessity of abandoning the objective reality of individual micro-objects.

That Planck's constant h represents a limit of validity of the principles of causality and continuity is further affirmed by the analysis of Landé, (1952) who showed that "the entire mathematical formalism of modern quantum theory was a logical consequence of the thermodynamic postulate of continuity of cause and effect. The latter requires that the quantum probability amplitude of transition from q to p values be represented by a complex exponential which is normalized to a constant." Equating this constant with Planck's h is tantamount to suggesting that h represents the limit of validity for the concept of continuity of cause and effect.

Recent tests of the foundations of quantum theory, particularly the work of Bell (1983), provide considerable evidence that quantum interactions must involve the intervention of a nonlocal force. In this regard it should be noted that the time $(l_{\oplus-\odot})/c$ (Eq. 55) not only defines a minimum time acausality inherent in h but it implicitly involves the intervention of our nonlocal solar center of gravitational mass in local terrestrial quantum phenomena. The resultant product $(\Delta E)[l_{\oplus-\odot})/c]$ could well represent the nonlocal force itself. Furthermore, in addition to our classical construct of h representing the geometric average of a gravitational and an inertial term, the ΔE term under the square root sign can be both positive and negative at the same time, that is, $(m_i - m_G)/m_G$ and $(m_G - m_i)/m_G$, which could provide an additional physical basis for the importance of the imaginary term in quantum mathematical formalism.

Finally, since the energy ΔE used in our construct for h represents the coherent energy of all the Earth's nucleons acting on a single nucleon (Eq. 44), there is a suggestion that a subquantum classical unit of action smaller than Planck's h might well exist. We shall address this question in Appendix A.

Astronomical Quantities, the Quantum Power Series $\sum_{p=1}^{\infty}(1/p^4)$, and the Electron

In our classical construct of Planck's constant h, we made use of the power series Eq. (50a) $\sum_{p=1}^{\infty}(1/p^4)$ and its variant, ΔK, Eq. (53). This series is a part of the important Stefan-Boltzmann constant, Eq. (52). It arises in quantum theory from purely mathematical considerations required to facilitate the integration of an exponential power series involving the vibrational frequencies of the electron, that is, $h\nu/kT$. In a theory based on gravitational binding mass nonequivalence, this power series used in microscopic physics and its variant ΔK have a direct physical, astronomical significance. For our own part we have used throughout this work other quantities as well, purely astronomical in nature (both planetary and artificial satellite-related), such as $[(P_{syn} - P_{sid})/P_{syn}]_{\oplus,spin}$, e_c, $P_{c,orbit}$, and $\dot{J}_{2,\oplus}$, to set limits on the validity of general and special relativity tests that are also microscopic in nature (see Appendix A).

In a nonequivalence model we have already noted that astronomical quantities have a direct physical connection with microscopic physics, because a detailed accounting of one's local astronomical environment is required. It is logical to expect that a theory that has the potential for unification at many levels of interaction inherent in the extreme weakness of $f_{g_i}(m_G - m_i)/m_G$, will involve both gravitational and inertial parameters ranging from those related to one's reference frame, the Earth, to the immediate solar system and ultimately to the universe.

The immediate question, therefore, is what do the power series and the aforementioned astronomical quantities share in common at the microscopic, quantum level? A clue to the resolution of this question lies in the utility of the above quantities in setting validity limits using the $TH\varepsilon\mu$ formalism. The $TH\varepsilon\mu$ parameters ε_0 and μ_0 measure the interaction of electric

charge with gravitation. It follows therefore that the astronomical parameters monitor the electronic-gravitational interactions that reflect the influence of our solar system. The fact that these interactions have heretofore not been detected quantum mechanically suggests that they could represent a series of hidden variables of the electron that are not found within the q, p quantum formalism. Bohm (1957) has addressed this question and has concluded that the present expression for the wave equation should be enlarged to include a term that reflects the influence of our local astronomical environment on the properties of the electron. Our central thesis is that a general gravitational binding mass inequality gives rise to such a class of variable, electronic interactions.

To quantify this astronomical-microscopic electron interaction, we begin by examining the electronic vibration series Eq. (50a), $\sum_{p=1}^{\infty} (1/p^4)$ where p represents an integral number of vibrations, as well as the related term ΔK. The latter has played a role in our construct of h (Eq. 55). We note, in particular, that ΔK is a component of the important electron group $e^- \dot{\xi}_{\oplus e^-}(R_\oplus/c)/\Delta K$ used in this construct. In our description of ΔK in Eq. (53), we noted that astronomical quantities such as the Earth's orbital period $P_{\oplus,\text{orbit}}$ and its synodic spin period $P_{\oplus,\text{spin}}$ are involved. As a consequence of nonequivalence in gravitational binding, both the orbital periods and the spin periods of the remaining eight planets are also involved in an electronic description of both ΔK and the related series Eq. (50a).

To test this thesis, we add the *synodic* orbital periods of the remaining eight planets (ranging in duration from 115.88 to 779.94 days) and divide by 8 in order to obtain an average planetary orbital period,

$$\sum_{i=1}^{8} P_{\text{i, orbit}}/8 \tag{56}$$

We have used the synodic orbital period with its special relevance to our terrestrial reference frame because nonequivalence requires that we specify in detail the particulars of one's reference frame. Employing the geometric average technique inherent in our gravitational binding nonequivalence model, we take the geometric average of this average planetary orbital period with the orbital period of the Earth, $P_{\oplus,\text{orbit}}$,

$$\sqrt{\left[\sum_{i=1}^{8} P_{\text{i, planets, orbit}}/8\right]\left[P_{\oplus,\text{ orbit}}\right]} \tag{57}$$

The identical averaging technique is also applied to the sidereal spin periods of the remaining eight planets. They range in duration from 244.3 days to less than 10 hours. This summation algebraically recognizes the fact that the retrograde spin of Venus is treated with a sign opposite to that used for the remaining seven planets with prograde spin. The resultant planetary spin average is geometrically averaged with the Earth's spin period $P_{\oplus,\text{spin}}$,

$$\sqrt{\left[\sum_{i=1}^{8} P_{\text{i, planets, spin}}/8\right]\left[P_{\oplus,\text{ spin}}\right]} \tag{58}$$

The division of the sum of these two geometric time averages by the orbital period P of the Earth numerically approximates (within 1%) the value 1.0823 obtained from the electronic vibrational series. The exact value of 1.0823, correct to four places, is obtained thus,

$$\sum_{p=1}^{\infty} \frac{1}{p^4} = \frac{\sqrt{\left[\sum_{i=1}^{8} P_{\text{i, planet, orbit}}/8\right]\left[P_{\oplus,\text{ orbit}}\right]} + \sqrt{\left[\sum_{i=1}^{8} P_{\text{i, planet, spin}}/8\right]\left[P_{\oplus,\text{ spin}}\right]}}{P_{\oplus,\text{ orbit}}} - \frac{P_{\oplus,\text{ spin}} + P_c\left[\dfrac{P_{\text{syn}} - P_{\text{sid}}}{P_{\text{syn}}}\right]\left[\dfrac{1 + e_c}{1 - e_c}\right]}{P_{\oplus,\text{ orbit}}} \tag{59}$$

by subtracting the sum of the spin period of the Earth, $P_{\oplus,\text{spin}}$ and the adjusted sidereal lunar orbital period used in Eq. (27) to quantify the solar normalized gravitational red shift, $P_C\,[(P_{\text{syn}} - P_{\text{sid}})/P_{\text{syn}}]_\oplus\,[(1 + e_c)/(1 - e_c)]$.

One can also obtain the precise value for the related electronic series $\Delta K = 1.0650$ by noting in Eq. (53) that it differs from the series Eq. (50a) by only the term $(2\pi/P_{\oplus,\text{orbit}})P_{\oplus,\text{spin}}$. An exact expression for $\Delta K = 1.0650$ is obtained, therefore, if we make the single substitution of the term $P_{\oplus,\text{spin}}(1 + 2\pi)$ for $P_{\oplus,\text{spin}}$ in equation (59).

Clearly, all the terms in our expression for the two related vibrational series ΔK and Eq. (50a) are astronomical in origin, thereby suggesting an intimate connection of our solar system with the microscopic, vibrating electron. It is the vibration of an electron that constitutes the basis of atomic time. The Earth's sidereal, orbital period provides the basis for ephemeris time. The magnitude of the fractional difference per unit time between atomic and ephemeris time $\dot{\xi}_{\oplus,e^-}$ quantifies the coupling of the electron to the solar system through the group $e^- \dot{\xi}_{\oplus,e^-}(R_\oplus/c)/\Delta K$ found in Eq. (55). ΔK represents an astronomical coupling to which the electron coupling given by the product $\dot{\xi}_{\oplus,e^-}(R_\oplus/c)$ is to be referred.

The magnitude of the coupling is determined by

the magnitude of the time $R_\oplus/c$. We suggest that our expression for Eq. (59) and that for ΔK detail the nature of the hidden variable, electronic interactions. The equations imply that the electron in a laboratory can detect a minute gravitational interaction due to the planetary spin and orbital components of our solar system. This should not be at all surprising since many, such as Sciama and Eddington, have suggested that a complete theory of the electron should reflect its interaction with the entire universe. That the latter interaction also exists is suggested by the fact that the proposed nonequivalence in gravitational binding, which is the ultimate cause of the general, extreme sensitivity of electrons to spin, orbital and eccentricities effects such as those that define ΔK, is itself intimately related to the details of the expansion of the universe (see Appendix B). We note that $(m_G - m_i)/m_G$ defines the deceleration of the universe and is directly related by means of the Sun's Schwarzschild radius to our solar system itself Eq. (B9), thereby completing the linkage of the laboratory electron to the Sun, the solar system, and, finally, to the entire universe.

Although it is premature to determine whether or not Bohm's two-parameter term for the wave expression does represent a valid solution for nonquantum, hidden variable, electronic interactions, it is interesting to note that the substitution of Eq. (59) or its ΔK variant into Eq. (60),

$$\left(\frac{1}{m_{e^-}}\right)\left(\frac{1}{2}\right)\left(e^-\right)^2\left[\frac{\dot{\xi}_{\oplus,e^-}\,(R_\oplus/c)}{\Delta K}\right]^2 \rightarrow$$

$$\left(\frac{1}{m_{e^-}}\right)\left(\frac{1}{2}\right)\left(e^-\right)^2\left[\frac{\dot{\xi}_{\oplus,e^-}\,(R_\oplus/c)\;P_{\oplus,\ \mathrm{orbit}}}{A}\right]^2$$

where

$$A = \sqrt{\left[\sum_{i=1}^{8} P_{i,\ \mathrm{planets,\ orbit}}/8\right]\left[P_{\oplus,\ \mathrm{orbit}}\right]} + \sqrt{\left[\sum_{i=1}^{8} P_{\mathrm{i,\ planets,\ spin}}/8\right]\left[P_{\oplus,\ \mathrm{spin}}\right]} - \left\{P_{\oplus,\ \mathrm{spin}}\,(1 + 2\pi) + P_c\left[\frac{P_{\mathrm{syn}} - P_{\mathrm{sid}}}{P_{\mathrm{syn}}}\right]\left[\frac{1 + e_c}{1 - e_c}\right]\right\} \tag{60}$$

that constitutes one of the elements of h Eq. (55), permits one to estimate the relaxation time required for Bohm's wave expression to revert to the standard Schrödinger wave equation. Bohm presented arguments suggesting that the time necessary for the randomization of hidden variable effects that connect the macroscopic world with the microscopic one might well be fixed by the quantum thermal equilibrium time given by $\hbar/kT \cong 10^{-13}$ sec. We note that the resultant time inherent in the group $[\dot{\xi}_{\oplus,e^-}(R_\oplus/c)\ (P_{\oplus,\mathrm{orbit}})] = 2.32 \times 10^{-14}$ sec is comparable to Bohm's estimate. This suggests that hidden variable experiments designed to detect the electronic currents arising from the spin and orbital interactions of the planets with the electron should involve times much smaller than 10^{-14} sec.

It is significant from an electric charge quantization standpoint to note that the magnitude of the time ratio (6.8×10^{-22}) found by dividing the product $\dot{\xi}_{\oplus,e^-}\ (R_\oplus/c)P_{\oplus,\mathrm{orbit}}$ (Eq. 60) by the sum of the two geometric time averages less the terrestrial and lunar time terms, that is, A in Eq. (60), is comparable to the longterm experimental lower limit $(e_p^+ - e^-)/e^- \cong 10^{-21}$ found by the most sensitive charge asymmetry tests designed to detect any difference between the charge of the proton and that of the electron. Equating these two ratios leads to a detailed elaboration of the astronomical current-current and linear current effects that give rise to charge asymmetry and provides new insight into the process of electron charge quantization.

Further, it should be noted that the time irreversibility which Bohm considers basic to his expression for the wave equation is already built into our fractional time term $\dot{\xi}_{\oplus,e^-}$. Finally, the 1/2 in our expression for h (Eqq. 55 and 60) could well represent the quantum spin 1/2. This suggests that the effects inherent in Eq. (60) represent a perturbation of the fourth quantum number, a point of view implicit in Bohm's work.

Conclusion

We have presented an extensive array of examples of the utility of the nonequivalence in gravitational binding concept for resolving theoretical and experimental difficulties presently confronting physics. For example, Fitch (1981) has noted that after more than twenty years of intense theoretical and experimental efforts, conventional physics can only define the magnitude of the energy associated with the $K_2^0 \rightarrow \pi^+\pi^-$ ΔCP problem. There is a very good reason for this difficulty and those encountered in many of the examples we have considered. The explanation is simply that the accepted structure of physics is wedded to the idea of *complete* equivalence between inertial and gravitational mass and therefore does not tolerate a slight easing of this absolute equality. It follows therefore that the present structure of physics is vainly committed to freeing itself of the coordinate depend-

ency inherent in gravitational binding nonequivalence; a situation that has long troubled the exponents of general relativity. To the extent that a ΔLPI violation exists due to nonequivalence in gravitational binding, physics can *not* free itself of this coordinate dependency. Instead of considering this situation a difficulty, coordinate dependency should be considered the path to far richer connections between astrophysical and local microphysical phenomena.

Acknowledgement

I wish to express my deep indebtedness to Drs. William H. Brantley and C. Stuart Patterson for their critical analysis of this work and their great help in preparing the manuscript.

The work related to the Lageos Satellite was done, in part, while I was a Fellow of the 1984 and 1985 NASA-ASEE Summer Faculty Fellowship Program at Goddard Space Flight Center. I am grateful to the program for the opportunity thus afforded me, and hereby acknowledge that program as well as my hosts at Goddard Space Flight Center.

Appendix A

General $TH\varepsilon\mu$ Limits on the Validity of Special Relativity Set by Nonequivalence in Atomic, Two-Clock Systems

There is reason to believe that a generalization of Eq. (33), to reflect the specific nature of the two "atomic clocks" used in the test of special relativity, leads to a complete description of the wide range of experimental upper limits set on the validity of special relativity.

The $TH\varepsilon\mu$ theoretical framework allows for nonuniversal coupling limits set by a new force in physics. In the present case, the force is that of gravitational binding nonequivalence.

In the $TH\varepsilon\mu$ formalism T_0 and H_0 are free parameters that describe the strength of the coupling between gravity and material particles. H_0 is directly related to spatial parameters and T_0 is related to those involving time. ε_0 and μ_0 describe the coupling between gravity and electromagnetic fields. A particular feature of the formalism is that the maximum speed of material particles c_0 need not be the same as that of light c. Recently, Haugen has adapted the $TH\varepsilon\mu$ formalism to give the dependence of frequencies, for nuclear magnetic resonance or other atomic transitions used in two-clock tests on the orientation of the atoms, based on their velocity relative to a preferred frame of reference. Haugen has done this in particular for the 2.71°K microradiation which is intimately linked to the origin of our gravitational binding nonequivalence (see Appendix B). For that reference frame Haugen finds that the $TH\varepsilon\mu$ relationship for the Hall-Brillet two-laser experiment is given by $(H_0 - T_0\varepsilon_0\mu_0)/H_0 \leqq 5\times10^{-9}$ compared with a $TH\varepsilon\mu$ value of $\leqq 1\times10^{-18}$ for the Prestage et al. NBS results.

A prepublication report (*Science* **229**: 745–747) of the Washington group, which involves two mercury isotopes ^{201}Hg and ^{199}Hg as the two atomic clocks, cites a value of $\leqq 1\times10^{-20}$. Our explanation of these widely varying $TH\varepsilon\mu$ upper limits, within the context of a common terrestrial coordinate orientation limit (that is, $\dot{J}_{2,\oplus}\{(P_{syn}-P_{sid})/\text{m.s. day}\}_{\oplus}\, t_{\oplus\to\odot} = 1.07\times10^{-18}$ is a constant) rests on the fact that the final orientation limit for a two-clock system must also reflect the specifics of the clocks themselves. For example, the fact that we were able to calculate a limit for the Prestage NBS two-clock system of ^{9}Be and ^{1}H, based solely on our terrestrial reference frame term, lies in the fact that the ratio of the mass number difference between ^{9}Be and ^{1}H, when divided by the maximum mass number in our two-clock system, 9, is practically unity, 8/9. It follows that the complete $TH\varepsilon\mu$ orientation invariance limit for the Prestage system is given by

$$\left[\frac{H_0 - T_0\epsilon_0\mu_0}{H_0}\right] = \left[\dot{J}_{2,\oplus}\left(\frac{P_{syn} - P_{sid}}{\text{m.s. day}}\right)_{\oplus} t_{\oplus\to\odot}\right]\left(\frac{8}{9}\right) = 0.95\times10^{-18}. \quad \text{(A1)}$$

In general, the $TH\varepsilon\mu$ orientation, Lorentz invariance limit for any two-clock system is simply given by

$$\left[\frac{H_0 - T_0\epsilon_0\mu_0}{H_0}\right] = \left[\dot{J}_{2,\oplus}\left(\frac{P_{syn} - P_{sid}}{\text{m.s. day}}\right)_{\oplus} t_{\oplus\to\odot}\right]\left(\frac{\Delta A}{A_{max}}\right), \quad \text{(A2)}$$

where $\Delta A = A_h - A_L$ is the mass number difference between the two atomic clocks. A_h is the larger mass number and A_L the smaller. $\Delta A/A_h = (A_h - A_L)/A_h$ represents the mass transfer analogue of the second law's temperature efficiency factor $(T_h - T_L)/T_h$. It measures the efficiency with which any two-clock system can detect the terrestrial coordinate frame nonequivalence effect represented by the product $\dot{J}_{2,\oplus}\, t_{\oplus-\odot}\,[(P_{syn}-P_{sid})/\text{m.s.d.}]_{\oplus}$.

Recently, an opportunity to test the generality of this relationship has arisen with the announcement by the Washington group that a $TH\varepsilon\mu$, two-clock orientation upper limit of 1×10^{-20} had been set for a

two-isotope-clock system (^{201}Hg and ^{199}Hg). The fact that the nucleon number difference between the two isotopes is 2 compared with the maximum isotope clock mass of 201, reduces the terrestrial coordinate orientation limit of 1.07×10^{-18} by a factor of approximately 100. It follows, therefore, that Eq. (A2) would predict for this system a limit of $\sim1\times10^{-20}$, in complete agreement with the announced Washington results.

A more severe test of the validity of Eq. (A2) lies in its application to the Hall-Brillet, two-laser $TH\varepsilon\mu$ limit of 5×10^{-9}. Not only is this upper limit, as calculated by Haugen, much larger than our common coordinate orientation limit of 1.07×10^{-18}, but it involves photons and not massive nucleons. To apply Eq. (A2) to photons we must (1) obtain the mass change Δm arising from the coupling of the two lasers, and (2) obtain an estimate of the rest mass of the photon.

Clearly, Δm in this laser experiment is simply the mass shift inherent in the beat frequency υ_0 between the two lasers ($\upsilon_0 = 35\times10^6$ Hz) used by Hall-Brillet, $\Delta m = h\upsilon_0/c^2$.

In *Mass, Measurement and Motion/Sequel 2: A New Look at Maxwell's Equations and the Permittivity of Free Space* we have shown in great detail that a limit to Coulomb's law due to nonequivalence in gravitational binding, leads to an estimate of the photon rest mass, $m_0' = 1.8\times10^{-49}$ gram. This value is about a factor of ten below the best experimental upper limits on this quantity. We have also shown in the same work that the limit to spherical symmetry inherent in classical electromagnetism leads to a second photon rest mass estimate of $m_0'' = 1\times10^{-50}$ gram. Consistent with our nonequivalence model and the detailed discussion accompanying the derivation of these two values, we take their geometric average to be the appropriate value of the photon rest mass, namely, $m_0 = 0.42\times10^{-49}$ gram. Substitution of $\Delta m/m_0$ for $(\Delta A/A_{max})$ in Eq. (A2), leads to a $TH\varepsilon\mu$ estimate $(H_0 - T_0\varepsilon_0\mu_0)/H_0 = 6.4\times10^{-9}$. This value is to be compared with Haugen's $TH\varepsilon\mu$ estimate of (5×10^{-9}) for the Hall-Brillet results.

Clearly, the ever decreasing $TH\varepsilon\mu$ limits of the two-atomic-clock orientation results do not necessarily reflect an increase in the validity of special relativity, but are a reflection of the differing composition of the atomic clocks being used. Furthermore, the ability of Eq. (A2) to handle the wide range of observations for mass particles and photons alike is a striking confirmation of the gravitational-binding nonequivalence model upon which this paper is based.

In conclusion, we wish to note that the gravitational terms in Eq. (A2) may well be identified with the permittivity ε and permeability μ of free space in the vicinity of the Earth, with the term $[(P_{syn}-P_{sid})/P_{syn}]_\oplus = \varepsilon$. Since Maxwell's theory requires that the product $\varepsilon\times\mu = (1/c^2)$, we can convert our terms into an equivalent dimensional relationship by the introduction of the square of a velocity v_i, yielding

$$\left(\frac{\dot{J}_{2,\oplus}\, t_{\oplus-\odot}}{v_i^2}\right)\left(\frac{P_{syn} - P_{sid}}{P_{syn}}\right) = \frac{1}{c^2}\,. \qquad \text{(A3)}$$

The resultant "ether" velocity required by equation (A3) is 3.1 cm/sec. Significantly, the Hall-Brillet, laser-light version of the Michelson-Morley ether experiment requires that the upper limit for the velocity of the Earth relative to the "ether" be no larger than ~7 cm/sec.

Evidence for a Subquantum Unit of Action, $h_{\gamma,ether}$

There is evidence to suggest that the photon rest mass $m_{0,\gamma}$ used in estimating the Hall-Brillet validity limit, and the terrestrial ether velocity v_i in Eq. (A3) can be combined to form a subquantum unit of action $h_{\gamma,ether}$ that is consistent with our classical derivation of Planck's constant, Eq. (53). To demonstrate this point one converts these two quantities into a subquantum unit of action $h_{\gamma,ether} = 1.33\times10^{-54}$ erg sec:

$$h_{\gamma,ether} = m_{0,\gamma}\, v_i^2 \sqrt{\left(\frac{1+e_c}{1-e_c}\right)\left(\frac{a'-c'}{c}\right)_c\left(\frac{b'-c'}{c}\right)_c} \qquad \text{(A4)}$$

by multiplying their product by the time acausality inherent in our description of $\dot{J}_{2,\oplus}$ in Eq. (7).

The resultant unit of ether action, $h_{\gamma,ether}$, can then be related to the Planckian spin-two graviton ($2\hbar$) via the process of graviton decay into two spin-one photons, that is, $(2\hbar\rightarrow(\beta^+ + \beta^- + \beta^+ + \beta^-) \rightarrow 2\gamma$. Rosen (*Phys. Rev.* **128**: 449 (1962)) demonstrated theoretically that graviton decay can occur solely by indirect means and the process must involve mediators. In the present application, involving the interaction of the Earth with the ether, the mediators could well be the mass of the Earth, $m_\oplus$, and two positron-electron pairs. Significantly, if we convert the subquantum $h_{\gamma,ether}$ into a spin-one subquantum by dividing by 2π, $\hbar_{\gamma,ether} = h_{\gamma,ether}/2\pi$, we can *quantitatively* link it to the Planckian spin-two graviton ($2\hbar_{Planck}$), if we assume that both the masses of the Earth and that of two positron-electron pairs are involved in the decay process,

$$2(1\hbar)_{\gamma,ether} = (2\hbar_{Planck})\sqrt{\left(\frac{2m_{\beta^+ + \beta^-}}{m_\oplus}\right)}\,. \qquad \text{(A5)}$$

Note that the action reduction factor in Eq. (A5) involves not only the terrestrial and electron masses, but also contains a square root sign as well, all quantities critical to our derivation of the classical Planck's constant h in Eq. (55). Equation (A5) serves to reinforce our contention that the components of the subquantum $h_{\gamma,\text{ether}}$ in equation (A4) that have been used throughout this study are of general validity.

Appendix B

The Origin of the Gravitational Binding Nonequivalence Between Inertial and Gravitational Mass

The origin of the proposed gravitational binding nonequivalence between inertial and gravitational mass lies in the behavior of the entire universe. Dingle pointed out that only motion and temperature depend upon the entire universe. Since motion is intimately linked to the equivalence principle it would appear reasonable that a derivation designed to quantify the magnitude of any difference between inertial and gravitational binding mass should be thermodynamic in nature and also involve the entire universe.

The proposed model is one in which an essentially empty universe behaves as an ideal gas composed of galaxies that are moving away from each other as a part of a general expansion. The expansion is monitored by the 2.71°K relic radiation. Within each galaxy, the stars, each subject to intense gravitational self-compressional binding effects that can in many cases lead to the final iron fusion stage, are moving randomly relative to each other. The primary standard environment in which inertial and gravitational binding mass are identically equal to each other is one in which the Kelvin temperature of the relic radiation is exactly zero. It follows that the relic radiation whose temperature is 2.71°K, monitors a universal temperature deviation $\Delta T = 2.71°C$ from this standard environment. Our general approach to a derivation of $(m_G - m_i)/m_G$ is based on the premise that radiant energy, being gravitationally unbound, obeys the strict equivalence principle between inertial and gravitational mass. This means that radiant energy associated with the expanding universe will obey a Lorentz-invariant Doppler temperature shift. On the other hand, all the elements associated with the expanding universe that involve gravitational binding such as the stars and their collective sum, the galaxies, will be affected by an epoch dependent nonequality between inertial and gravitational binding mass.

For an ideal gas such as our relatively empty universe composed of galaxies, the fluctuation in the pressure of its unbound radiation as a function of volume at constant entropy is given by

$$\left(\frac{\partial P}{\partial V}\right)_{S,U} = \frac{\overline{\Delta P}^2}{kT} . \tag{B1}$$

We can represent the pressure fluctuation in the unbound radiant energy as a change in radiant mass localized in a volume fluctuation $\Delta mc^2/\overline{\Delta V}$. In general, there are four gravitational states of *unbound mass*, that is, active and passive gravitational masses, $m_{G,A}$, $_{G,P}$, ordinary inertial mass, m_i, and that form of inertial mass that participates in pair formation, $m_{i,\text{pair}}$. The existence of these four states of mass requires that the term $(\partial P/\partial V)_{S,U}$ in Eq. (B1) be squared, since $(\partial P/\partial V)_{S,U}$ involves only two energy density fluctuations. Further, since radiation is unbound energy, the four aforementioned unbound radiation energy densities are exactly equal to each other, that is, $(\Delta m_i c^2/\overline{\Delta V}) = (\Delta m_{G,A} c^2/\overline{\Delta V}) = (\Delta m_{G,P} c^2/\overline{\Delta V}) = (\Delta m_{i,\text{pair}} c^2/\overline{\Delta V})$. The latter follows from the fact that unbound energy, such as radiation, obeys strict equivalence. It is only the gravitationally bound energy that violates strict equivalence.

Although the formation of galaxies and their stars is an entropy decreasing process, the overall entropy change accompanying the expansion of the universe is an increase. It follows, therefore, that the term $(\partial P/\partial V)^2_{S,U}$ must be perturbed by an entropy increasing effect. A clue to the nature of this effect lies in the fact that any difference between inertial and gravitational binding masses will lead to a violation of Newton's third law, the latter requiring that any emission of radiation be accompanied by an equivalent recoil momentum.

The thermal aspect of the Mössbauer effect not only involves photon emission but is also accompanied by an apparent lack of recoil. In the Mössbauer case however, the photon recoil momentum is spread amongst $\sim 10^{10}$ atoms in a lattice leading to a negligible recoil in the atom actually undergoing the photon emission. In addition, the thermal, Mössbauer, Doppler-two effect accounts for a difference in temperature between the source of emission and the absorber. This also is similar to the relic radiation of the universe at $T = 2.71°K$ emitting radiation to a zero temperature absorption sink.

The conventional second order thermal Doppler shift is given by

$$\frac{1}{2}\frac{C_p \Delta T}{c^2} = \frac{1}{2}\frac{\overline{v}^2}{c^2} , \tag{B2}$$

where C_p is the heat capacity per gram of the photon emitter and $\Delta T = 2.71°K$ is the temperature difference between the emitter and the absorber. It is well known that, although the mean velocity $\overline{v}$ for an oscillating

system is zero, the mean square velocity, $\overline{v}^2$, is not zero. The factor of ½ in Eq. (B2) arises from the fact that the random kinetic energy (thermal energy) of an atomic lattice is one-half of the lattice energy.

In view of the above discussion, we propose to quantify the increase in the entropy of our ideal gas, expanding universe by a Mössbauer thermal term,

$$\left(\frac{\partial P}{\partial V}\right)^2_{S,U} \frac{1}{2} \frac{C_P \Delta T}{c^2} . \tag{B3}$$

The rationale behind Eq. (B3) is the premise that at zero Kelvin the inertial and gravitational binding masses are identically equal to each other. Since the Doppler-two term describes a recoiless situation involving an "apparent" violation of Newton's third law, the temperature difference between the relic radiation and the zero Kelvin standard environment could in principle constitute a monitor of the real Newton's third law violation that arises from a gravitational binding mass nonequivalence between inertial and gravitational mass. To determine the size of this gravitational binding nonequivalence requires that we construct a mechanical motional analogue of the second-order Doppler shift of the ideal gas term $(\partial P/\partial V)^2_{S,U}$ inherent in Eq. (B3). In the present case we shall use the gas fluctuations inherent in the term described by

$$\left(\frac{\partial P}{\partial V}\right)^2_{T,U} = \frac{(kT)^2}{\overline{\Delta V^4}} . \tag{B4}$$

Our analogue to Eq. (B3) requires that the constant temperature term Eq. (B4) be perturbed by the gravitational packing fraction f_{g_i}, where f_{g_i}, can be written in a Doppler-two velocity ratio format

$$f_{g_i} = \frac{\text{gravitational binding energy}}{(1 \text{ nucleon mass})(c^2)} = \frac{v_i^2}{c^2} , \tag{B5}$$

analogous to that in Eq. (B2). For an average star like our Sun, $f_{g_\oplus} = -2.2 \times 10^{-6}$. The limiting magnitude that accompanies the formation of stars and galaxies if $f_{\min} = -8.46 \times 10^{-4}$. Significantly, this limit is characteristic of the ^{56}Fe atom. It has long been recognized that stars will continue to fuse nucleons as a counteractant to the stars' gravitational compression until the iron phase is reached. At that point no net energy can be released by fusion. In order to make the product $(\partial P/\partial V)^2_{T,U} f_{g_i}$ analogous to Eq. (B3), we multiply the product by the fractional difference $(m_G - m_i)/m_G$ between the inertial and gravitational binding mass. We reiterate that at the standard zero Kelvin environment, $m_{G,\text{binding}} = m_{i,\text{binding}}$. At any other point, the fractional difference $(m_G - m_i)/m_G$ in gravitational binding will be epoch-dependent, just like that of the temperature of the relic radiation in Eq. (B3). To obtain an estimate of $(m_G - m_i)/m_G$, we equate Eq. (B3) with its gravitational binding analogue, thereby obtaining

$$\left(\frac{\partial P}{\partial V}\right)^2_{S,U} \frac{1}{2} \frac{C_P \Delta T}{c^2} = \left(\frac{\partial P}{\partial V}\right)^2_{T,U} \frac{1}{2} f_{g_i} \left(\frac{m_G - m_i}{m_G}\right) , \tag{B6}$$

where the factor of ½ on the right hand side arises from the fact that a one-way time acausality required by nonequivalence is always one-half of the roundtrip time acausality.

In view of our preceding discussion on the role of ^{56}Fe in stellar gravitational collapse, we shall use the value of $f_{\min} = -8.46 \times 10^{-4}$ characteristic of the iron atom in order to obtain an estimate of $(m_G - m_i)/m_G$ from Eq. (B6). Further, for ^{56}Fe the value of the heat capacity per gram per degree is 2.2×10^{-15}. For an ideal gas, $(\partial P/\partial V)_T/(\partial P/\partial V)_S = 1.67$. Inserting these quantities into Eq. (B6), one obtains a value of $(m_G - m_i)/m_G = -5.05 \times 10^{-12}$.

It should be emphasized at this point that all of our tests of the equivalence principle involve the use of the same epoch-dependent value of $(m_G - m_i)/m_G = -5.05 \times 10^{-12}$ in combination with different values for f_{g_i} depending upon the nucleonic size of the system under investigation.

There is reason to believe that the universal gravitational binding difference $(m_G - m_i)/m_G = -5.05 \times 10^{-12}$ can be directly related to the quantities that characterize our expanding universe, since we have claimed that nonequivalence should be related to the dynamics of the universe.

The expansion of the universe is quantified by the Hubble recessional constant $H = 55$ km/sec/megaparsec $= 1.78 \times 10^{-18}$/sec. While the universe is expanding, it is slowly decelerating $(\partial^2 l/\partial t^2)_U$ due to the self-gravitational binding drag effect of all the matter in the universe. This effect is quantified by the deceleration constant q_0 given by

$$q_0 = \frac{\left(\frac{d^2\ell}{dt^2}\right)_U \ell}{\left(\frac{d\ell}{dt}\right)^2_U} , \tag{B7}$$

where $(dl/dt)/l$ is simply the Hubble constant H. The product $q_0 H$ therefore is given by

$$q_0 H = \frac{\left(\frac{d^2\ell}{dt^2}\right)_U}{\left(\frac{d\ell}{dt}\right)_U} . \tag{B8}$$

In order to relate Eq. (B8) with the numeric $(m_G - m_i)/m_G$ we must multiply Eq. (B8) by an estimate of the time over which the deceleration of the universe operates. On average, the deceleration $(d^2l/dt^2)_U$ originates at the present edge of the universe, $R_U = 1.48 \times 10^{28}$ cm, and terminates at an average Sun's Schwarzchild radius, $2L_\odot = 2.965 \times 10^5$ cm, for the gravitational limit, and at the Moffet spin analogue of the Schwarzschild radius, $l_\odot = 3.02 \times 10^8$ cm, for the inertial spin limit. It follows that equating these dynamic quantities to $(m_G - m_i)/m_G = -5.05 \times 10^{-12}$,

$$q_0 H(R_U^2 \ell_\odot 2L_\odot)^{1/4} \frac{1}{c} = \frac{m_G - m_i}{m_G}, \qquad \text{(B9)}$$

requires a value of $q_0 = 0.23$, a magnitude characteristic of an open universe. In light of Eqq. (B8) and (B9), we can rewrite Eq. (B6) as follows:

$$\left(\frac{\partial P}{\partial V}\right)^2_{S,U} \frac{1}{2} \frac{C_P \Delta T}{c^2} = \left(\frac{\partial P}{\partial V}\right)^2_{T,U} \frac{1}{2} f_{\min} \frac{(d^2\ell/dt^2)_U (R_U^2 \ell_\odot 2L_\odot)^{1/4}}{(d\ell/dt)_U c}. \qquad \text{(B10)}$$

It is of interest to note that one of the solutions proposed by Bell and Katz to resolve the gravitational energy problem confronting general relativity involves a flat space special condition characteristic of special relativity and requires that the entire universe be involved in the specification of gravitational energy. It should be noted in this regard that our Eqq. (B10) and (B6) not only involve the Doppler-two term characteristic of special relativity but the product $(Hq_0/c)(R_u^2 l_\odot 2L_\odot)^{1/4}$ contains a detailed description of the dynamics of the universe.

References

Adair, R., and E. Fowler, 1963. *Strange Particles*. New York: John Wiley.

Bahcall, J., et al. 1980. *Phys. Rev. Lett.* **15** (11): 945–948.

Ballinger, J., et al. 1985. *Phys. Rev. Lett.* **54** (10): 1000–1003.

Bell, D., and J. Katz. 1985. *Mon. Not. R. Astron. Soc.* **213**: 21–25.

Bell, J. S. 1983. *Open Questions in Quantum Physics*.

Blin-Stoyle, R. and J. Freeman. 1970. *Nucl. Phys. A* **150**: 369–378.

Bohm, D. 1957. *Causality and Choice in Modern Physics*. New York: Van Nostrand.

Bohm, D. 1966. *Rev. Med. Phys.* **38**(3): 453.

Bridgman, P. W. 1961. *The Nature of Thermodynamics*. New York: Harper, 107–113.

Cabbibo, N. 1975. *In*: L. H. Ryder. *Elementary Particles and Symmetries*. London: Gordon and Breach, 148–153.

Canuto, V., and I. Goldman. 1982. *Nature* **296**: 709–712.

Chapra, K. P. 1961. *Rev. Mod. Phys.* **133** (2): 153–189.

Cook, A. H. 1969. *Gravity and the Earth*. London: Wykeham, 68.

Cronin, J. 1981. *Science* **212**: 1221–1228.

Davis, R., Jr. 1978. Brookhaven National Laboratory Report, No. 8NL50879 **1**: 1. Unpublished.

Drever, R. 1961. *Philos. Mag.* **6**: 683.

Fitch, V. 1981. *Rev. Mod. Phys.* **53**: 367–371.

Ford, K. 1968. *Basic Physics*. Waltham, Mass.: Ginn, 916–917.

Garland, G. D. 1965. *The Earth's Shape and Gravity*. Oxford: Pergamon, 37.

Harrison, B. K., et al. 1965. *Gravitational Theory and Gravitational Collapse*. Chicago: University of Chicago Press, 93.

Heilings, R. W., et al. 1983. *Phys. Rev. Lett.* **51** (18): 1609–1612.

Jastrow, R., and C. A. Pearse. 1957. *J. Geophys. Res.* **62**: 413–423.

Kaula, W. M. 1968. *Introduction to Planetary Physics of the Terrestrial Planets*. New York: John Wiley, 174–175.

Kaula, W. M. 1983. *Nature* **303**: 756 (June 30).

Knetchel, E. D., and W. D. Pitts. 1964. *AIAA J.* **2** (6): 1148–1151.

Kovalevsky, J. 1963. *Introduction to Celestial Mechanics*. New York: Springer, 101–102.

Kuchaeviacz, B. 1976. "Neutrinos from the Sun," *Rep. Prog. Phys.* **39**: 21–343 (April).

Lambeck, K., and S. M. Nakeboglu. 1983. *J. Geophys. Res. Lett.* **10** (9):857–860 (Sept.).

Landé, A. 1952. *Am. J. Phys.* **20**: 353 and *Phys. Rev.* **87**: 267.

McCrea, W. H. 1964. *Nature* **201**: 589.

Maddox, J. 1985. *Nature* **314**: 129 (March 14).

Peltier, W. R. 1983. *Nature* **304**: 434–436 (Aug. 4).

Penrose, R. 1982. *Proc. R. Soc. London Ser. A* **381**: 53–63.

Pound, R., and G. Rebka. 1960. *Phys. Rev. Lett.* **4**: 337–341.

Prestage, J., et al. 1985. *Phys. Rev. Lett.* **54** (22): 2387–2390.

Rubincam, D. P. 1980. *Geophys. Res. Lett.* **7** (6): 468–470 (June).

———. 1982. *Celest. Mech.* **26**: 361–382.

———. 1984. *J. Geophys. Res.* **89** (B2): 1077–1087 (Feb. 10).

Ryder, L. H. 1975. *Elementary Particles and Symmetries*. London: Gordon and Breach, 148–153.

Sciama, D. W. 1959. *Unity of the Universe*.

Smith, D. E. and P. J. Dunn. 1981. *Geophys. Res. Lett.* **7** Eq. (6): 437–440 (June).

Soldano, B. A. 1974. *Bull. Am. Phys. Soc.* **19** (5): 682 (May).

———. 1978. *Bull. Am. Phys. Soc.* **23** (9): 544 (April).

———. 1979. *In*: W. H. Brantley, ed., *Mass, Measurement and Motion: Report of the Spring 1979 Meeting of the SACS/AAPT*, 3.

———. 1982. Abstract on solar neutrinos. *Bull. Am. Phys. Soc.* **27** (4): 546 (April).

———. 1983. *Bull. Am. Phys. Soc.* **28** (9): 1138–1139 (November).

———. 1984. *Bull. Am. Phys. Soc.* **29** (4): 683 (April).

———. See also these references: Soldano *in*: G. Ottewell, *Astronomical Calendar 1979*, Greenville, S.C.: G. Ottewell, Dept. of Physics, Furman University. Soldano, *Mass, Measurement and Motion/Sequel 1: Nonequivalence and Quantum Electrodynamics, 1980; Sequel 2: A New Look at Maxwell's Equations and the Permittivity of Free Space*, 1982; and *Sequel 3*, in press. These are edited by W. H. Brantley and published in Greenville, S.C. by Grenridge Publishing. See also the following Soldano contributions to the *Bull. Am. Phys. Soc.*: **6** (1): 79, 1961; **19** (4): 440, 1974; **21** (2): 180, 1976; **21** (4): 621, 1977; **24** (2): 106, 1979; **28** (1): 31, 1983; **29** (9): 1495, 1984; **30** (3): 276, 1985.

Turneaure, J., et al. 1983. *Phys. Rev. D* **27** (8): 1705–1711 (April 15).

Vessot, R., et al. 1980. *Phys. Rev. Lett.* **25** (26): 2081–2084 (Dec. 29).

Weinberg, S. 1980. *Rev. Mod. Phys.* **52** (3): 515–523.

Will, C. 1981. *Theory and Experiment in Gravitational Physics*. Cambridge: Cambridge University Press, 31–66.

———. 1983. *Sky and Telescope* **66** (4): 294–299. (Oct. 1).

Wyatt, P. J. 1960. *J. Geophys. Res.* **65** (6): 1673–1678.

Yoder, C. F., et al. 1983. *Nature* **303**: 757–763 (June 30).

Zatsepin, G. 1982. *Neutrinos '82*, Supplement. Budapest, 53–68.

Note Added in Proof (Jan. 20, 1986)

Fischbach, et al.[1] have just claimed confirmation of the existence of a fifth force, hypercharge, based in part on a nonnull result obtained upon reanalysis of the Eötvös gravitational acceleration experiments. The postulate of a fifth force was presumably intended to isolate the implications of the nonnull result and therefore leave unaffected the theories of special and general relativity. Heretofore, however, the interpretation of the Eötvös results as null had constituted one of the proofs of a universal equivalence of inertial and gravitational mass for all forces. It will be shown that the work of Fischbach, et al. provides additional confirmation of our universal gravitational binding nonequivalence postulate, and that the much sought after[2] exponential contribution to gravity to which they call attention, Eq. (N1), is of a form which can readily accommodate our central premise of an antibinding gravitational nonequivalence within the format of Newton's universal law of gravitation.

Geophysical measurements of Newton's gravitational constant suggest G values consistently higher than those measured in the laboratory, G_0. The assumption that the discrepancy between these two sets of G values is real leads to an equation of the form

$$V(r) = -G_\infty \frac{m_1 m_2}{r}(1 + \alpha e^{-r/\lambda}) = V_N(r) + \Delta V(r) \qquad \text{(N1)}$$

$V_N(r)$ is the usual Newtonian expression for potential energy of two masses m_1 and m_2 separated by distance r. Fischbach concludes that the discrepancy between the G value at infinity (G_∞) and that found in the laboratory (G_0) in Eq. (N1) can be accounted for by a hypercharge-related, fifth force, which he suggests constitutes the basis for the nonnull Eötvös results. Fischbach, on the basis of his Eötvös reanalysis, agrees with Stacey and others[2] that the best fit for Eq. (N1) requires that the empirical constants α,λ have the following values: $\alpha = -(7.24 \pm 3.6)\times 10^{-3}$ and $\lambda = (200 \pm 50)m$. Further, he interprets the fact that the empirical constant α in Eq. (N1) is less than zero as evidence that the fifth force described by the second term is repulsive, with the exponential r dependence characteristic of a massive hypercharge field.[3] The quanta of this field are hyperphotons of mass m_γ given by $1/\lambda \cong 1\times 10^{-9}$eV, with their exchange being described by a potential of the form $\Delta V(r)$, Eq. (N1).

United Press International carried a report[4] on Fischbach's public assurances that his "own theory does not contradict Einstein, but that hypercharge will have to be accounted for when calculating the acceleration of objects to the center of the Earth." Such assurance that the equivalence principle, so key to general relativity, was not jeopardized by his findings is quite surprising in view of the fact that the crucial constant α in Eq. (N1) remains empirical, and possible deviations from the Eötvös null interpretation heretofore have been considered evidence for a nonequality between inertial and gravitational mass. Further, as we shall show, nonequivalence between inertial and gravitational binding mass would lead to an antibinding repulsion consistent with that attributed to Fischbach's hypercharge.

The suggestion that the equivalence principle has been spared by the Fischbach interpretation of Eq. (N1) is refuted by the following. First, if the Newtonian gravitational constant at infinite range is different from that found in the laboratory, then the factor α in Eq. (N1), which in part quantifies this difference, should represent a statement, characteristic of our terrestrial reference frame, that details how this change in G occurs. Some of the attempts to characterize changes in G have involved an examination of the role of time factors or time ratios. (We will use the latter in our analysis.) Of paramount importance, however, is the fact that any nonnull Eötvös effect strongly suggests that the principle that absolutely equates inertial and gravitational mass, the equivalence principle, must now be restricted. We have addressed in detail the consequences of a nonequality between inertial and gravitational mass restricted to the gravitational binding fraction of mass alone that pervades the entire structure of science.

Turning to the specific elements to be introduced in order to account for the empirical α and λ in Eq. (N1), we begin by making the following crucial point. General relativity, a theory uniquely linked to the equivalence of inertial and gravitational mass, permits no variation in the gravitational constant.[5] The fact that Fischbach is forced to use an equation that describes a change in the Newtonian gravitational constant, clearly underscores the fact that his "hypercharge force" is dealing with a nonequivalence phenomenon that is alien to general relativity. Further, it strongly suggests that the two empirical constants in Eq. (N1) must be related to nonequivalence.

It is not surprising therefore, to find that our terrestrial reference frame, nonequivalence expression for the fine structure constant in Eq. (47), with a value $= 7.29\times 10^{-3}$, that is,

$$\alpha = (1 \text{ rad})\dot{\eta}_{\oplus,\gamma}/(2\pi\,\dot{\xi}_{\oplus,e^-}),$$

not only is comparable in magnitude to the empirical constant α contained in Eq. (N1), but the antibinding

inherent in the $\dot{\eta}_{\oplus,\gamma}$ portion in Eq. (48) of our expression for the fine structure constant, that is,

$$f_{g\oplus}\,(m_i - m_G)/m_G$$

(where $m_i > m_G$ and $f_{g\oplus}$ is negative) ensures that our term will be negative as required. Of greater significance, however, is the fact that the term $\dot{\eta}_{\oplus,\gamma}$, which describes a photon interaction, represents a binding nonequivalence deviation from the Lorentz invariance inherent in the description of the Earth's aberration constant, 20."49 in (Eq. 48). Since the light aberration process involves the photon, any deviation from it could be related to the process of hyperphoton emission due to mass nonequivalence in gravitational binding. It should also be noted that the magnitude of the gravitational binding fraction $f_{g\oplus}$ in the term $\dot{\eta}_{\oplus,\gamma}$ in Eq. (48), which is required to describe the size of binding nonequivalence, is proportional to the number of nucleons or the hypercharge, see Eq. (1). So our explanation involves hypercharge, as does Fischbach's, but our position is that it is the nonequivalence in this nucleonic gravitational binding effect that gives rise to hyperphoton emission quantified by the term $\dot{\eta}_{\oplus,\gamma}$. Further support for identification of our expression for the fine structure constant in Eq. (47) with the empirical term α in Eq. (N1) arises from the fact that Eq. (47) also contains the term $\dot{\xi}_{\oplus,e^-}$, which represents the fractional difference between ephemeris and atomic time, see Eq. (46). This is pertinent when one is removing the empiricism in Eq. (N1), since this non-Newtonian expression describes the gravitational potential energy over the entire range of r values. The latter requires that atomic time factors at short range and ephemeris time factors at long range be properly combined over the entire range of r values. Furthermore, the entire basis of ephemeris time, namely, the Earth's orbital period about the Sun, is a component of the Earth-light aberration effect inherent in $\dot{\eta}_{\oplus,\gamma}$, Eq. (48).

The specific connection between Fischbach's hypercharge coupling f^2 and our gravitational binding nonequivalence is detailed by our substitution of the ratio $(1\ \text{rad})\dot{\eta}_{\oplus,\gamma}/(2\pi)\dot{\xi}_{\oplus,e^-}$ for α in the Fischbach relationship, Eq. (N2),

$$\frac{f^2}{G_o\, m_P^2} \simeq \frac{\alpha}{1 + \alpha} \tag{N2}$$

where m_P is the mass of a nucleon, yielding Eq. (N3).

$$\left[f^2 \left(\frac{1\text{AU}}{c_\gamma}\,\dot{\xi}_{\oplus,e^-}\right) 2\pi\ \omega_{\oplus,\ \text{orbit}}\ \frac{1 + \alpha}{\sqrt{1 - e_\oplus^2}}\right] + \left[G_o\, m_P^2\, f_{g\oplus} \left(\frac{m_i - m_G}{m_G}\right) \hat{u}_n \cdot \vec{\omega}_{\oplus,\ \text{spin}}\right] \cong 0 \tag{N3}$$

We note in Eq. (N3) a complete symmetry between the bracketed terms. For example, the product of $\dot{\xi}_{\oplus,e^-}$ and the minimum time required to send a signal to our local center of gravitational mass, the Sun, (1AU/c), and Fischbach's hypercharge coupling f^2, is analogous to $G_O m_P^2 f_{g\oplus}(m_i - m_G)/m_G$ in the other bracket of Eq. (N3). Further, both brackets involve either a spin or orbital angular velocity. Eq. (N3) clearly demonstrates that the hypercharge coupling f^2 originates in gravitational binding nonequivalence $f_{g\oplus}(m_i - m_G)/m_G$.

An additional argument for use of our terrestrial frame, nonequivalence, description of α, in both Eqq. (N1) and (N3), lies in the discrepancy noted between Fischbach's higher (by a factor of 16.4) estimate of the magnitude of the hypercharge $f^2 = (4.6 \pm 0.6) \times 10^{-42} e^2$ based solely upon the nonequivalence Eötvös data, and the value $(f^2 = (2.8 \pm 1.5) \times 10^{-43} e^2$ obtained using Eq. (N1). He attributes the discrepancy between the two estimates to hypercharge distribution effects. However, it should be noted that the time term $\dot{\xi}_{\oplus,e^-}$, which is a multiple of f^2 [see Eq. (N3)], is 21.8 times larger than the $\dot{\eta}_{\oplus,\gamma}$ term that contains the nonequivalence effect of our reference frame. Fischbach's graphical analysis of the Eötvös results, using the term $f^2/(G_O\, m_P^2\, a)$, with a an empirical numeric, could implicitly involve $[f^2 = (\dot{\xi}_{\oplus,e^-}/\dot{\eta}_{\oplus,\gamma} = f^2_{\text{Eötvös}}]$. This would have the effect of increasing the Eötvös hypercharge coupling estimates by a factor of 21.8, an increase comparable to the factor of 16.4 encountered by Fischbach.

On the basis of the preceding arguments, we propose to substitute our nonequivalence time relationship for the empirical α term into Eq. (N1), thereby leading to Eq. (N4). Eq. (N4) suggests that hyperphotons

$$V(r) = -G_\infty \frac{m_1\, m_2}{r}\left[1 + \left(\frac{1\ rad\ \ \dot{\eta}_{\oplus,\gamma}}{2\pi\ \dot{\xi}_{\oplus,e^-}}\right) e^{\frac{-r}{\lambda}}\right] \tag{N4}$$

where $\lambda = \sqrt{2L_\oplus \times R_{\oplus,barycenter}} = 203.34$ meters

generated by nonequivalence in gravitational binding, described by the term $\dot{\eta}_{\oplus,\gamma}$, mediate the gravitational process quantified by $\Delta V(r)$. Further it suggests that terms such as the angular spin of the Earth, $\omega_{\oplus,\text{spin}}$, and its orbital spin velocity, $\omega_{\oplus,\text{orbit}}$, that are inherent in $\dot{\eta}_{\oplus,\gamma}$ also are playing a role in this process. In addition, the aforementioned time term $\dot{\xi}_{\oplus,e^-}$ is also involved.

S. Weinberg[3] has shown that hyperphoton coupling is exponentially dependent on the range λ. Since the hyperphoton range λ arises from nonequivalence in gravitational binding inherent in $\dot{\eta}_{\oplus,\gamma}$ [Eq. (48)], its

value is simply the gravitational complementary field length for the three-body system (Sun, Earth, Moon) as referenced to the Earth, with the gravitational component, the Schwarzschild radius of the Earth $2L_{\oplus}$. The inertial component is given by the distance separating the Earth's center of mass from the barycenter of Earth-Moon, that is, $R_{\oplus,barycenter} = 0.7325\ R_{\oplus}$. This inertial length is required because the binding nonequivalence perturbs the terrestrial spin coupling to the lunar orbital motion. The resultant range $\lambda = 203.34$ meters [Eq. (N4)] accounts for 0.56 of the decrease in the Earth's angular spin rate 0.0015 sec/century (in press).

References

1. E. Fischbach, D. Sudarsky, A. Szafer, C. Talmaadge, S. Aronson, *Phys. Rev. Lett.* **56**(1): 3 (Jan. 6, 1986)
2. (a) D. R. Long, *Nature* **260**: 417 (1974); (b) D. R. Long, *Nuovo Cimento* **558**: 252, (1980); (c) G. W. Gibbons and B. F. Whiting. *Nature*. **291**: 636, (1981); (d) F. D. Stacey and G. J. Tuck. *Nature*. **292**: 230. (1981); (e) S. C. Holding, G. J. Tuck. *Nature*. **307**: 714, (1984).
3. S. Weinberg. *Phys. Rev. Lett.* **13**: 495 (Oct. 12, 1964).
4. United Press International release by Jan Ziegler, Jan. 13, 1986.
5. H. Bondi. *Cosmology*. Cambridge Monographs in Physics, p. 162, (1961).

The Importance of Eugenio Beltrami's Hydroelectrodynamics

by Giuseppe Filipponi

Milan, Italy

Editor's Note

As part of a continuing project of bringing the works of Bernhard Riemann and his collaborators directly before the scientific community, we are happy to present translations of two papers by Eugenio Beltrami that were key in the development of hydrodynamics. We have also translated a short portion of Beltrami's attack upon the electrodynamics of James Clerk Maxwell.

The first paper develops the work of Hermann Helmholtz [translated in IJFE (Helmholtz 1978)] into a generative treatment of vortices. As the note by Dan Wells in this issue (page 59) illustrates in connection with his own work, Beltrami's method has proven critical to the treatment of the development of vortices in plasmas, providing a crucial tool for studying what was otherwise dismissed as turbulence. In his introduction to the translations, Dr. Giuseppe Filipponi develops the connection between the discoveries of Beltrami and the Italian tradition of research in hydrodynamics begun by Leonardo da Vinci.

The role of Leonardo da Vinci as father of the Italian Renaissance and the political activity of Leibniz during the late 17th century clearly demonstrate that scientific advancements are historically born of the political activity required to build republican states committed to scientific, technological, and cultural advancements.

This is exactly the case of the great hydrodynamic school that was developed in Italy during the mid-19th century with the decisive contribution of Bernhard Riemann. Riemann came from Göttingen University to Italy to spend his last years in Pisa and Maggiore Lake. Enrico Betti, Eugenio Beltrami, Felice Groiti, Francesco Brioschi, Luigi Cremona, Masotti, and Carlo Matteucci were the principal representatives of this hydrodynamic school, and they had a decisive role in the political and military struggles that directly led to the formation of the modern Italian state in 1860.

In fact, during the period 1840-1860, as a result of the work of some of these scientists, the Annual Congress of Italian Scientists, which brought together scientists from throughout the Italian peninsula, became one of the centers of the patriotic conspiracy. The Congress was considered so dangerous that two orders were issued in 1850—one by the Austrian governor of Lombardo-Veneto and the other by the Vatican Curia—banning the future participation of scientists from those regions, which were then independent states.

This was also the period during which the Count of Cavour imposed a crash program for the industrialization of the Piedmont region, (then ruled by the King of Savoy) based on steel production and agricultural development. This crash effort provided the essential logistical means for sustaining the military offensives leading into the national unification of Italy.

In spite of World War I and the disastrous fascist regime, the Italian hydrodynamic school, centered in these educational institutions, survived until World War II in the form of the modern aerodynamic school, with Arturo Crocco and Antonio Ferri in Rome, Carlo Ferrari in Turin, and Enrico Pistolesi in Pisa. In 1935, this school founded the Aerodynamic Research Center in Guidonia, near Rome, where Ferri built the most advanced supersonic wind tunnel then found in the world.

This Italian school was intimately connected with the Prandtl-Busemann School in Germany. After 1945, Antonio Ferri and Adolf Busemann worked in close collaboration at Langley Air Force Base in Virginia.

The Hydroelectrodynamics of Eugenio Beltrami

These historical developments are most important for properly locating the work of Eugenio Beltrami, a student and then colleague of Betti and Riemann, and probably the most brilliant product of the Italian hydrodynamic school. As Betti explicitly reports, the Riemann contribution to the Italian hydrodynamic school was essential for breaking the intellectual chains represented by the mathematical-algebraic approach otherwise prevalent throughout Italian academies and universities.

Under these circumstances, the role of Riemann was essential in forcing Betti, Beltrami, and others to incorporate the method of synthetic geometry into the study of mathematical physics.

Ironically, in the official history of science, Betti and Beltrami are presented as the masters of elasticity theory. What is not reported, however, is that Betti and Beltrami in particular developed this theory for the purpose of demonstrating that the Maxwellian interpretation of electromagnetic phenomena as elastic tension was wrong.

In his paper "On the Mechanical Interpretation of Maxwell's Equations" (see page 51), Beltrami demonstrates that with the Maxwell hypothesis of an elastic ether, it is possible to explain the propagation of electromagnetic potential only in one special case: the potential must result from a geometrical configuration of distribution that can be contracted to a single point.

If the Maxwell hypothesis of an elastic ether has been demonstrated to be wrong, what alternative interpretation do Beltrami, Betti, and Riemann offer in order to explain electromagnetism? This interpretation is presented implicitly in Beltrami's first papers on hydrodynamics presented to the Academy of Science of the Bologna Institute between 1871 and 1874.

These papers, collected under the title "Research on Flow Configuration," describe electromagnetic phenomena as hydrodynamic phenomena. In them, Beltrami elaborated in a three-dimensional field the theory of the potential generated by fluid dynamic vortices and the analogy between the action of these vortices and the electromagnetic action of electrical currents (Figure 1).

This hypothesis was not originally Beltrami's. Riemann had developed the theory of complex functions uniquely to explain hydrodynamic and electrodynamic phenomena, as well as the transmission of heat on two-dimensional surfaces.

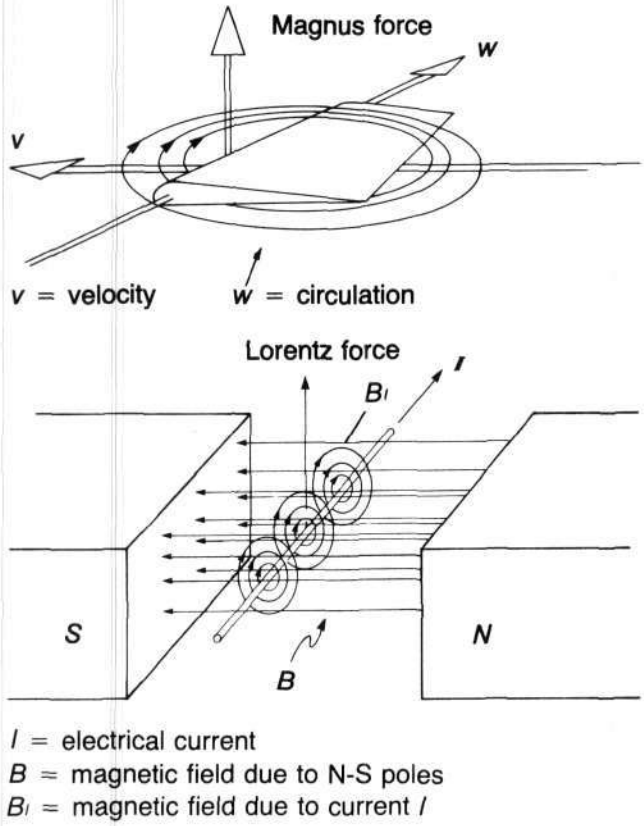

Figure 1. The analogy between the action of fluid dynamic vortices and the electromagnetic action of electrical currents, according to Beltrami.

In 1858, Helmholtz also published a paper on vortices, noting the analogy between the vortices and electromagnetic action. Helmhotz rested his theory on the principle of the Conservation of Energy combined with that of the Conservation of Vorticity. He failed to take into consideration any explanation of the generation of vortices and their evolution.

Beltrami, on the contrary, focused his research on the different possible configurations of fluid vortices in order to discover the principles of the behavior of hydrodynamic and electrodynamic systems. In other words, Beltrami studied hydrodynamic vortices in the same way that the first individuals who developed the techniques of flight found it necessary to study fluid motion both in air and water.

From this standpoint, it can be seen how Beltrami focused his studies on the actual electrodynamic and fluid configurations without concentrating on axiomatic presumptions, such as the conservation laws (as Helmholtz did), and with a particular emphasis on the pathologically unique, extreme cases.

In his 1889 paper, "Hydrodynamic Considerations," Beltrami presented the hydrodynamic configuration that today bears his name, the Beltrami vortex, in which both the flux and vortex lines are always parallel or antiparallel; that is, when extended to the electrodynamic case, a configuration in which the electric current and magnetic field lines are also always parallel (or antiparallel). In this case, it is found that the "Lorentz" force is zero, and the electric currents do not have to do any work against the magnetic field.

As Beltrami demonstrated, this "force free" configuration is not just some theoretical speculation, but really exists, and precisely describes geometrical configurations that he termed "helicoidal."

The morphology of Beltrami vortices may be seen today in the magnetic geometry of the plasma spheromak configuration and field-reversed pinch. Dr. Winston Bostick of Stevens Institute of Technology in New Jersey discovered the formation of pairs of these force-free filaments in magnetic plasma and plasma pinches as early as 1966 (Figure 2).

Nature then, given the opportunity, demonstrates a pronounced tendency to organize itself according to configurations that correspond to force-free, least-action systems. Research focused on such systems under these conditions can give us the key to comprehending more general physical phenomena, such as the electron, proton, neutron, and so on, if we consider them, not simply as elementary particles, but rather as complex hydrodynamic and electrodynamic systems. The same can also be said for such phenomena as superconductivity and superfluidity in which

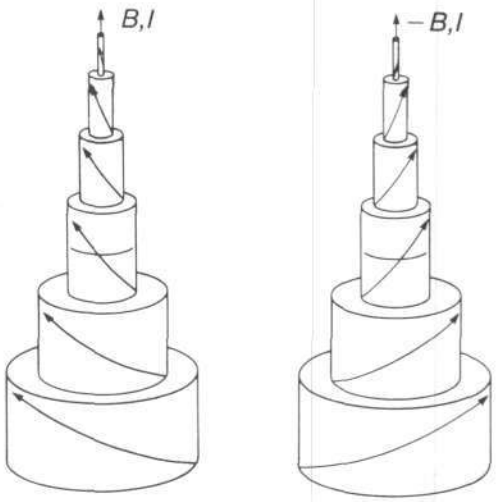

Figure 2. The formation of a pair force-free filaments in magnetic plasma and plasma pinches, according to Dr. Winston Bostick.

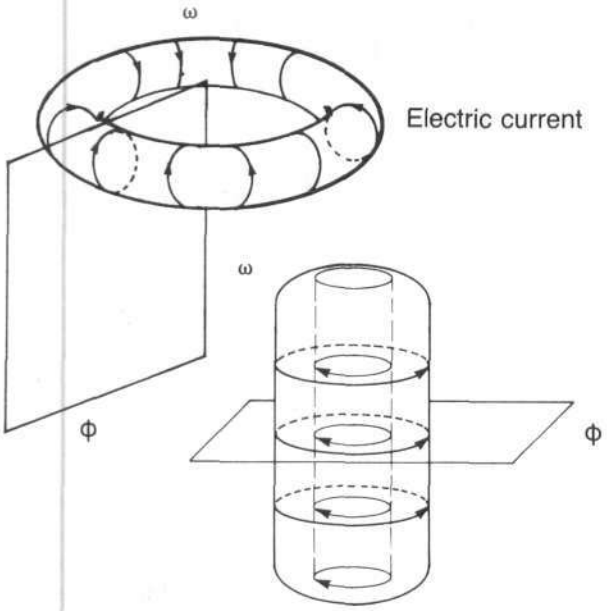

Figure 3. Beltrami's neutral solenoid configuration.

frictional forces tend toward zero and the efficiency of action is maximal. The Beltrami studies, even if they do not give us a comprehensive theory of hydrodynamic and electrodynamic phenomena, always followed this approach.

In fact, however, in 1871, in one of Beltrami's first papers, "The Mathematical Theory of Electrodynamic Solenoids," he demonstrated: "Given a surface (ω) shaped as a tube which goes inside itself (torus), which is triply connected, of all the electric currents that can circulate on it, those that exercise the minimum electromagnetic potential on themselves are those that circulate on planes (φ) that are always perpendicular to the (ω) surface (Figure 3).

It is not a coincidence that these configurations are the same configurations found today in leading magnetic fusion experiments like the tokamak, stellarator, and compact tori, which are used to contain the hot fusion plasma.

Beltrami called these configurations neutral solenoids, because the magnetic action is confined inside the surface of solenoids, and outside is zero. The research concerning neutral solenoids is part of Beltrami's work directed toward finding all possible analogies between electrostatic and electrodynamic actions. In the case of neutral solenoids, the analogy is with that of the distribution of electric charges on the surface of a conductor, because the electric action exists only outside the conductor and is zero inside.

The analogies between electrostatic and electrody-

namic phenomena bring us directly to the problem mentioned earlier, that of the possible explanation of the so-called elementary particles as force-free, least-action electrodynamic systems.

The first significant attempt in this direction was carried out by Winston H. Bostick (1985), who describes the electron as a Beltrami electric vortex whose mass is formed by the self-contained electromagnetic energy.

Following the Bostick example, we should be able to develop a model of the neutron according to these conceptions. The idea of developing an electrodynamic model of the neutron is not original. In fact, immediately after the neutron was discovered in 1932, several indirect scattering experiments were done in order to describe the neutron shape. Although the entire science community thought of describing the neutron by the usual Rutherford model—the positive charge in the middle and the negative charge surrounding—the experiments nevertheless showed that there was no "hard" positive charge inside, and that the interior of the neutron was an empty space. Therefore several attempts were made at that time to develop an electrodynamic model of the neutron (Hughes 1959), attempts that were abandoned as the esoteric statistical approach and the quark theory became dominant.

These models were more or less based on the flow of two antiparallel electric currents, one of positive and the other one of negative charges, around a toroidal configuration (Beltrami's tube which goes inside itself). In this electrodynamic configuration, the electrical and magnetic fields are always zero outside the toroidal shape with the exception of the "tube" axis where the magnetic momentum of the two electrical currents are parallel. The neutron does in fact have a magnetic momentum, even if it does not have an electrical charge (Figure 4).

Arturo Crocco, a pioneer of the Italian flight technique, once said that modern aerodynamics had pulled

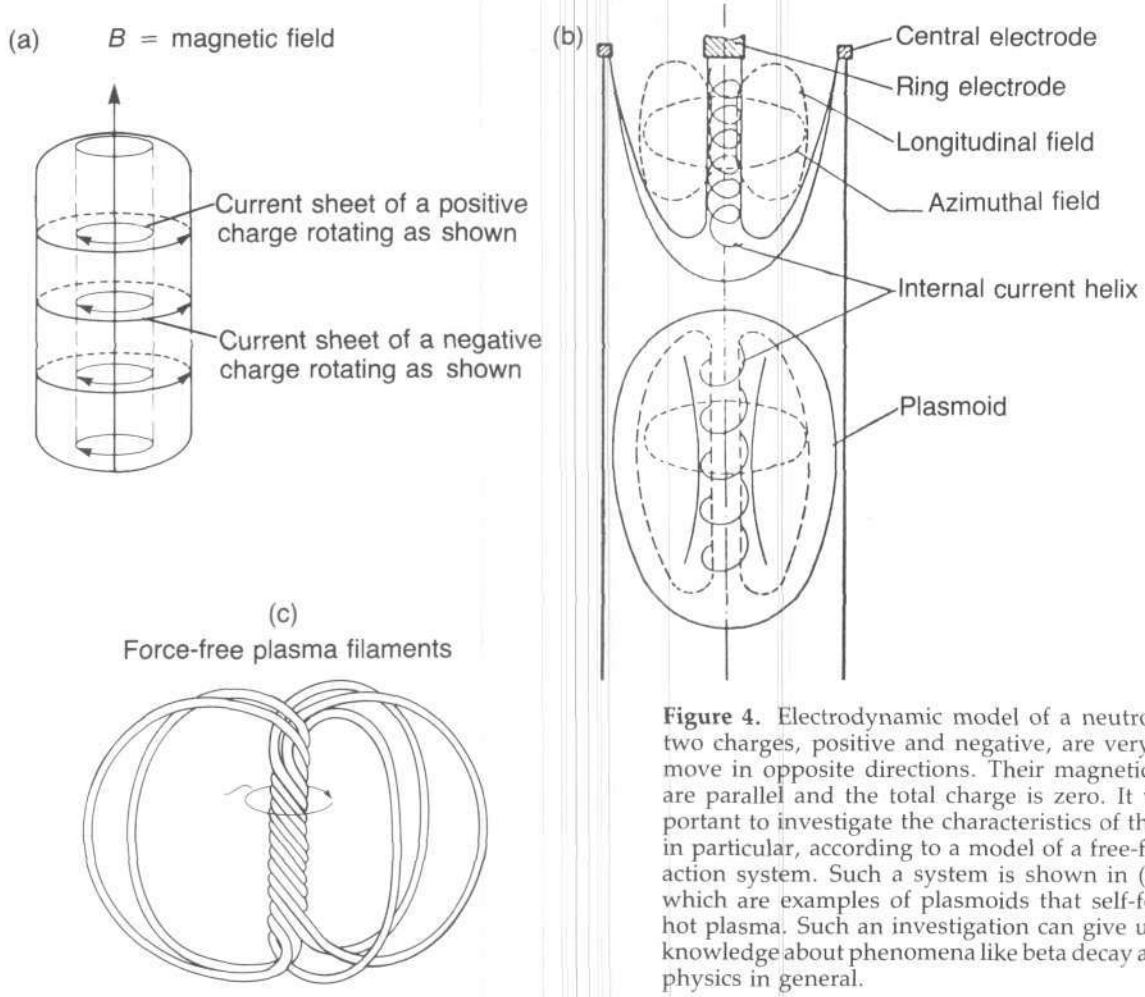

Figure 4. Electrodynamic model of a neutron (a). The two charges, positive and negative, are very close and move in opposite directions. Their magnetic momenta are parallel and the total charge is zero. It will be important to investigate the characteristics of the neutron, in particular, according to a model of a free-force, least-action system. Such a system is shown in (b) and (c), which are examples of plasmoids that self-form in the hot plasma. Such an investigation can give us a deeper knowledge about phenomena like beta decay and nuclear physics in general.

the vortices of Helmholtz down from Olympus and humanized them. The vortices that Helmholtz described as gods were never born and never die. We can say that plasma physics, so-called particle physics, and other sectors of science can also be brought down from Olympus if we take the same approach to understanding physical phenomena first introduced by Leonardo and refined by the school of Riemann.

References

Bostick, Winston H. 1985. "The Morphology of the Electron." *IJFE* **3**(1): 9. (Jan.).

Helmholtz, Hermann. 1978. "On Integrals of the Hydrodynamic Equations That Correspond to Vortex Motions (1858)." Trans. Uwe Parpart. *IJFE* **1**(3-4): 41.

Hughes, Donald J. 1959. *The Neutron Story*. New York, Doubleday, Science Study Series.

Notes on the Mathematical Theory Of Electrodynamic Solenoids

by Eugenio Beltrami

This paper was translated from the Italian by Dr. Giuseppe Filipponi. It was originally published in 1871-72 in Il Nuovo Cimento, *Series II, Vol. VII-VIII pp. 285-301. It also appears as paper No. 34 in Beltrami's collected works* Opere Matematiche *published in Milan in 1904 by Ulrico Hoepli.*

The solenoids considered in this note are continuous systems of currents in which the law of distribution is much more general than is ordinarily admitted.

I assume that they are formed in the following way:

Take a closed space, S, which is bounded in every direction by a closed surface, ω. If a function ϕ $(x, y, z,)$ which has the coordinates of the points of S is assumed, the only condition on this function is, that in this space it is single-valued, finite, and continuous, and so are its partial derivatives. The surfaces represented by the equation ϕ = constant, which I will indicate with the symbol (ϕ), are all distinct from each other, and the lines, in which they intersect the surface ω, are also distinct from each other and closed. These lines divide the surface, ω, into an infinity of elementary strips, each of which corresponds to the infinitesimal increment $d\phi$ of the function ϕ. Then the current is made to circulate in each of these strips in a determinate sense. The intensity of the current is κ $d\phi$, where κ is a constant and $d\phi$ is the increment of the function ϕ passing from one strip to the other. All of these currents form the general solenoids that I wish to study at this time.

It will be useful at this point to review some general information about this system. First, note that the way in which the system is formed does not exclude that the geometrical locus of the effective currents can be an open surface rather than one which is closed. In fact, if we make one part of the ω surface coincide with a portion of one of the (ϕ) surfaces, the boundary line of this common portion becomes a terminal current of the solenoid because the intensity of the currents is zero, which in the general case would circulate on the common portion.

Second, if we suppose the κ factor to be constant, we do not thereby restrict the law by which the intensity varies. In fact, if we want to make κ change

Editor's Note

Δ_1 and Δ_2 are differential operators of the first and second degree or kind. These are defined in a paper entitled *Richerche di analizi applicate alla Geometrie* in his *Collected Works*, Vol. 1, page 143. Beltrami's differential operators may be expressed in terms of Einstein's notation as follows:

$$\Delta_1 f = g^{ij} f_{,i} f_{,} = g^{ij} (\partial f / \partial x^i) (\partial f / \partial x^j) \qquad (1)$$

This is the Beltrami operator of the first kind that assigns to each scalar field f the length of the gradient of f, grad f, or ∇f.

$$\Delta_2 f = -g^{ij} f_{,ij} \partial^2 / (\partial x^i \partial x^j) - g^{ij} \Gamma^s_{ij} \partial / \partial x^s \qquad (2)$$

This operator is of the second kind and is identical with $-\Delta$ where Δ denotes the Laplacian:

$$\nabla^2 f = \text{div grad } f = \nabla \cdot \nabla f =$$
$$1/\sqrt{g}\ \partial [\sqrt{g}\ g^{ij} (\partial f / \partial x^j)] / \partial x^i$$

from one strip to the other, for example, if $\kappa = F(\phi)$, it will be sufficient to substitute for ϕ a function $\Psi = \int F(\phi) d\phi$. In such a case, there would be a new system substantially equivalent to the first, in which the intensity of each of the elementary currents will be expressed $d\Psi$. In order to simplify, I will suppose that $\kappa = 1$, since multiplying the final result by κ if it reenters the first hypothesis.

Furthermore, I can say that the necessity for the condition that requires the derivative of the function ϕ to be single-valued does not imply that the function must necessarily be single-valued as well. It is useful to be able to take a function that is not single-valued (this means that it has periodic form) in order to apply this method of the solenoids to more general cases; but, in this case, I will consider the ϕ functions as single-valued in order to simplify the research on the potential function of the solenoids, which is almost intuitive, and at the end of the note, I shall give a second demonstration of the formula derived, from which it will be very easy to study the value of functions which are not single-valued.

For greater clarity, I shall consider the hypothesis that the successive lines of intersection of the ω surfaces (ϕ) correspond to the values of the preceding ϕ parameter, from a minimum value ϕ_1 to a maximum value ϕ_2. In fact, if the ω surface is not consistent with this hypothesis, we can change it by substituting closed surfaces that do satisfy these conditions, and in this way we can add some diaphragms that have circulating currents, or portions of currents of equal intensity on each of their two faces, that move in opposite directions.

I denote, with n, the direction of the inwardly facing normal to an element of the surface $d\omega$, and with r, the distance of this element, which has x, y, z as coordinates, from a point m_1, which has as coordinates x_1, y_1, and z_1, on which we suppose the electromagnetic action of the solenoids to act. I consider that this last point is at a finite distance from the ω surface, from the internal to the external part.

Now consider one of the elementary strips in which the ω surface is divided, and let ϕ, and ϕ plus $d\phi$ be the values of the parameter corresponding to the two lines that have this strip between them. I will suppose the increment $d\phi$, to be positive, of the pair of all the analogous increments; it is not necessary that the rest of these increments be equal. Let ω' be the portion of ω that is the locus of all the lines (ϕ) in which the parameters are between the intermediate value ϕ and the maximum value ϕ_2. This portion of the surface is totally determined by the closed line of the ϕ parameter; therefore, because of Ampere's fundamental theorem on the electromagnetic action of closed currents, the potential on a point m_1, of the current with intensity $d\phi$, which circulates around the surface ω', can be expressed by the integral

$$d\varphi \int \frac{d\frac{1}{r}}{dn'} d\omega',$$

extended to all the surfaces ω'. Now the potential Φ of the entire solenoid is evidently the sum of all the expressions like this, relative to the successive increments of ϕ, from ϕ_1 to ϕ_2. Summing these, and collecting all the factors that are to be multiplied, for each element $d\omega$ of the total surface, we have

$$\Phi = \int \left(\frac{d\frac{1}{r}}{dn} \sum d\varphi \right) d\omega.$$

Then it is clear that

$$\Sigma d\phi = \phi - \phi_1,$$

where ϕ is the value of the parameter on the element $d\omega$: then

$$\Phi = \int \varphi \frac{d\frac{1}{r}}{dn} d\omega - \varphi_1 \int \frac{d\frac{1}{r}}{dn} d\omega,$$

that means, according to a well-known theorem

$$\Phi = \int \varphi \frac{d\frac{1}{r}}{dn} d\omega - 4\pi\epsilon\varphi_1,$$

where ε is 1 or 0, according to whether the point m_1 is internal or external to the space S.

The function Φ so determined is continuous in all the space. But it is much more useful to replace this function (which I will continue to denote with the same symbol)

$$\Phi = \int \varphi \frac{d\frac{1}{r}}{dn} d\omega, \qquad (1)$$

which has the same derivatives of the preceding, even if it is discontinuous in all the points of the ω surface. This last circumstance is not influential, because, as I said, the point m_1, need never cross this surface.

We remember now Green's equation

$$\int \left(\varphi \frac{d\frac{1}{r}}{dn} - \frac{1}{r} \frac{d\varphi}{dn} \right) d\omega = \int \frac{\Delta^2 \varphi}{r} dS + 4\pi\epsilon\varphi(x_1, y_1, z_1),$$

where ε has the same meaning as before, and where we pose

$$\Delta^2\varphi = \frac{\partial^2\varphi}{\partial x^2} + \frac{\partial^2\varphi}{\partial y^2} + \frac{\partial^2\varphi}{\partial z^2}.$$

If for brevity these notations are used

$$P = \int \frac{\Delta^2\varphi}{r} dS, \quad \Pi = \int \frac{d\varphi}{dn} \frac{d\omega}{r},$$

we will have

$$\Phi = P + \Pi + 4\pi\varepsilon\phi_1, \tag{2}$$

where ϕ_1 represents the value of the function ϕ at the point m_1.

The two functions P and Π are two Newtonian potentials, one of space, the other of a surface that corresponds to the well-known distribution of matter in the space S and on the surface ω, distributions that I shall call p and π. The total masses of these two distributions are equal in their absolute value, but contrary in sign, because of the equation

$$\int \Delta^2\varphi \cdot dS + \int \frac{d\varphi}{dn} \cdot d\omega = 0.$$

Of the two expressions (1) and (2) of the potential Φ, the second is, in the greater number of cases, far more useful than the first one. Therefore we will not speak about the significance of equation (1), but only about the results contained in equation (2):

The electromagnetic action of the general solenoid Σ, is equal to the resultant Newtonian action at each point external to S, that is, due to the distribution p and π; and, in each internal point, the resultant action is not only due to the distribution of these two actions and to a third, whose potential is $4\pi\phi$.

This theorem is true without modification also in the case in which ϕ is a multivalued function with a single-valued differential function, provided that the branching lines are external to space S. This results immediately from the demonstration that I will give of equation (1), since all that I am about to say refers to the multi-valued functions, it is understood with the restriction or so-called branch lines. Furthermore, because it is possible to satisfy the conditions of the (LaPlacian equation) $\Delta^2\phi = 0$, in the majority of the cases, and, because it is really true in each case which we know today of the general theorem that we enunciated previously, I shall suppose that the condition be true. That means that we suppose that the distribution p be 0, then $P = 0$, then we must consider finally the distribution π, with the surface potential Π relative to π.

The simplest way to satisfy the equation $\Delta^2\phi = 0$ is to take as ϕ a linear function of the coordinates x,y,z. In this case, the solenoid Σ is formed by currents placed in parallel planes, and with the intensity constant, if the distance between planes is constant. With these hypotheses, the previous theorem reproduces what is called the Riecke theorem.[1] The observation that the author Riecke made, about the possibility of substituting the surface distribution π, which has a variable density, a certain space distribution, with constant density is nothing but a corollary of another general property about which I recommend that the reader refer to my monograph "Research on Fluid Kinematics"[2] because this theorem is related to the motion of a fluid.

Second, suppose that the surface ω be formed by a tubular portion, where the axis is orthogonal to the surface (ϕ) [at each point], and where it is closed at its two ends by the intersection of two surfaces. In this case, the distribution π exists only on the two terminal portions of the tube because on all the tubular part we have $d\phi/dn = 0$. The electric currents circulate only around the tubular portion, and the theorem describing the action of these currents is the same as the theorem of Lipschitz.[3]

These two theorems, by Riecke and Lipschitz, have a particular case in common in which they agree. It is when ϕ is a linear function and ω is a cylindrical surface whose axis is perpendicular to the planes ϕ = constant, and whose ends are closed by terminal sections that coincide with two of these planes. The theorem about this cylindrical solenoid with an arbitrary axis was already given a long time ago by F. Neumann[4] and was recently discussed with great accuracy by Emilio Weyr.[5]

A case that is in some ways reciprocal to Neumann and Weyr is as follows: If ϕ is a cylindrical potential, ϕ_1 and ϕ_2 the parameters of two equipotential surfaces outside of the acting mass, and ϕ_1 is internal to ϕ_2; and lastly, let ρ' and ρ'' be the portions that are cut by these surfaces. Applying the general theorem to the surface ω that is formed by the two plane bases ρ' and ρ'' of the cylindrical portions ϕ_1 and ϕ_2, it is clear that the distribution π exists in this case only on

the latter two, and the electrical current circulates around the two former; and therefore the actions of these are equivalent for external points; however, they differ at internal points, because of the action of the potential ϕ. Suppose, for example, that $\phi = \log r$, where r is the distance between the point (x, y, z) and a given straight line, which means that the cylindrical potential must be the same as that of an infinite straight line; and let the radii of the two cylindrical surfaces ϕ_1 and ϕ_2 be a_1 and a_2. Because a_1 is less than a_2 we have

$$\frac{d\varphi}{dn} = \frac{1}{a_1} \qquad \text{on the surface } \varphi_1,$$

$$\frac{d\varphi}{dn} = -\frac{1}{a_2} \qquad \text{on the surface } \varphi_2,$$

and the potential of the electrical currents that circulate around the two rings, ρ' and ρ'', are given by

$$\Pi = \frac{1}{a_1}\int \frac{d\omega_1}{r_1} - \frac{1}{a_2}\int \frac{d\omega_2}{r_2} + 4\pi\epsilon \log r,$$

where the indices 1,2 are used to distinguish between the relative quantities of the two cylindrical portions ϕ_1 and ϕ_2. The two integrals found in this formula are evidently the Newtonian potentials for two strata, having the density of 1, that are deposited on the two cylindrical surfaces. The electric current circulates around the two rings ρ' and ρ'', which are concentric circles at the two boundaries, with an intensity inversely proportional to the respective radii, supposing that the width of the strip be constant. If we put one of these base planes, for example, ρ'', at infinity, we are left with only ρ', having two electric currents, and preceding formula reproduces the results of Emilio Weyr, arrived at in a different way, published in Volume 13, in *Schlomilch's Journal* (1868) p. 437. The general theorem explains, at the same time, the difference that occurs in the electromagnetic action, between the case where the point at which the electromagnetic action is acting is projected inside the rings and that in which it falls outside.

I will suppose now that the surface ω be orthogonal at each point to (ϕ), which cuts the surface. Generally speaking, that means that ϕ must be a multivalued potential function, and that, in this case, the form of the surface ω is like that of a tube which goes inside of itself. With this hypothesis we have $P = 0$, and $\Pi = 0$, and we have

$$\Phi = 4\pi\varepsilon\phi,$$

which means that: the external action of the solenoid built in such a way is 0, while the internal action is given by the product of 4π and the actions of the external currents that produce the potential ϕ. I regard the first of these two properties that it is already a condition of the other; it can be demonstrated that it is a kind of configuration called a neutral solenoid.

The neutral solenoids have many characteristics in common with electrical strata in equilibrium over the surface of a conductor. In order to show this case better, we will use Green's formula, and we will write this in the following way:

$$\frac{1}{4\pi}\int\left(\varphi\frac{d\frac{1}{r}}{dn} - \frac{1}{r}\frac{d\varphi}{dn}\right)d\omega = \frac{1}{4\pi}\int\frac{\Delta^2\varphi}{r}\,dS + \epsilon\varphi_1.$$

Then we will observe that:

First, if ϕ be the magnetic potential of a system of masses and if ω is an equipotential closed surface that contains within itself all of the masses, we have over this surface the potential ϕ = constant = ϕ_0, and then

$$\frac{1}{4\pi}\int\frac{d\varphi}{dn}\frac{d\omega}{r} = (1-\epsilon)\varphi_1 + \epsilon\varphi_0.$$

This formula contains all of the theory of the so-called level strata which, as is well known and as is derived from the previous equation, can be substituted for the masses at all external points ($\varepsilon = 0$); and for the internal points the action is zero where ($\varepsilon = 1$).

Second, if ϕ is the electromagnetic potential of a system of electric currents and ω is a closed surface orthogonal to the equipotential surfaces, which do not contain any currents inside of themselves, we have over these surfaces $d\phi/dn = 0$ and then

$$\frac{1}{4\pi}\int\varphi\frac{d\frac{1}{r}}{dn}\,d\omega = \epsilon\varphi_1.$$

This formula contains all of the theory of the so-called neutral solenoids which, as we have said before, and as we saw from the preceding equation, can be substituted for the electrical currents at all of the internal points ($\varepsilon = 1$), and the action is 0 for all of the external points ($\varepsilon = 0$).

The comparison between these two statements in which I have underlined the words and phrases that constitute the difference, illustrates the duality which exists for many problems, between electrostatics and electrodynamics, and shows reciprocity, to which I alluded before, because it is well known that the electricity in equilibrium over the surface of a conductor distributes itself in such a way as to form a level strata.[6]

Boltzmann has already spoken about this analogy.[7] He demonstrated that the potential that a neutral solenoid exerts upon itself is a minimum of all the configuration of systems of the currents which can circulate around the given surface ω subordinated to certain other conditions which it is not necessary to specify. From this, the result follows that in neutral solenoids the electrical currents are themselves kept in equilibrium, and this is the same as occurs in the distribution of static electricity upon the surface of a conductor. This minimal property is intimately connected with the so-called Dirichlet Principle because, in virtue of a formula that was demonstrated at the conclusion of the § 17 of the cited monograph (in which I extended Helmholtz's theorem in his paper on vortices), the potential of the neutral solenoid upon itself is equal to the product of 2π and the integral

$$\int \left[\left(\frac{\partial \varphi}{\partial x}\right)^2 + \left(\frac{\partial \varphi}{\partial y}\right)^2 + \left(\frac{\partial \varphi}{\partial z}\right)^2 \right] dS$$

extended on all of the space S inside the solenoid.

A singular circumstance is that the general theorem demonstrated previously, which we can apply in a simple way for many problems, cannot be simply applied to the most simple solenoids, which are known as Ampère solenoids.[8] In such cases, the potential function of these solenoids, which are formed by elementary currents, both equal and equidistant, and which are perpendicular to the axis, can be immediately calculated from the potential of a single current, by integrating along the axis. It can be shown, however, that the method of calculating their potential is a special case of the calculation for the general solenoid Σ.

The function ϕ in such cases is not explicitly dependent upon x, y, z, but depends upon the equation $F(x, y, z, \phi) = 0$. In such a case, if we represent with Δ the sum of the squares of the first derivative with respect to x, y, and z we have

$$\Delta\varphi = \frac{\Delta F}{F'^2}, \quad \Delta^2\varphi = \frac{1}{F'}\left[\left(\frac{\Delta F}{F'}\right)' - \Delta^2 F\right],$$

where the prime indicates the partial derivative with respect to ϕ in F, and then also in ΔF. If we take as F a function which has the following forms

$$F = (x - \xi)\frac{d\xi}{d\varphi} + (y - \eta)\frac{d\eta}{d\varphi} + (z - \zeta)\frac{d\zeta}{d\varphi},$$

where ξ, η, ζ are the coordinates and ϕ is the arc of any line L, so that the surfaces (ϕ) are in this case planes normal to this line. In this hypothesis, we found that $\Delta F = 1$, and $\Delta^2 F = 0$ and then

$$\Delta\varphi = \frac{1}{F'^2}, \quad \Delta^2\varphi = -\frac{F''}{F'^3},$$

$$F' = (x - \xi)\xi'' + (y - \eta)\eta'' + (z - \zeta)\zeta'' - 1,$$

$$F'' = (x - \xi)\xi''' + (y - \eta)\eta''' + (z - \zeta)\zeta'''.$$

The x, y, z that are found in these equations by virtue of the equation $F = 0$, the coordinates of a point m existing in the plane normal to the line L at point μ, which has coordinates ξ, η, ζ and with parameter ϕ. In order to fix the position of m in such a plane, I imagine two orthogonal lines lying on the plane, determined by each point μ, well-defined for each value of ϕ, the normal principal and the perpendicular to the osculating plane I call u, v the coordinates of the point m with respect to these two axes. In such a way, the position of any point in space is determined by three values of the quantity ϕ, u, v, which three numbers are totally separate if the point remains in the region around the line L. Because of these conventions, and also because of the theorems that we know from differential geometry, calling γ and δ the curvature of the first and second species of the line L and at point ϕ, we have

$$F' = \gamma u - 1, \; F'' = \gamma' u - \gamma\delta v,$$

and from this we get $u = 0$, $v = 0$, if $\Delta\phi = 1$, and $\Delta^2\phi = 0$. This result can be formulated in the following manner: considering the arc ϕ as a function of the coordinates x, y, z of a point on a plane normal to a line L, at the variable extremity of the arc itself, the equations $\Delta\phi = 1$ and $\Delta^2\phi = 0$ are satisfied for the coordinates x, y, z, at all points on the line L.

In consequence of this property, the expressions $\Delta\phi - 1$, and $\Delta^2\phi$ are infinitely small in each point which is infinitely close to the line L, and are the same order of distance of this point from the line. Therefore if this line is the direction of an Ampère solenoid, in formula (2) we can pose

$$\Delta\phi, = 1, \; \Delta^2\phi = 0,$$

and thus,

$$P = 0$$

because, since derivative $d\phi/dn = 0$, on all the tubular surfaces, we have only an error of the third order, and the remaining quantities are of the second order. These quantities are the value of Π, which depend upon the two boundary sections, and because we have $d\phi/dn = \pm\sqrt{\Delta\phi} = \pm 1$ (the sign + is relative to the origin of the arc, and the sign − to the end), it is clear

that the previous formula precisely reproduces the result which we know.

What remains now is the analytical demonstration of the equation (1), and we will first define the following lemma. Because of the condition of being single-valued which we ascribed to the function ϕ, we have, the transformations

$$\int \frac{\partial^2 \varphi}{\partial y \partial z}\, dS = -\int \frac{\partial \varphi}{\partial y}\frac{dz}{dn}\, d\omega = -\int \frac{\partial \varphi}{\partial z}\frac{dy}{dn}\, d\omega ,$$

then the relation follows

$$\int \left(\frac{\partial \varphi}{\partial y}\frac{dz}{dn} - \frac{\partial \varphi}{\partial z}\frac{dy}{dn}\right) d\omega = 0.$$

I will demonstrate that this is true also in the case of substituting the function ϕ/r for the functions ϕ. That is very clear when the point m_1 is external to the space S. But when m_1 is inside, the function ϕ/r becomes infinite in m_1, and we cannot use the previous transformation. I will suppose then, for a moment, that the surface ω be a spherical surface ω_1, whose center is m_1, with a finite radius r; then I shall rewrite the previous equation, substituting the product of $r(\phi/r)$ for ϕ. We have then, taking the derivative of the product

$$r\int \left(\frac{\partial \frac{\varphi}{r}}{\partial y}\frac{dz}{dn} - \frac{\partial \frac{\varphi}{r}}{\partial z}\frac{dy}{dn}\right) d\omega_1 +$$

$$\frac{1}{r}\int \varphi \left(\frac{\partial r}{\partial y}\frac{dz}{dn} - \frac{\partial r}{\partial z}\frac{dy}{dn}\right) d\omega = 0.$$

Now the element of the second integral is always 0 because of the hypothesis that we have

$$\frac{\partial r}{\partial x} = -\frac{dx}{dn}, \quad \frac{\partial r}{\partial y} = -\frac{dy}{dn}, \quad \frac{\partial r}{\partial z} = -\frac{dz}{dn},$$

then, in order to have $r > 0$, we have

$$\int \left(\frac{\partial \frac{\varphi}{r}}{\partial y}\frac{dz}{dn} - \frac{\partial \frac{\varphi}{r}}{\partial z}\frac{dy}{dn}\right) d\omega_1 = 0,$$

We have this equation that has the same form as the previous one, but refers to a spherical surface ω_1, with a finite radius with its center in m_1, where the function ϕ/r becomes infinite. We can see now if ω is any closed surface from which the point ω_1 is a finite distance, we can always inscribe a spherical surface ω which will not extend beyond the space S which is bounded by the surface ω. In the space between the two surfaces, the function ϕ/r satisfies the condition true for ϕ; then the integral

$$\int \left(\frac{\partial \frac{\varphi}{r}}{\partial y}\frac{dz}{dn} - \frac{\partial \frac{\varphi}{r}}{\partial z}\frac{dy}{dn}\right) d\omega$$

has the same value for the closed surface ω and thus for point m, at a finite distance from all of its points. (It would be equally provable that such an equation could exist, substituting for r a function of r, so that $r = 0$).

$$\int \left(\frac{\partial \frac{\varphi}{r}}{\partial y}\frac{dz}{dn} - \frac{\partial \frac{\varphi}{r}}{\partial z}\frac{dy}{dn}\right) d\omega = 0 \qquad (3)$$

Returning now to the argument, I shall indicate with s, the arc of any of the lines (ϕ), and I shall determine the direction in the following manner: from a point (x, y, z) from this line (ϕ) I will produce two radii, one in the direction of the normal internal to ω, and the other in the direction of the minimal distance $d\sigma$ of the same point on the contiguous line ($\phi + d\phi$) which we take from the part where $d\phi$ is positive. Then I assume as the direction of the arcs s that is growing, that is, of the positive ds, the direction that is like the positive z axis, placed with respect to the positive x and y axis. In this hypothesis, through very easy geometrical steps we have

$$\begin{aligned}
\frac{\partial \varphi}{\partial y}\frac{dz}{dn} - \frac{\partial \varphi}{\partial z}\frac{dy}{dn} &= -\frac{dx}{ds}\frac{d\varphi}{d\sigma}, \\
\frac{\partial \varphi}{\partial z}\frac{dx}{dn} - \frac{\partial \varphi}{\partial x}\frac{dz}{dn} &= -\frac{dy}{ds}\frac{d\varphi}{d\sigma}, \\
\frac{\partial \varphi}{\partial x}\frac{dy}{dn} - \frac{\partial \varphi}{\partial y}\frac{dx}{dn} &= -\frac{dz}{ds}\frac{d\varphi}{d\sigma}.
\end{aligned} \qquad (4)$$

Now it is well known that the components of magnetic action of a system of currents are given by

$$\begin{aligned}
\frac{\partial \Phi}{\partial x_1} &= \frac{\partial Z}{\partial y_1} - \frac{\partial Y}{\partial z_1}, \\
\frac{\partial \Phi}{\partial y_1} &= \frac{\partial X}{\partial z_1} - \frac{\partial Z}{\partial x_1}, \\
\frac{\partial \Phi}{\partial z_1} &= \frac{\partial Y}{\partial x_1} - \frac{\partial X}{\partial y_1},
\end{aligned} \qquad (5)$$

where

$$X = \int d\varphi \int \frac{dx}{r}, \quad Y = \int d\varphi \int \frac{dy}{r},$$

$$Z = \int d\varphi \int \frac{dz}{r}.$$

Then we have by virtue of equation (4), making $ds\, d\sigma = d\omega$,

$$X = -\int \left(\frac{\partial \varphi}{\partial y} \frac{dz}{dn} - \frac{\partial \varphi}{\partial z} \frac{dy}{dn} \right) \frac{d\omega}{r},$$

That means for equation (3)

$$X = \frac{\partial}{\partial z_1} \int \frac{dy}{dn} \frac{\varphi d\omega}{r} - \frac{\partial}{\partial y_1} \int \frac{dz}{dn} \frac{\varphi d\omega}{r},$$

and similarly

$$Y = \frac{\partial}{\partial x_1} \int \frac{dz}{dn} \frac{\varphi d\omega}{r} - \frac{\partial}{\partial z_1} \int \frac{dx}{dn} \frac{\varphi d\omega}{r},$$

$$Z = \frac{\partial}{\partial y_1} \int \frac{dx}{dn} \frac{\varphi d\omega}{r} - \frac{\partial}{\partial x_1} \int \frac{dy}{dn} \frac{\varphi d\omega}{r}.$$

Substituting these values in the second members of (5), and observing that we have

$$\Delta^2 \int \frac{dx}{dn} \frac{\varphi d\omega}{r} = 0,$$

$$\Delta^2 \int \frac{dy}{dn} \frac{\varphi d\omega}{r} = 0,$$

$$\Delta^2 \int \frac{dz}{dn} \frac{\varphi d\omega}{r} = 0,$$

$$\frac{\partial}{\partial x_1} \int \frac{dx}{dn} \frac{\varphi d\omega}{r} + \frac{\partial}{\partial y_1} \int \frac{dy}{dn} \frac{\varphi d\omega}{r} + \frac{\partial}{\partial z_1} \int \frac{dz}{dn} \frac{\varphi d\omega}{r}$$

$$= -\int \varphi \frac{d\frac{1}{r}}{dn} d\omega,$$

We find that the three derivatives of the potential Φ and of the functions

$$\int \varphi \frac{d\frac{1}{r}}{dn} d\omega \tag{6}$$

are equal to each other. These two functions can be taken, one for the other, in the calculus of the components, and in this we establish equation (1), which is now demonstrated.

We observe that when the function ϕ is multivalued with one or more periodic forms, we can always, by making perpendicular cuts in the space S, (in a number equal to the forms) transform it into a single-valued function. The presence of such sections, each of which penetrates the space twice on either side of the cutting plane, on the new overall surface I'll call Ω, does not change the surface integrals whose elements contain ϕ as a factor. Then we need to write

$$\int \frac{dx}{dn} \frac{\varphi d\Omega}{r}, \quad \int \frac{dy}{dn} \frac{\varphi d\Omega}{r}, \quad \int \frac{dz}{dn} \frac{\varphi d\Omega}{r}$$

in place of

$$\int \frac{dx}{dn} \frac{\varphi d\omega}{r}, \quad \int \frac{dy}{dn} \frac{\varphi d\omega}{r}, \quad \int \frac{dz}{dn} \frac{\varphi d\omega}{r},$$

and then we have

$$\int \varphi \frac{d\frac{1}{r}}{dn} d\Omega$$

in place of

$$\int \varphi \frac{d\frac{1}{r}}{dn} d\omega,$$

that means of Φ. But this substitution does not influence the proposition that we made around equation (2), because the integrals P and Π are not changed by substituting the Ω [the surface after the cut] for ω.

This proposition then, is true, under the condition that the branches, in which the derivative of ϕ ceases to be single-valued, is finite and continuous, and external to the space S. And this is what we said above.

In other words, the integral

$$\int \varphi \frac{d\frac{1}{r}}{dn} d\Omega$$

is the same as the primitive

$$\int \varphi \frac{d\frac{1}{r}}{dn} d\omega$$

added to the sum of the potential of the currents which cirulate around the transverse sections, with equal intensity with respect to the periodic form and this is explained in § 70 of my monograph.

Notes

1. *Nachrichten von der K. Gesellschaft d. W.*, Göttingen, (1870); *Annalen der Physik und Chemie von Poggendorff*, Vol. CXLV, (1872).
2. Memoria XXXV of this work (*Opere*), Vol. II
3. *Journal für die reine und angewandte Mathematik*, Vol. LXIX (1868), pp. 125-126.
4. *Journal für die reine und angewandte Mathematik*, Vol. XXXVII, (1848), p. 47.
5. *Sitzungberichte der K. Böhmischen Gesellschaft d. W.*, (1871), p. 25.
6. *Cf.* Section XI of the excellent *Teorica delle forze che agiscono secondo la legge di Newton*, (Theory of the forces which agitate according to Newton's law) published by Betti in this same journal.
7. *Journal für die reine und angewandte Mathematik*, Vol. LXIII (1871), pp. 116-119.
8. *Mémoires de l'Académie Royale des Sciences de l'Institut de France*, Vol. VI (1823), p. 175.

On the Mechanical Interpretation Of Maxwell's Formulae

by Eugenio Beltrami

This short excerpt from Beltrami's paper was translated by Dr. Giuseppe Filipponi. The original paper was published in 1886 in Series IV, Vol. VII (pp. 1-38) of the Memorie della R. Accademica delle Scienze dell'Istituto di Bologna *and also appears as paper No. 82 in Beltrami's collected works,* Opere Matematiche, *published in Milan in 1920 by Ulrico Hoepli (vol. 4).*

The research that is the object of this present memorandum concerns the same formulae that I studied from another point of view in the memorandum that I had the honor to present last year to this illustrious academy ("On the Use of Curvilinear Coordinates in Potential and Elasticity Theory," published 1885). I allude to the formulae which Maxwell used to define the system of pressures which generate, in elastic media, the same force field which ordinarily is considered to be represented by a Newtonian potential function.

These formulae, which I reproduce with the same symbols that I used in the previous memorandum, are the following:

$$
\begin{aligned}
X_x &= -\frac{1}{4\pi}\left(\frac{\partial V}{\partial x}\right)^2 + \frac{1}{8\pi}\Delta_1 V, \\
Y_y &= -\frac{1}{4\pi}\left(\frac{\partial V}{\partial y}\right)^2 + \frac{1}{8\pi}\Delta_1 V, \\
Z_z &= -\frac{1}{4\pi}\left(\frac{\partial V}{\partial z}\right)^2 + \frac{1}{8\pi}\Delta_1 V, \\
Y_z &= Z_y = -\frac{1}{4\pi}\frac{\partial V}{\partial y}\frac{\partial V}{\partial z}, \\
Z_x &= X_z = -\frac{1}{4\pi}\frac{\partial V}{\partial z}\frac{\partial V}{\partial x}, \\
X_y &= Y_x = -\frac{1}{4\pi}\frac{\partial V}{\partial x}\frac{\partial V}{\partial y}, \\
\Delta_1 V &= \left(\frac{\partial V}{\partial x}\right)^2 + \left(\frac{\partial V}{\partial y}\right)^2 + \left(\frac{\partial V}{\partial z}\right)^2;
\end{aligned}
\qquad (1)
$$

where V is the Newtonian potential function, and X_x, X_y, and so forth, are the same as the Kirchoff symbols, conventionally represented with X_n, Y_n, Z_n, the components, according to the three orthogonal axes x, y, z, of the normalized components of pressure over a plane element with n being the normal.

Now we come to the question that I wish to develop, and which I think would present itself naturally to anyone who reflects on the significance of the meaning that is attributed in the theory of elasticity to the pressures and tensions that exist in an elastic medium. We do not use any preconceptions about the possible physical correlation between the so-called action at a distance and the pressures and tensions defined by the Maxwell formulae, and we consider these pressures and tensions as simply generated in the middle of the elastic medium by a slight deformation of it, that is, by a slight displacement of each of its points (relative to an initial equilibrium state). If we look at the problem from this aspect, we can ask ourselves, does a deformation really exist that is capable of generating these pressures, and, if it exists, what are the components of the displacement of each point of the medium?

In order to answer these questions, we must first establish some things about the nature of the elastic medium in which we suppose the pressures and tensions defined by the Maxwell formulae to be generated. From a purely mathematical point of view, we could demand that the constitution of the medium is defined only by the condition of continuity, but, in order to reduce the calculations implied by this research, we wish to restrict the generality; therefore,

I will suppose that the medium is homogeneous and isotropic, and I will further suppose that the constants of isotropy can be different in different regions of the space in which are found different conditions with respect to the masses that produce the potential function. In order to avoid too much generality, we can say that the masses that are responsible for the potential function are three dimensional, with constant density, in the same way that we developed the constant density of the ordinary isotropic medium. We can say that this restriction is not so important in the theory in which Maxwell's formulae are presented, because the potential functions of the surface do not generally exist in this theory.

With this restriction, it is possible to interpret the mathematical treatment, and the object of this work is to do exactly that. The conclusions of this work are almost entirely negative, because they establish that in a real isotropic medium, the deformations capable of reproducing the system of pressures defined by Maxwell's equations do not exist, except in that case where the potential function is linear with respect to the coordinates; this special case is not only without any interest, but it is impossible to realize when the space in question is infinite. If we wish to escape the necessity of giving such a particular shape to the potential function, which is, of course, not always admissable, we must concede the existence of an isotropic medium, *sui generis*, whose characteristics do not correspond to any reality that we now know. In order to conceive of the nature of such a medium, we remember that the elementary elasticity potential of such a medium, according to Green's formula, can be considered to be composed of two parts, which are the elasticity potentials of two media which are different and irreducible, and which in combination can form any isotropic medium. The first of these two corresponds to a real entity that is well known, whose properties are the same as those of ordinary elastic fluids in which only longitudinal waves are transmitted. No known entity corresponds to the second, in which only transversal waves are transmitted, because in this medium the conditions of stability at equilibrium do not exist. Now, by only considering the existence of the second medium, he has a model that fits the analysis which we reproduce here. While, initially, it looks possible to extend the inquiry about the deformations into the space outside of the masses that produce the potential function, further development of this analysis demonstrates that, in the infinite space around the masses, the deformations are not possible, generally speaking; they are possible only when the potential function has the simple form that it generally has if all of the masses can be treated as one mass collected at a fixed point. If we have an arbitrary potential function, then we can correctly say that, generally, it is not possible to reproduce the system of pressures defined by Maxwell's equations through the deformations of an isotropic medium.

I was pushed to publish these results, despite my hesitation, not because I wanted to attack the Maxwell theory, but only because I wanted to demonstrate the necessity for developing another direction for the mechanical interpretation of the electromagnetic phenomena.

Considerations on Hydrodynamics

by Eugenio Beltrami

This paper by Eugenio Beltrami was translated by Dr. Giuseppe Filipponi. The full paper appeared in 1889 in Rendiconti del Reale Instituto Lombardo, *Series II, Vol. 22. It also appears in Italian as paper No. 87 in Beltrami's collected works,* Opere Matematiche, *Vol. 4, published in Milan in 1920 by Ulrico Hoepli.*

In the general theory of the motion of fluids, there are two doubly infinite systems of lines that have a fundamental importance for kinematic and dynamic studies of the motion itself. One of these systems is that of the lines of flux, defined by the differential equation

$$\frac{dx}{u} = \frac{dy}{v} = \frac{dz}{w}, \quad dt = 0,$$

where u, v, w, are the velocity components at the point (x, y, z) and at the instant t; the other system is the vortical lines, defined by the differential equation

$$\frac{dx}{p} = \frac{dy}{q} = \frac{dz}{r}, \quad dt = 0,$$

where p, q, r are the components of the rotation at the same point, and are defined by the well-known equation

$$2p = \frac{\partial w}{\partial y} - \frac{\partial v}{\partial z}, \quad 2q = \frac{\partial u}{\partial z} - \frac{\partial w}{\partial x},$$

$$2r = \frac{\partial v}{\partial x} - \frac{\partial u}{\partial y}.$$

These two systems of lines are not, evidently, independent of each other, even if their mutual dependence is not explicit. They appear only in a very indirect way in the well-known hydrodynamic theorems. We will not speak about this question in general, but only about two cases that can be considered as extreme cases. The first is the case in which the lines of the two systems cross each other at right angles in each instant of time and in each point of the space occupied by the fluid. It is defined by the equation

$$pu + qv + rw = 0$$

which must be true for the whole duration of the motion, throughout the whole space. This equation has a well-known interpretation, which expresses the necessary and sufficient condition in which the trinomial

$$udx + vdy + wdz$$

always can be integrated. The class of motion of the fluid in which this property is true is fully represented by the formulae

$$u = \mu\frac{\partial\varphi}{\partial x}, \quad v = \mu\frac{\partial\varphi}{\partial y}, \quad w = \mu\frac{\partial\varphi}{\partial z},$$

where μ and ϕ are two arbitrary functions of the space and time coordinates.

On the contrary, the second case takes place when these lines always meet at a 0 angle. In other words, they coincide at each point in time and space. The analytic conditions for this coincidence are

$$\frac{p}{u} = \frac{q}{v} = \frac{r}{w}, \tag{1}$$

otherwise

$$qw - rv = 0, \; ru - pw = 0, \; pv - qu = 0 \tag{1$_a$}$$

which of these last equations, it can be said that one of them can be derived from the other two. Can this second case actually be verified? If not, then, with the hypotheses,

$$u = \frac{\partial \varphi}{\partial x}, \quad v = \frac{\partial \varphi}{\partial y}, \quad w = \frac{\partial \varphi}{\partial z},$$

p, q, r must be 0, which means that the vortical lines do not exist.

We shall begin by considering a particular class of motions, in which each molecule of fluid moves in parallel to a fixed plane, which we suppose to be the xy plane. In this case we have $w = 0$ and then

$$2p = -\frac{\partial v}{\partial z}, \quad 2q = \frac{\partial u}{\partial z}, \quad 2r = \frac{\partial v}{\partial x} - \frac{\partial u}{\partial y},$$

That means that equations (1_a) are the following:

$$\frac{\partial v}{\partial x} - \frac{\partial u}{\partial y} = 0, \quad u\frac{\partial u}{\partial z} + v\frac{\partial v}{\partial z} = 0.$$

Providing that the following conditions hold

$$u = \frac{\partial \varphi}{\partial x}, \quad v = \frac{\partial \varphi}{\partial y}, \quad w = 0, \qquad (2)$$

where ϕ is a function of x, y, z, and t, subject to the condition

$$\frac{\partial}{\partial z}\left[\left(\frac{\partial \varphi}{\partial x}\right)^2 + \left(\frac{\partial \varphi}{\partial y}\right)^2\right] = 0.$$

A particular manner, but sufficient for our purposes, to solve this equation is this. Let F be an arbitrary function of the complex binomial $(x + iy)$ and the time t, and let Z be another arbitrary function, which however has only real values, and of z again take the time as t, posing

$$Fe^{iZ} = \phi + i\psi, \qquad (2_a)$$

which means that the real part is denoted with the symbol ϕ, and the coefficient of the imaginary unity with ψ. The function ϕ satisfies the condition just found. In fact we have

$$2\phi = Fe^{iZ} + F_1 e^{-iX},$$

where F_1 is the conjugate function of F, we have

$$2\frac{\partial \varphi}{\partial x} = F' e^{iZ} + F_1' e^{-iZ},$$

$$2\frac{\partial \varphi}{\partial y} = iF' e^{iZ} - iF_1' e^{-iZ},$$

where the prime indicates finding the derivative with respect to the binomial $(x + iy)$. From which we results

$$\left(\frac{\partial \varphi}{\partial x}\right)^2 + \left(\frac{\partial \varphi}{\partial y}\right)^2 = F' F_1',$$

and because the second member (F', F'_1) by hypothesis depends only upon the variables x, y and t, it is clear that the derivative with respect to the variable z is 0, which is the result which we sought.

We have, at least in the case in which motion is parallel to a fixed plane, a class of real motions in which what we require, that is, the coincidence of flux and vortical lines, exists. We note that each function ϕ, which we have created through the previous process, satisfies the equation

$$\frac{\partial^2 \varphi}{\partial x^2} + \frac{\partial^2 \varphi}{\partial y^2} = 0,$$

which means that this class of motion refers to an incompressible fluid (2). But we note that, having

$$\frac{\partial \varphi}{\partial x} = \frac{\partial \psi}{\partial y}, \quad \frac{\partial \varphi}{\partial y} = -\frac{\partial \psi}{\partial x},$$

the differential equations of the flux lines become

$$d\psi = 0, dz = 0, dt = 0,$$

that means these lines, identical with the vortical lines, are represented by the finite equations

$$\psi = \text{const}, z = \text{const}, t = \text{const} \qquad (2_b)$$

We can make a very simple example.
Taking

$$F = x + iy, Z = -2Tz$$

where T is some function of t, we find

$$Fe^{iZ} = (x + iy)e^{-2iTz},$$

from which

$$\varphi = x \cos 2Tz + y \sin 2tz$$
$$\psi = -x \sin 2Tz + y \cos 2Tz.$$

thus the solution is obtained

$$u = \cos 2Tz,\ v = \sin 2Tz,\ w = 0,$$

in which the required property is immediately verifiable, since we find

$$p = -T\cos 2Tz,\ q = -T\sin 2Tz,\ r = 0$$

and from which

$$\frac{p}{u} = \frac{q}{v} = -T.$$

The flux and vortical lines are straight lines,

$$-x\sin 2Tz + y\cos 2Tz = \text{const},$$
$$z = \text{const},\ t = \text{const}.$$

This particular example easily leads to another example which also relates to an incompressible fluid, but in which the fluid molecules no longer move more parallel in a plane. If, in fact, we take

$$u = T_2\cos 2Ty + T_3\sin 2Tz,$$
$$v = T_3\cos 2Tz + T_1 \mathit{sin}\ 2Tx,$$
$$w = T_1\cos 2Tx + T_2\sin 2Ty,$$

where T, T_1, T_2, and T_3 are four arbitrary functions of time, we immediately find

$$\frac{p}{u} = \frac{q}{v} = \frac{r}{w} = T.$$

Another class of solutions can be indicated, in which the motion is neither parallel to the plane nor in general relates to an incompressible fluid.

Let ϕ be a general function of x, y, and t, then pose

$$u = -\frac{\partial\varphi}{\partial y}, \qquad v = \frac{\partial\varphi}{\partial x},$$

keeping the third component w, indeterminate for the moment. From this is derived

$$2p = \frac{\partial w}{\partial y}, \quad 2q = -\frac{\partial w}{\partial x}, \quad 2r = \frac{\partial^2\varphi}{\partial x^2} + \frac{\partial^2\varphi}{\partial y^2}.$$

The third equation (1_a) will become

$$\frac{\partial\varphi}{\partial x}\frac{\partial w}{\partial y} - \frac{\partial\varphi}{\partial y}\frac{\partial w}{\partial x} = 0$$

and that shows that w must have the form

$$w = w(\varphi, z, t),$$

from this results

$$\frac{2p}{u} = \frac{2q}{v} = -\frac{\partial w}{\partial\varphi}.$$

The equality of the first two relationships (1) with the third is thus expressed by the equation

$$\frac{\partial^2\varphi}{\partial x^2} + \frac{\partial^2\varphi}{\partial y^2} + \frac{1}{2}\frac{\partial(w^2)}{\partial\varphi} = 0.$$

But, because ϕ is an independent function of w, and because of this same equation,

$$\frac{\partial^2(w^2)}{\partial\varphi\partial z} = 0,$$

then w^2 must have the form

$$w^2 = F(\varphi, t) + Z(z, t),$$

and ϕ must satisfy the equation

$$\frac{\partial^2\varphi}{\partial x^2} + \frac{\partial^2\varphi}{\partial y^2} + \frac{1}{2}\frac{\partial F}{\partial\varphi} = 0.$$

Supposing that ϕ and F depend only upon $\rho = \sqrt{x^2+y^2}$ and from t, this equation becomes

$$2\phi'(\rho\phi')' + \rho F' = 0,$$

where the prime indicates the derivative with respect to ρ. In these particular hypotheses, the various preceding formulae can thus be summarized:

$$u = -\frac{\partial\varphi}{\partial y}, \quad v = \frac{\partial\varphi}{\partial x}, \quad \varphi'(\rho\varphi')' + \rho w w' = 0,$$

$$\frac{2p}{u} = \frac{2q}{v} = \frac{2r}{w} = -\frac{w'}{\varphi'} = \frac{(\rho\varphi')'}{\rho w}$$

If, for example, the component of the motion parallel to the xy plane is that which is due to a rotation with constant angular velocity Ω, around the z axis, we can pose

$$\varphi = \tfrac{1}{2}\Omega\rho^2$$

and the differential relation between ϕ and w becomes

$$2\Omega^2\rho + ww' = 0,$$

From which making the integral

$$2\Omega^2\rho^2 + w^2 = Z(z, t).$$

We have definitively

$$u = -\Omega y\,, \quad v = \Omega x, \quad w = \sqrt{Z - 2\Omega^2\rho^2}\,,$$

$$u^2 + v^2 + w^2 = Z - \Omega^2\rho^2\,,$$

$$\frac{p}{u} = \frac{q}{v} = \frac{r}{w} = \frac{\Omega}{\sqrt{Z - 2\Omega^2\rho^2}}$$

the flux lines are given by the equations

$$\rho = \text{const},$$

$$\arctan\frac{y}{x} - \int \frac{\Omega dz}{\sqrt{Z - 2\Omega^2\rho^2}} = \text{const},$$

$$t = \text{const}.$$

The motion defined by these formulae (which can be limited to a cylindrical space) is the motion of an incompressible fluid, if not when Z is independent of z: in this case, the flux lines are helical, all of which have the same z axis. These examples are sufficient to establish the existence of a large and interesting class of fluid motions, which (by an obvious analogy) can be called *helical motions*, and in which the flux lines coincide at each instant, and at each point, with the vortical lines. The necessary and sufficient conditions to define this class of motions are equations (1) and (1_a); but another form can be used that can easily be given for these equations. The first of the equations (1_a) is the following:

$$\left(\frac{\partial u}{\partial z} - \frac{\partial w}{\partial x}\right) w - \left(\frac{\partial v}{\partial x} - \frac{\partial u}{\partial y}\right) v = 0\,,$$

it can be written, in fact as

$$\frac{\partial u}{\partial y} v + \frac{\partial u}{\partial z} w = \frac{\partial v}{\partial x} v + \frac{\partial w}{\partial x} w\,,$$

and from this equation we can immediately pass to the first of the following three:

$$\begin{aligned} u' &= \frac{\partial u}{\partial t} + \frac{1}{2}\frac{\partial(\omega^2)}{\partial x}\,, \\ v' &= \frac{\partial v}{\partial t} + \frac{1}{2}\frac{\partial(\omega^2)}{\partial y}\,, \\ w' &= \frac{\partial w}{\partial t} + \frac{1}{2}\frac{\partial(\omega^2)}{\partial z}\,, \end{aligned} \tag{4}$$

where u', v', and w' are the complete derivatives of u, v, w; and where, for brevity, we pose

$$u^2 + v^2 + w^2 = \omega^2.$$

These new equations, of which one is the consequence of the other two, can be considered as characteristics of each helical motion.

Now, from the well-known forms of the equations of motion of perfect fluids, we know that if the external forces have a potential function, the trinomial

$$u'dx + v'dy + w'dz$$

is a perfect differential, with respect to the coordinates, that means that the potential function for the accelerations exists. Having, from equations (4)

$$\frac{\partial w'}{\partial y} - \frac{\partial v'}{\partial z} = 2\frac{\partial p}{\partial t}\,, \quad \frac{\partial u'}{\partial z} - \frac{\partial w'}{\partial x} = 2\frac{\partial q}{\partial t}\,,$$

$$\frac{\partial v'}{\partial x} - \frac{\partial u'}{\partial y} = 2\frac{\partial r}{\partial t}\,,$$

it is immediately recognized that the existence of such potential functions for the accelerations cannot agree with the hypotheses of helical motion if the quantities p, q, r in this motion are independent of time. Furthermore, if we denote with μ the common value of the three ratios (1), that means we pose

$$p = \mu u,\ q = \mu v,\ r = \mu w, \tag{4_a}$$

and if p_1, q_1, r_1, are indicated with three expressions formed with p, q, r, in the same way in which these are formed with u, v, w, we have the relationships

$$\begin{aligned} 2p_1 &= 2\mu p + \frac{\partial\mu}{\partial y} w - \frac{\partial\mu}{\partial z} v\,, \\ 2q_1 &= 2\mu q + \frac{\partial\mu}{\partial z} u - \frac{\partial\mu}{\partial x} w\,, \\ 2r_1 &= 2\mu r + \frac{\partial\mu}{\partial x} v - \frac{\partial\mu}{\partial y} u\,, \end{aligned}$$

from which follows

$$pp_1 + qq_1, + rr_1 = (p^2 + q^2 + r^2)\mu.$$

When the quantities p, q, r and the quantities p_1, q_1, and r_1 are thus independent of time, the factor μ cannot depend upon this variable, and then, consequently, (4_a), the components of the velocity cannot also be functions only of the coordinates of position. In this way, we obtain the following theorem: When the potential of acceleration exists, then helical motion cannot be verified if this motion is not also stationary. Reciprocally, from equation (4) it follows that for each stationary helical motion there exists a potential of acceleration, a potential whose value is $\frac{1}{2}\omega^2$.

If this property of helical motion is considered, taking the ordinary derivatives of equations (4_a) with respect to x, y, and z and summing them, and denoting the density by ε, then we have

$$\mu\varepsilon' - \mu'\varepsilon = 0:$$

then: *in each stationary helical motion, the ratio between μ and ε remains constant for each fluid molecule, in the whole course of the motion.*

The equations (4) are not particular cases of the other three, which exist unconditionally. In fact, if to the second member of the equation

$$u' = \frac{\partial u}{\partial t} + \frac{\partial u}{\partial x}u + \frac{\partial u}{\partial y}v + \frac{\partial u}{\partial z}w$$

we add and subtract the binomial

$$\frac{\partial v}{\partial x}v + \frac{\partial w}{\partial x}w,$$

we get the first of the following equations:

$$u' = \frac{\partial u}{\partial t} + \frac{1}{2}\frac{\partial(\omega^2)}{\partial x} + 2qw - 2rv,$$

$$v' = \frac{\partial v}{\partial t} + \frac{1}{2}\frac{\partial(\omega^2)}{\partial y} + 2ru - 2pw,$$

$$w' = \frac{\partial w}{\partial t} + \frac{1}{2}\frac{\partial(\omega^2)}{\partial z} + 2pv - 2qu,$$

from which result the equations (4), when we impose the proportionalities (1).

From the same equation (a), adding and subtracting to the second member the quantity s multiplied by u, where

$$s = \frac{\partial u}{\partial x} + \frac{\partial v}{\partial y} + \frac{\partial w}{\partial z},$$

we can also calculate the first of the following equations:

$$u' = \frac{\partial u}{\partial t} + \frac{\partial(u^2)}{\partial x} + \frac{\partial(uv)}{\partial y} + \frac{\partial(uw)}{\partial z} - su,$$

$$v' = \frac{\partial v}{\partial t} + \frac{\partial(vu)}{\partial x} + \frac{\partial(v^2)}{\partial y} + \frac{\partial(vw)}{\partial z} - sv, \qquad (5a)$$

$$w' = \frac{\partial w}{\partial t} + \frac{\partial(wu)}{\partial x} + \frac{\partial(wv)}{\partial y} + \frac{\partial(w^2)}{\partial z} - sw,$$

and the comparison with the preceding gets the following identities:

$$\frac{\partial\left(u^2 - \frac{\omega^2}{2}\right)}{\partial x} + \frac{\partial(uv)}{\partial y} + \frac{\partial(uw)}{\partial z} = su + 2qw - 2rv,$$

$$\frac{\partial(vu)}{\partial x} + \frac{\partial\left(v^2 - \frac{\omega^2}{2}\right)}{\partial y} + \frac{\partial(vw)}{\partial z} = sv + 2ru - 2pw,$$

$$\frac{\partial(wu)}{\partial x} + \frac{\partial(wv)}{\partial y} + \frac{\partial\left(w^2 - \frac{\omega^2}{2}\right)}{\partial z} = sw + 2pv - 2qu. \qquad (6)$$

when a potential of motion φ exists, we have

$$s = \Delta_2\phi,\ p = q = r = 0$$

and the preceding relationships are the well-known Maxwell formulae.

Very similar formulae also exist in the case in which the motion is without a potential but appears instead in the class of helical motions.

Taken in all of its generality, the relationships in (6) reproduce the other formulae which Maxwell calls the electromagnetic force equations (Second Edition of the *Treatise*, Vol. II, Art. 643.) In order to establish the agreement between equations (6) with Maxwell's, we must write

$$\begin{aligned} \alpha, \beta, \gamma &\text{ to replace } u, v, w, \\ 2\pi u, 2\pi v, 2\pi w &\text{ to replace } p, q, r, \\ 4\pi m &\text{ to replace } s, \end{aligned}$$

where α, β, γ are, according to Maxwell, the components of magnetic force; u, v, w are those of the specific intensity of the current, and m is the density of the Newtonian distribution equivalent in external action, to the magnetic polarization of the field.

Information for Contributors

Manuscripts should be sent to David Cherry at the Fusion Energy Foundation, P.O. Box 17149, Washington, D.C. 20041-0149.

Manuscripts should be submitted in triplicate (with three sets of illustrations, of which one is an original.) They should be typewritten on one side of letter (quarto) paper and double spaced with at least 25mm (1 inch) margins. All pages must be numbered in sequence beginning with the title page.

TITLE PAGE of the manuscript should contain the complete article title; names and affiliations of all authors; name, address, telephone number, and cable or Telex number for all correspondence.

ABSTRACT of no more than 200 words should summarize the work and major conclusions.

TEXT should define all abbreviations at first mention. American measuring units should be accompanied by metric translation. In general, the meter/kilogram/second/ampere system of units should be used. Letters of permission should be submitted with any material that has been previously published.

FOOTNOTES should appear at the bottom of the respective page and must be numbered consecutively.

REFERENCES should be referred to in the text by the author's name and the date of the work. The references should also be listed alphabetically on a separate page. The references should include for articles: author, year of publication, title, periodical name, volume no., and pages; for books: author, year of publication, title, place of publication, and publisher's name.

TABLES, FIGURES, and ILLUSTRATIONS must be prepared each on a separate page, numbered in order of appearance, and have a title and descriptive legend. Photographs should be glossy black and white prints.

ACKNOWLEDGMENTS. Illustrations from other publications must be acknowledged. Include the following when applicable: author(s), title of journal or book, publisher and place of publication (if book), volume number, page(s), month and year of publication. The author is responsible for obtaining the publisher's permission to reprint.

REPRINT order forms will be sent to the author with proofs of the article.

Reports

The Application of Beltrami's Work to Plasma Research Today

by Dan Wells, Ph.D.

Fusion scientist Dan Wells, a corresponding editor of the IJFE, is currently a professor at the University of Miami. This article is excerpted from a presentation he gave at a Fusion Energy Foundation seminar on how he discovered the relevance of Beltrami vortices to his own work with the magnetic vortices that develop in plasmas.

We were originally interested in the construction of force-free coils at the Princeton Plasma Physics Laboratory, back in the early 1950s, and our job was to design large electromagnets that would produce high magnetic fields. When you produce high magnetic fields, you also produce high forces which tend to break the magnets apart. In order to get around this, we were studying methods of winding coils in complicated ways in order to produce either force-freeness, where there were no breaking forces in the coils, or force-reduced coils. My working assignment at the laboratory was coil-winding and designing coil-winding.

The actual progression of my thinking was from the force-free coils to a graduate project I was doing with Dr. Winston Bostick at Stevens Institute, where I was completing work on my doctorate. Bostick suggested that I look at certain structures that were being produced by Wanniack's conical theta pinches. Ralph Wanniack, working all by himself somewhere in California, had built conical theta pinches and fired them at each other. Bostick asked me to look at them because Wanniack said something very strange was happening.

The structures looked like vortices to me. They looked like the kind of things I saw in studying and testing aircraft and in wind tunnels, when I had worked in flight testing during the Second World War. I told Winston that these looked to me like vortex rings, and then we began to probe them, and it turned out they were indeed vortex rings.

Here was a very stable vortex that had a toroidal shape, and the coils I was winding also had toroidal shapes. Therefore, I began to look for toroidal fields, and to speculate that these were force-free or quasi-force-free structures because they were relatively stable.

At that time, I came across some articles on force-free fields that had been published by the Indian scientist Subrennanyan Chandrasekhar on astrophysics. He was concerned with electromagnetic forces on plasmas in the plane of the galaxy and why certain phenomena were produced. He applied the concept of a geometric arrangement of the currents and magnetic fields present in the plane of the galaxy to the problem of the motion or lack of motion of the plasma in and near the galactic plane. From this, I was led to Beltrami's basic papers on Beltrami flow.

I obtained Beltrami's papers through the library at Langley Field, Virginia, where my colleague Joe Norwood, also one of Bostick's students, was employed. (Aerodynamicist Adolf Busemann was also there at the time.) These papers were apparently pretty well known to the aerodynamicists at Langley, but they were something of a revelation to us—all these beautiful solutions of the force-free equations done in every conceivable coordinate system.

We were looking for equations to describe minimal free energy structures. We knew what the equations were, and here Beltrami had already considered them and solved them in all the different coordinates. Therefore, we used it as a working paper.

My approach has always been one where I have induced velocities in the plasma and then tried to maintain them, at least for some time into the experiment. The Beltrami equations were concerned with fluid flow. Thus they are applicable to magnetohydrodynamic flow. But, the *form* of the Beltrami equation is identical to this *form* of the force-free equation for the Lorentz force ($\mathbf{j} \times \mathbf{B}$) and thus its solutions are good for plasma forces *even if there is no flow!*

The Beltrami papers enabled us to study the detailed solutions for the force-free fields under various geometrical constraints or conditions. I was particularly interested in applying these ideas to plasmas, because I was a graduate student at the time, and I was interested in doing research work on the stability of plasma structures or closed plasma configurations.

The basic difference between a force-free electromagnetic coil and a force-free plasma structure is that the plasma structure has both the currents and magnetic fields and the velocity fields of the flow. And if there is any vorticity present, the vortex filaments are also wrapped up in this structure. Therefore, from the very beginning in my work, in adapting the force-free coil configurations to closed plasma configurations, I included the possibility of flow of the plasma and actual vorticity in the flow of the structures, as well as the currents and magnetic fields.

The reason that the vorticity and the flow seemed

obviously to be important to me in my work was that we were producing the structures that we were studying with a device that produced high-velocity flows. Therefore I could not see how one could study the stable states of these structures without including the flow, which was really creating some of the dominant forces in the plasma. We looked at the so-called magnus forces, which are the forces produced by the interaction of the flow fields and the vorticity filaments. It turns out that if the conditions exist for a force-free electromagnetic field, where the current density and magnetic induction vectors are parallel, there also will be, in the low-energy state, a condition in which the velocity of flow and the vortex filaments are also parallel. Therefore, there is complete force-freeness for both the electromagnetic forces, or so-called Lorenz force, and the hydromagnetic force, which is the so-called magnus force.

Later work done by people like J.B. Taylor and company, and the work of Harold Furth at Princeton on spheromaks, until at least the last year or two, has excluded—explicitly excluded—any consideration of the plasma flow velocity in calculations. This is because these researchers believe that the spheromak maintains a steady-state, zero-velocity equilibrium in which there are no flows. When they cannot ignore the flows, they try to get rid of them. Any flow velocity in the spheromaks that they talk about, is due to instabilities—or pump-out, as they call it—and they don't want those. Therefore, they ignore the velocity terms in the equations.

We adapt the Beltrami equations in this way: If you write down the equation for the force-fields for the electric currents and magnetic induction fields, and you write down the equations for the forces produced by the vorticity interacting with the mass-flow fields, the two equations are the same mathematical equation. If they settle down to the lowest energy state, then the equations align themselves so that all four fields—the electric, magnetic, flow, and vorticity—are parallel.

Beltrami is talking about a flow of normal fluid, so there is no electrical conduction current and there is no magnetic induction field. For example, in the case of a wind tunnel, with air in it, not a plasma, there aren't any current densities and there aren't any magnetic induction fields—they are just zero. The same equations can also apply to currents and magnetic fields, as Beltrami showed. We have applied his formalism twice to describe four fields, although he dealt only with two.

The "hydrodynamic" and "electrodynamic" fields can interact. There can be an interconnection between the two—that is, instead of the magnetic forces containing electrical charges, hydrodynamic flows can confine these electric charges hydrodynamically.

Therefore, in the overall balance of so-called forces, what would ordinarily be missed by a static approach is the fact that a situation could exist where the magnetic force was not sufficient to contain the electrical charges.

Spying on Carcinoma Cells Through an NMR Looking Glass

by James Frazer, Ph.D.

Nuclear magnetic resonance (NMR) is providing us with new ways of characterizing and understanding cancer. The following is an account of some work we are doing using NMR at M.D. Anderson Cancer Institute in Houston, Tex.

The biological material we are using comes from Dr. Garth Nicholson's group at M.D. Anderson, which has worked for several years to obtain clones of mammary adenocarcinoma (laboratory cell cultures derived from single cells of tumor) with defined metastatic potential to a variety of specific organs: brain, liver, or lung. He develops these clones by first taking cells from a tumor that has metastasized, for example, from the breast to the lung; reintroducing that lung metastasis cell clone to the breast of a healthy animal, and again waiting for metastasis to the lung, and so on, until he gets a repeatable and predictable tumor line that metastasizes to the lung with regularity.

Recently, with the help of Dr. Steven Tomasovich at M.D. Anderson, we have been growing these clones in the lab to about 1 gram quantities and examining their NMR resonance spectra compared to "normal" cells. The most studied breast tumor clone metastasizes repeatably to lung (termed MTNL 3).

As a result of earlier work, we know that macrophages (certain immune system cells) present in tumors will not cytolyse (kill by secreting lethal substances) the more metastatic clone, but will cytolyse those clones of the same general cell type that can form only local tumors. This seems to imply that those tumors that have more metastatic potential have some way of evading the ability of macrophages to kill cancer cells.

In attempting to define that critical difference, Dr. Peter Steck at M.D. Anderson isolated several cell surface glycoproteins (proteins with carbohydrates attached) secreted by the more invasive cell clone.

With Dr. Lawrence Dennis, we chose to examine these well-characterized clones by means of NMR spectroscopy using both a continuous wave (CW) and a pulsed spectrometer so that relaxation rates (pulsed NMR spectroscopy is based on measuring the released

radiation after an input pulse, termed "relaxation") and co-relaxations (the relaxations of chemical groups with resonances close to the ones of interest) could be well measured. Our early work, with Dr. Stephen Bines, showed that there was a significant chemical shift of water (change in NMR relaxation time, associated with decrease in the amount of long-range ordering of the water) in the more metastatic clones as compared with more sessile (nonmetastatic) clones.

We also noticed, using the CW spectrometer, that there were significant differences in a 1.2 parts per million (ppm) peak (a frequency differing from the standard of 42.024 megacycles per tesla for tetramethyl silane, by 1.2 parts per million cycles) which may be at least partly due to membrane cholesterol. Dr. Caroline Mountford, working in Australia, also noticed this in leukemia cells using a pulsed NMR spectrometer.

Using a pulsed spectrometer, we have picked up a glycoprotein signal at approximately 3.5 ppm in the more metastatic line, which is nearly absent in less metastatic clones. Interestingly, a similar glycoprotein was found in the supernatant (that is, outside the cells) from the more metastatic clone. We would like to know if this glycoprotein has a functional significance in the metastatic potential of this cell line. Also, there is considerable evidence that there is significantly more protein hydrolysis (digestion) of the culture medium of the metastatic clone as compared to the nonmetastatic clone. Is this hydrolytic process also related to metastatic potential?

We are attempting to further characterize these interesting surface glycoproteins. Through work with a student, James de Gregori, we obtained the spectra of individual amino acids (protein-building blocks), then calculated the theoretical spectra of our protein assuming a simple addition relation (as modified by data from short chains of amino acids). We have found that the total integrated area of the spectrum of the whole protein, as compared to the spectra of the individual constituent amino acids, is decreased to as little as 25 percent of theoretical magnitude. Denaturing the protein (changing the overall shape without breaking any chemical bonds) in a solution of 8 molar urea allowed us to recover to approximately 50 percent of the theoretical magnitude. This disturbed us, since previous work using deuterium oxide instead of usual water, with pH carefully controlled, indicated that full recovery (that is, full spectrum amplitude corresponding to the amplitudes of the constitutent amino acids making up the protein) should be possible. We used hydrogen (rather than deuterium) in our studies and a spin inversion technique to suppress the large water spectrum with pH carefully controlled, and still only obtained at most 50 percent of the theoretical requirement.

What this all suggests is that the state of the protein determines the amplitude and shape of its spectrum, which may allow predictions of long molecule conformations (geometries) in solution. This may provide information on the degree of extended state of surface molecules that may be involved in the above suggested processes. Information concerning these surface molecule states may be valuable in planning studies of their functioning, such as affecting interactions with the immune system.

Our observations may have near-term practical utility in the examination of human cells. We are now "decoding" patients whose cells, obtained from the cell-phoresis unit (automated cell-sorter used for blood tests) at M.D. Anderson, have been examined by NMR. We are attempting to build a "bank" of normal and disease-related spectra for use as a diagnostic technique.

On a more theoretical plane, we hope to use the spectra as a way of measuring fluidity changes in membranes of cells undergoing a variety of adaptive responses. This is a viable goal because several of the glycoproteins we are examining are constituents of cell surface receptor sites. We think the reason for lack of macrophage activity against more metastatic tumors may be due to the release of glycoprotein by the tumor cells, adsorption of this glycoprotein on the macrophage cell-surface receptor site, and thus inactivation of the macrophage site. We will have to do much more investigation to see if this hypothesis holds true.

The Spectroscopy of Photosynthesis

by Ned Rosinsky, M.D.

The Fusion Energy Foundation's interest in optical biology has included a review of the past five years' literature on chlorophyll spectroscopy, as well as the work of Philip Callahan (1985) on insect sense of smell being based on infrared absorption and emission and James Frazer's use of Nuclear Magnetic Resonance (NMR) to characterize the spectral properties of cancer tissue (Frazer 1985). "Spectroscopy" here refers both to normal absorption and emission of radiation by functioning plant tissue, as well as diagnostic techniques such as those we will describe below, based on variants of NMR.

Although chlorophyll is known to be the initial absorber of visible light photons in the process of pho-

tosynthesis in green plants, its spectrum implies that there are at least two distinct states of chlorophyll in each functional photosynthetic unit (PTU). The PTU is the smallest unit that can engage in all the initial events of photosynthesis, including light absorption as well as the use of that excitation to chemically reduce a substance (known now to be ubiquinone) as the first step in the chain of oxidation/reduction reactions that ultimately produce sugar from water and carbon dioxide. In advanced green plants, each PTU contains 300-1,000 molecules of chlorophyll, as well as several other pigments, numerous proteins, membranes, water, ions, and the substance ubiquinone. The two states of chlorophyll correspond to the two main functions of the PTU: light capture and ubiquinone reduction.

Experimentally, this is implied by there being two distinct spectral groupings of chlorophyll. The chlorophyll closely associated with ubiquinone can be separated out of the PTU and has a peak absorption at wavelength 700 nanometers (nm) (termed P700). This is a very small fraction of the total chlorophyll. All the rest has a peak at 670 nm (P670).

Furthermore, if the P700 is treated with conditions to separate the chlorophyll molecules, it becomes P670. This implies that P700 is a modified state of P670. The complex of P700, ubiquinone, and the associated proteins are termed the photo-reaction center (PRC) of the PTU (though it should be pointed out that the actual geometric relationship of the PRC to the larger PTU is not yet understood). Since P670 is not directly associated with ubiquinone, it is considered to be primarily involved with light capture, and is therefore termed antenna chlorophyll. It is significant that there is a small downshift in the resonant frequency between antenna chlorophyll and PRC chlorophyll. This may serve as a photon trap, serving to *concentrate photons at the PRC for use in the reduction process.*

The recent innovations in spectroscopic techniques relevant to these questions are related to NMR and measure aspects of magnetic fields on the scale lengths of molecules. They can therefore indicate geometric ordering as well as electromagnetic interaction on these scale lengths.

How is it that the antenna chlorophyll has a different absorption peak from that of the PRC chlorophyll? Joseph Katz at Argonne National Laboratory has done spectroscopic studies of PRC chlorophyll and concluded that the spectral shift is the result of the close association of two molecules of chlorophyll (which he terms the special pair or Chl sp), forming a functionally larger absorber and emitter of radiation. He postulates the function of this spectral difference to be the formation of a photon trap, in which photons flowing through the array of antenna chlorophylls can be absorbed by the P700, but cannot flow back to the antenna since the antenna chlorophyll resonates at a slightly higher frequency. This serves to greatly concentrate the photons at the PRC. It is further possible that the antenna chlorophyll exists in a variety of degrees of partial pairing, creating a range of characteristic spectral peaks that guide the photons toward the reaction center; that is, the spectral potential is in the form of a funnel with the PRC at the bottom.

The existence of this special pair, or chlorophyll dimer, is implied by evidence from electron paramagnetic resonance (EPR), a variant of NMR. EPR measures how many molecules are acting in a coherent unit with respect to an electron excitation. Katz demonstrates that the EPR data imply that the molecular spatial extent of the photo-excited electron state in the PRC is approximately twice the size of one chlorophyll molecule. EPR, as the electron magnetic equivalent of NMR, utilizes a constant external magnetic field to spin-align the electrons (as compared to the spin-alignment of positively charged nuclei in NMR), and a second alternating field that, at resonant frequencies, changes the spin alignment of electrons of specific energies (that is, specific local magnetic flux densities) away from the direction of the constant field. This change of alignment occurs, as in any quantum effect, in discontinuous energy jumps, which are associated with energy absorption from the alternating field input, resulting in a characteristic absorption spectrum. The significant finding here concerns the width of the shape of the absorption peak lines, rather than the specific frequency of the absorption maximum. The narrower the width, the larger the number of (hydrogen) protons that are closely coupling with the electron in question. In the case of P700, the EPR peak is 40 percent narrower than the isolated monomer form of Chl *a*, and this corresponds to a doubling of the absorption unit size, since quantum predictions suggest that the peak width should scale inversely with the square root of the number of molecules sharing the excited state (Katz 1979). This idea is backed up by similar spectra occurring in molecules which are built up in the laboratory by chemically bonding together two chlorophyll molecules.

A second variant of NMR combines NMR with EPR, resulting in electron nuclear double resonance (ENDOR) spectroscopy. Here, as in EPR, an external constant magnetic field is applied that aligns the spins of the hydrogen nuclei (protons) as well as the unpaired excited electron. Then, an alternating field at the resonant frequency of the excited electron saturates an electron absorption band; however, a second alternating field is then introduced at the resonant

frequency of the hydrogen protons. The resulting spin shift of the protons affects local magnetic flux and changes the maximum amplitude of the electron absorption. This can be used as a measure of the degree of coupling between the excited electron and nearby hydrogen (protons). The electron-nuclear hyperfine coupling constant for the individual monomer is N times the constant for the N-fold functional aggregate; in this case N is found to be close to 2, varying from 1.9 to 2.2 for different classes of protons (different peaks within the overall ENDOR spectrum) (Norris 1979).

Both the EPR and ENDOR results, however, could still possibly be explained by environmental effects other than a chlorophyll special pair model, particularly since the excited electron state is presumed to "ring" the molecule and therefore is accessible to near neighbor effects. However, the nitrogens within the macrocycle ring are less exposed, and the spectrum of the nitrogens is additional evidence in favor of the special pair notion, as measured by the technique of electron spin-echo spectroscopy (ESE). This technique utilizes the secondary field effects of the relaxing or flipping back of the electron spin that occurs in the course of usual EPR (see above), and is particularly useful for studying the hyperfine interactions between nitrogen and excited electrons. The ESE pattern for P700 is radically different from P670, indicating that the primary electron-donor for ubiquinone reduction cannot be monomeric chlorophyll (Norris 1980).

While the usual quantum-mechanical interpretations of the above spectral experiments are frequently reductionist in methodology, the spectra themselves are provocative, and indicate that qualitative differences exist in the various forms of chlorophyll in the PSU, which the NMR-type spectral results indicate are differences in something akin to long-range phase coherence (as in the case of the simpler NMR of "structured" water).

Quantum Upshift

The indication that photons are concentrated at the PRC prompted J.E. Hunt at Argonne to push P700 to the limit with intense laser irradiation. With nanosecond pulses in the megawatt range, he showed recently that 700 nm radiation results in 400 nm fluorescence, an *upshift* of almost doubling the frequency (Hunt 1983). The quantum efficiency of this under his experimental conditions was very small, 1/100,000. He also showed that the hyperexcited state of the chlorophyll could reduce a dye substance whose reduction required that higher amount of energy, opening up the possibility that the Chl *sp* may function in this fashion in normal physiological conditions. That is, the question raised by this finding is whether such an upshift of quantum size is part of the usual functioning of chlorophyll. Such an upshift would represent a work aspect of the photosynthetic apparatus apart from the above-mentioned concentrating of photons at the PRC, and the transduction of the excited electron state to the reduction of ubiquinone.

While mean sunlight intensity is far below the laser pulse used by 10 orders of magnitude, the concentrating of photons into the reaction center by the antenna could at least partially make up for this and increase the flux; also, if the directionality of photon flux is established by antenna geometry, and the Chl *sp* is designed to reduce ubiquinone only after receiving a second photon, then in the living state such an upshift could be the dominant mode. This is now a very hot point of debate, and workers in the area feel that this is a definite possibility. As an aside, if the in vitro PSU is irradiated with blue light at 400 nm, it will not fluoresce; it will only do so if it receives intense red light (700 nm), and then will fluoresce in the blue. In the normally functioning state, chlorophyll does not fluoresce at all or only minimally, since most of the photons are utilized to reduce quinones for the eventual production of carbohydrates. (Or, if the PSU is overcharged by intense sunlight, the excess energy is transferred to other pigments in the PSU that reradiate the energy to the environment at lower frequencies.) This stands out as a strange and anomalous finding. Hyperexcited chlorophyll can also be made to lase, and should respond differently to polarized light. However, this polarization experiment, simple as it is, is yet to be done.

Thus, the overall picture of the PSU that emerges is that of a photon potential trap with the Chl *sp* at the bottom, in which a slight change downward in spectral frequency toward the PRC, combined with an almost 100 percent efficiency of photon transfer within the PSU, results in an immense increase in photon flux at the PRC, and may very well include a sizable upshift in frequency at the PRC. If *chlorophyll* is thought of as actually a mode of self-induced transparency, the variation in characteristic absorption and emission wavelength within the PSU can be seen as a varying retarded potential, serving to perform the above described concentrating and upshifting functions.

Related Processes

The porphyrin macrocycle portion of chlorophyll is also involved in numerous other work transformations in the cell. The heme in hemoglobin, which is involved in oxygen transport, is almost identical, with iron substituting for magnesium. The cytochromes in

the ATP-forming oxidative respiration that goes on in the mitochondria (the "powerhouses" of the cell) are protein-porphyrin enzyme complexes with stepwise varying redox potentials. Thus the metabolic construction of porphyrin represents an entire array of work functions. Likewise, the simpler pyrrole compounds represent a lower array of functions. Thus the stepwise metabolic construction of chlorophyll may correspond, at each qualitative step, to a historical evolutionary state of life. For example, the simpler pigments may have originally had more of a sensory function to direct the microorganism toward a pond surface for food-gathering: such as the current use of retinene in the mammalian eye that is closely related to the carotene in plants, or the plant sensory pigment phytochrome that is closely related to chlorophyll, and later evolved the photon-food conversion function (retinene, carotene, and chlorophyll are all constructed metabolically from the same isopentene, with the pyrrole compounds differing topologically in being closed on themselves in loops). This would be an example of extreme physiological transformation that requires a comparatively straightforward and simple topological change in geometric (metabolic) construction.

Since the characteristic geometry involved in these construction pathways is dominated by pentagonal-golden mean self-similar forms, we must investigate further the role of such geometries, which as Leonardo da Vinci first showed, characterize life and, more generally, the process of evolution.

References

Callahan, Philip S. 1985. "Insects and the Battle of the Beams." *Fusion* 7(5): 27 (Sept.-Oct.).

Frazer, James. 1985. "New Frontiers of Biophysics." *IJFE* 3: 63.

Hunt, J.E. et al. 1983. "Energy-transfer Processes from the Excited Singlet Manifold of Chlorophyll." *Chemical Physics* **82**: 413.

Katz, Joseph J. 1979. "Structure and Function of Photoreaction-centre Chlorophyll." *Chlorophyll Organization and Energy Transfer in Photosynthesis*, CIBA Foundation Symposium **61** (new series), Excerpta Medica.

_____. 1979. "Chlorophyll-lipid Interactions." In *Advances in the Biochemical Physiology of Plant Lipids*. Eds. L.A. Applequist and C. Liljenberg. Elsevier: North Holland Biomedical, p. 37.

Norris, J.R. et al. 1979. "ENDOR Spectroscopy of the Chlorophylls and the Photosynthetic Light Conversion Apparatus." *The Porphyrins*, **IV**, Academic Press.

Norris, J.R. et al. 1980. "Electron Spin Echo Spectroscopy and the Study of Biological Structure and Function." *Advances in Biological and Medical Physics* **17**: 365.

Acronym List

Chl	Chlorophyll
EPR	Electron paramagnetic resonance, sometimes called ESR
ESR	Electron spin resonance
ENDOR	Electron nuclear double resonance: NMR and EPR are used together
ESE	Electron spin echo
NMR	Nuclear magnetic resonance
PTU or PSU	Photosynthetic unit
P700, P670	Components of chlorophyll with peak spectral absorption at 700 nm and 670 nm respectively
PRC	Photo-reaction center

Modeling Chromophore Interaction with Protein to Alter Its Spectral Absorption

by Carol Shaffer Cleary

The "tuning" of chlorophyll, as described by Ned Rosinsky (p. 61), suggests the question of how other biologically active chromophores are tuned. An interesting and closely related example in green plants

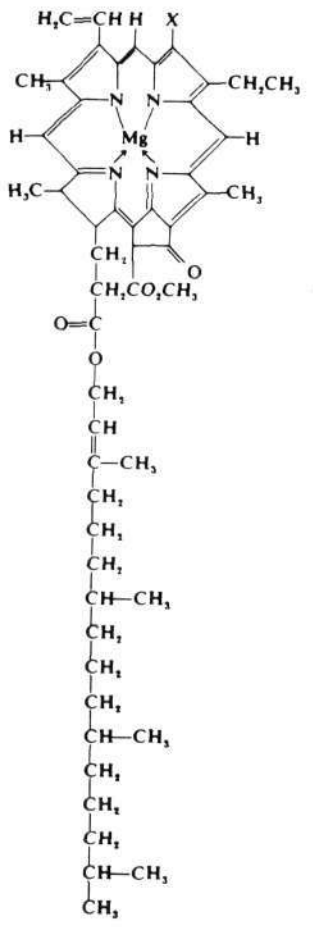

Figure 1. Chlorophyll, shown here, has a closed tetrapyrrole ring. Unlike phytochrome, it does not contain protein.

is the issue of how plants "sense" such spectral changes as the length of day, which is known to somehow stimulate both subtle and radical changes in the physiology of the plant, such as flowering. Each species of flowering plant has a characteristic season in which it blooms, which has been shown to be directly related to the length of night under artificially controlled conditions. By examining the specific frequency of light that controls this plant behavior, and correlating this action spectra with the variety of plant pigments, or chromophores, the particular pigment responsible has been identified as the phytochrome.

Interestingly, phytochrome bears a strong resemblance to chlorophyll (Figure 1). Notice that one of the major differences between phytochrome and chlorophyll is that the macrocycle (overall chain) is not closed (Figure 2). The fact that it is not closed allows for a different sort of tuning from that occurring in a chlorophyll that contains a photo-reaction center (PRC). In photosynthesis, the PRC is tuned by a process of dimerization that effectively increases the size of the antennae—the chlorophyll chromophore. In the case of the chromophore of phytochrome (phytochromobilin protein), the open topology of the tetrapyrrole chromophore allows for a more subtle tuning involving degrees of straightening or bending of the tetrapyrrole chain.

This is a fascinating example of pathways in biological evolution in which a change in topology opens up an entirely new area for biological differentiation.

Phytochrome is a biliprotein—an open chain tetrapyrrole chromophore embedded in a 120,000 molecular weight (MW) protein to which the chromophore is covalently linked.

Like phytochrome, biliproteins in their native state—embedded in protein—have spectral properties drastically modified by that protein (Figures 3 and 4). When the bulk of the protein is cleaved off, such as by means of boiling methanol, the remaining bilin chromophore, with its 10-15 amino acid peptide fragment attached, curls up into an unclosed ring. This unclosed ring behaves spectrally very much like free bilin chromophores. The chemical structure of phytochromobilin—this unclosed ring—was confirmed by total synthesis of the racemic compound (Weller, Grossauer 1980).

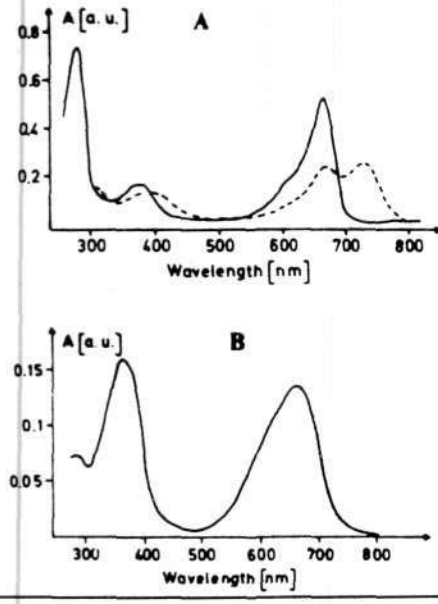

Figure 3. Electronic spectra of phytochrome and its 11 amino acid chromopeptide. The electronic spectra for native P_r, the inactive form of phytochrome (solid line) and P_{fr}, the active form of phytochrome (dashed line) are shown in (a). Both P_r and P_{fr} are in 0.1 molar sodium phosphate buffer, pH 7.8. Phytochromobilin 11 amino acid peptide in 10 percent acetic acid as shown in (b).
Source: Rüdiger, et al. 1983.

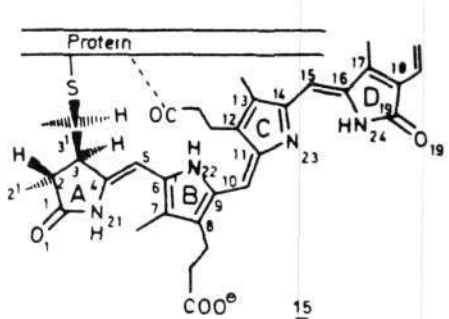

Figure 2. The chromophore of phytochrome, in contrast, has an open tetrapyrrole chain.

In plants, phytochrome builds up in large concentrations in the dark. This dark, inactive form of phytochrome (P_r) has an absorption spectrum maximum at 660 nm. Exposure to light in the 600-660 nm range converts this inactive phytochrome to P_{fr}, an active form that has an absorption spectrum maximum around 730 nm. The active P_{fr} form of phytochrome is energetically unstable and can ordinarily revert back to the P_r form in the dark as well as in the presence of far red light.

$$P_R \underset{730\text{ nm}}{\overset{660\text{ nm}}{\leftrightarrows}} P_{FR} \rightarrow\rightarrow\rightarrow \text{Biological Activity}$$
$$\uparrow \quad \text{In dark} \quad \uparrow$$

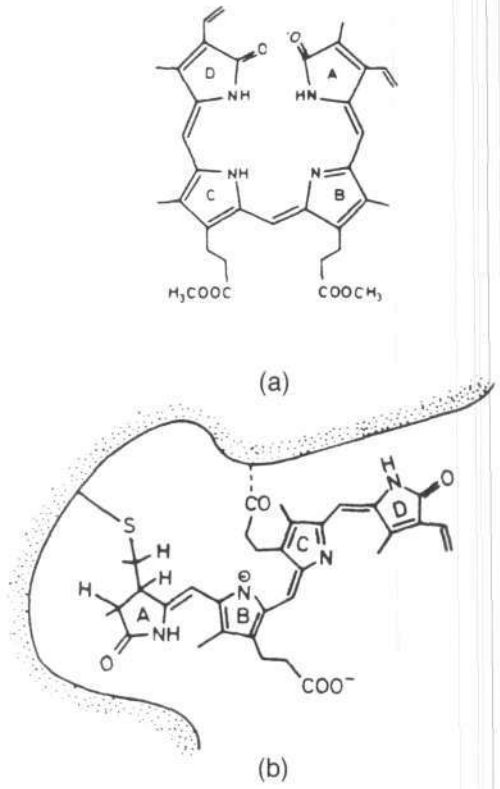

Figure 4. Once the main part of the protein is cleaved off, the phytochromobilin chromophore curls up in a ring (a). Note that the ring isn't closed at the top; the two oxygens are not bonded together. In its native form, with its full 124,000-MW protein attached, the phytochromobilin chromophore is held open in a bent position (b). **Source:** Rüdiger, et al. 1983

Both the phototransformation from P_r to P_{fr} and P_{fr} to P_r are multistepped reactions (Lagarias 1980).

In its natural state, the protein part of the phytochrome provides a matrix for the chromophore to be maintained in a confirmation that is opened up—a stretched out tetrapyrrole that may be tuned continuously by different degrees of bending. Both photoconversions involve conformational changes in the chromophore and its protein. While the protein holds the chromophore in a matrix in which finely tuned spectral shifts are possible by conformational changes, the stimulation of P_r with light alters the chromophore's conformation in a way that, in turn, forces the protein into a new conformation—its active form. Hence, the two are mutally interdependent. This spectral fine-tuning interdependence of the protein and the open-chain tetrapyrrole chromophore are supported by the fact that denaturation of the protein, under conditions that should not alter the chromophore chemically, leads to a loss of photoreversibility, a large bathochromic shift (shift toward the blue, see Figure 3) in the visible absorbance peak, and a reduction in extinction coefficient (Smith 1983).

The same sort of bathochromic spectral shift toward the blue or free chromophore spectrum can be achieved by degrading the phytochrome protein, such as by unfolding it in guanidinium chloride (Grombein 1975).

In vivo, in solution, and even in very dilute solution, the 120,000-MW phyrochrome is found as a dimer noncovalently-linked complex. Equilibrium centrifugation gives a molecular weight twice that of the monomer obtainable by denatured electrophoresis. Gel filtration indicates that this dimer has an elipsoidal—nonspherical—geometry (Smith 1983). Little is now known about the effect this dimerization has on phytochrome function. One cannot yet rule out that dimerization may create some allosteric interactions, as are found in hemoglobin.

Phytochrome research might appear to be the biochemist's dream system, being a soluble protein chromophore somewhat analogous in the plant world to the model protein chromophore hemoglobin in the animal world, particularly since phytochrome is readily perturbed in a well-defined way in response to light. However, in reality, phytochrome research has been plagued by the poor stability of the phytochrome. Only five laboratories in the world have been able to isolate reasonably stable phytochrome that appear not to be denatured, and this progress in phytochrome preparation has occurred only in the last five years. Although these laboratories have produced preparations that are stable enough not to denature in the middle of an experiment, they are not stable enough to ship. Unfortunately, these isolation procedures are not trivial. Prior experimentation on phytochromes, in retrospect, has been found to be on denatured phytochrome, creating much confusion in the literature as older data are reevaluated and, in some cases, experimentation repeated. Some of the inconsistencies in current data may still be due to the possibility that some laboratories are working with purified undegraded phytochrome mixed with some partially degraded phyrochrome (Smith 1983).

Considerable work has been done on the 11-peptide fragment chromophore of phytochrome with nuclear magnetic resonance (NMR) by J. Lagarias at Lawrence Berkeley Laboratory at the University of California and by W. Rüdiger at the University of Munich in West Germany. Pill-Soon Song at Texas Tech University in Lubbock, Tex., has begun work with the full 120,000-MW phytochrome protein using NMR. Partly because of the concentrations of phytochrome

needed and its instability, work with electron spin resonance (ESR), electron spin echo (ESE), and electron nuclear double resonance (ENDOR) has not yet been attempted on phytochrome. Phytochrome does not have a metal cation and the chromophore is not paramagnetic. Hence, to use ESR, ESE, or ENDOR, one would need to spin label—preferably with an organic spin label like anoxide—some amino acid near the chromophore and probably also, in a separate experiment, spin label one away from the chromophore to look for conformational changes.*

Peter Quail at the University of Wisconsin, Madison, is preparing ground-breaking work that will enable him to utilize recombinant deoxyribonucleic acid (DNA) to alter the amino acid sequence in the 120,000-MW phytochrome protein. Quail's group has now cloned the gene for the phytochrome of oats, and derived its amino acid sequence. His group has also begun studying the genetic control of that gene in preparation for such recombinant DNA work.

Deliberate man-made alterations in the protein part of the phytochrome would provide, in combination with the sophistication of NMR, ESE, ESR, and ENDOR, an opportunity to elaborate the role the protein plays in altering or tuning the tetrapyrrole chromophore spectrally to absorb specific wavelengths. A better grasp of how the protein and chromophore interact to shift the spectrum will be crucial for the agriculture of the 21st century, for as man colonizes other planets, he will need to know how to alter the ubiquitous tetrapyrrole ring, which plays many different roles, with different absorption spectrums in the evolution of life.

References

Grombein S., et al. 1975. "The Structure of the Phytochrome Chromophore in Both Photoreversible Forms." *Hoppe-Seyler's Z. Physiol Chem* **356**: 1709.

Lagarias, J., et al. 1980. "Chromopeptides from Phytochrome, the Structure and Linkage of the P, Form of the Phytochrome Chromophore" *J of Amer Chem Soc* **102**: 4821.

Smith, W.O. 1983. "Phytochrome as a Molecule" *Encyclopedia of Plant Physiology New Series*, Vol. 16: *Photomorphogonesis*, ed. W. Shropshire Jr. and H. Mohr, Springer-Verlag Berlin Heidelberg.

Weller, J.P., Gossauer A. 1980. "Synthese und Photoisomerisierung des Racem. Phytochromobilindimethylesters" *Chem Ber* **113**: 1603.

Note

*Such a project would cost about $30,000 a year: $20,000 for a postdoctoral student and $10,000 for supply money, assuming the availability of the necessary equipment at an appropriate research center that has learned to isolate purified undenatured phytochrome in a relatively stable form. This is definitely the sort of project that should be funded.

The Plant Cell Wall: Crucial in Plant Tissue Differentiation and Defense Against Invading Microbes

by Carol Shaffer Cleary

Complex carbohydrates are crucial in cell-cell recognition in humans and animals, as the work of James Frazer shows (Frazer 1985), which is vital to tissue-tissue recognition in rejection of cancers or foreign tissue transplants, including blood type rejection. Complex carbohydrates in a similar way are crucial in the bacterial and plant world. Unlike animals, plants and microbes have a cell wall in addition to the cell membrane. In the plant world and microbial world, the cell wall is the first line of communication with the environment, including defense against pathogenic agents.

The cell wall of the growing plant cell (called the primary cell wall) consists of roughly 90 percent polysaccharides and 10 percent glycoproteins, plus some methyl, acetyl, feruloyl, and other esters. The polysaccharide component includes both long polymerized linear polysaccharides, cellulose, and very complicated branching polysaccharides called matrix polysaccharide. Twenty to 30 percent of the primary cell wall is cellulose, organized as microfibrils consisting of 40 linear chains of D-glucose linked by beta glycosidic bonds between the first and the fourth carbon. Sixty to 70 percent of the primary cell wall is matrix polysaccharide, composed of two or more sugars connected by several kinds of glycosidic bond—generally generating branching structures.

For example, rhamnogalacturonan, a matrix polysaccharide, is composed of 65 units of 10 different sugars, linked by alpha and beta bonds in 20 different ways. Rhamnogalacturonan makes up 3 percent of the primary cell wall in dicotyledons—plants with broad leaves with netted vein patterns, like tomatoes and soybeans—and less in both monocotyledons—plants with narrow leaves with parallel veins like grasses and grains—and gymnosperms—plants like conifers and ferns (McNeil 1984).

Involvement in Tissue Differentiation

It has been widely observed that the newly laid down cellulose microfibrils in the primary plant cell wall run parallel to each other, wrapped around the cell much like thread wrapped around a spool, and that these microfibrils are perpendicular to the cell's principal axis of growth. The orientation of these microfibrils is assumed immediately after cell division, and is apparently indirectly controlled by the microtubules. This orientation, combined with the turgor stresses on the outer epidermal wall, determines

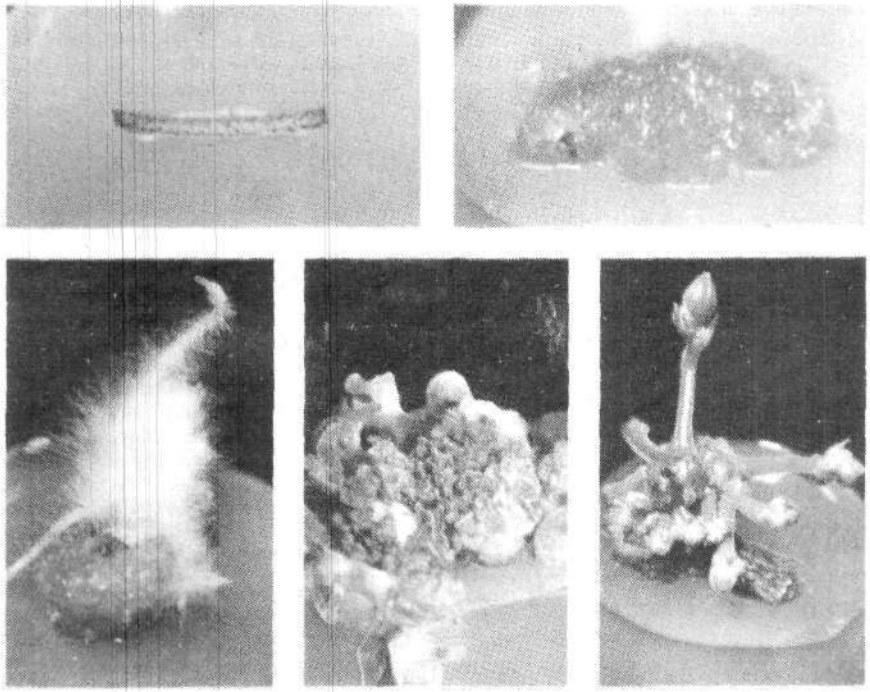

Single explants of the flower of a tobacco plant grown on solid azar. Top left, explants; top right, differentiation into undifferentiated callus; bottom right, floral shoots; bottom center, vegetative shoots and leaves; bottom left, roots exposed to oligosaccharins. The active heptaglucoside fragment, which appears as the dark area in the bottom center photo, is an elicitor for soybean production of phytoalexins in response to invasion by a fungus. This is the first oligosaccharin identified by Albersheim's group to play a role in plant cell defense.
Source: Peter Albersheim and Alan G. Darvill, "Oligosaccharins," *Scientific American*, **253**: 64 (Sept. 1985).

whether grass shoots straight up or curls around itself, and is very closely tied to the golden mean relationships of developing leaves spiraling out of the stem at the apial meristem or the petals spiraling out of the base of a flower (Green 1980).

As the primary cell wall matures into its more rigid final form, called the secondary cell wall, cellulose becomes much more polymerized with the microfibrils becoming thicker and carefully crosslinked in their parallel arrangement by hydrogen bonds. This gives the cellulose of the secondary cell wall a high degree of crystallinity, thus maintaining plant organ shape in a well-defined orientation (McNeil 1984).

One of the glycoproteins in the cell wall, peroxidase, can oxidize and inactivate the plant hormone, indoleacetic acid. The synthesis and secretion of peroxidase is modulated by various environmental influences, including light, temperature, drought, salinity, and plant growth regulators. Thus it may be a crucial link in the observed dependency of plant cell response to plant hormones on physiological and environmental factors (McNeil 1984).

Indoleacetic acid is an auxin, a hormone that generally increases the plasticity of the cell wall and increases the motion of hydrogen ions out of the cell. High concentrations of auxin in the stem tip stimulates cell division, but high concentrations at the root growth tip inhibit root growth. Lower concentrations of auxins in the stem of the plant stimulate cell elongation, but lower concentrations in the nongrowth tip area of the root stimulate root growth. Diminished production of auxins in the leaves stimulate abscission, part of the process by which deciduous trees (in autumn) and other plants shed their leaves. When applied to the stigma of the fruiting body of the plant, auxin causes the production of seedless fruit. The pleiotropic role of the auxins is typical of plant hormones—each triggers a multitude of different responses in different tissues, and even different responses at different concentrations in the same tissue. Not all the pleiotropic roles of each plant hormone are yet known, nor is the exact mechanism by which these responses are activated in the plant cell.

Peroxidase is also hypothesized to catalyze the crosslinking of extensin. Extensin is another glycoprotein, but unlike peroxidase, it is very tightly bonded covalently to the plant cell wall. Extensin is hypothesized to help restrict cell expansion. A negative correlation has been observed between plant growth rate and peroxidase concentration (McNeil 1984).

Kiem Tran Thanh Van's group at the Laboratoire du Phytotron at Gif-sur-Yvette, France, developed a tissue culture system for testing the impact of potential growth factors, such as plant hormones, added to a

culture medium on which thin strips of tobacco plant flower stem are floated (see figure). They found that the ratio of auxin to cytokinin and the acidity of the culture medium determined whether these tobacco explants formed undifferentiated callus, flowers, vegetative buds, or roots. In collaboration with Albersheim's group at the University of Georgia in Athens, they tested mixtures of oligosaccharides isolated from sycamore cells added to the culture medium. Different mixtures of oligosaccharins prompted explants to form roots rather than the otherwise expected vegetative buds; or vegetative buds rather than the otherwise anticipated flowers. The oligosaccharins were present in 1/100 to 1/1,000 of the concentration of the auxins and cytokinin present in the medium. A cooperating group has begun to look at whether oligosaccharins can be used to help solve the great impasse in plant tissue culture: teasing monocotes to redifferentiate whole plants out of a single cell. Until this impasse is resolved, recombinant DNA advances in grain cultivars will be very difficult (Tran Thanh Van 1985).

Involvement in Defense Against Pathogens

To attack plant tissue successfully, pathogens must penetrate the walls of the plant host. To accomplish this, pathogens secrete a mixture of cell wall degrading enzymes. Plants have proteins within the cell wall that may inhibit specific wall-degrading pathogen enzymes (extensin) and also some enzymes that can degrade microbial walls. Hence, each side bombards the other with chemical warfare until one side triumphs, leaving the other's cell wall in shambles. In this chemical bombardment, both glycoproteins and oligosaccharins in the cell wall play a key role.

Research has discovered a positive correlation between disease resistance and high concentrations of the glycoprotein extensin (or high concentrations of its precursors) found in the plant cell wall. One of the hypothesized mechanisms for this result is the observed high resistance of extensin to protein digesting enzymes that the pathogen produces to help digest the plant cell wall. Another hypothesized mechanism is that extensin, as a polycation, agglutinates bacteria and thus prevents their spread (McNeil 1984).

One of the ways plants defend themselves chemically from microbial onslaught is by secreting nonprotein antimicrobial compounds of low molecular weight, called phytoalexins. These phytoalexins are the rough equivalent of antibodies. Phytoalexins are not present in healthy plants, but are synthesized de novo in response to elicitors. After exposure to elicitors, plant cells in tissue culture stop growing, and begin synthesizing the messenger RNA and enzymes required for the de novo synthesis of phytoalexins. The concentration of phytoalexins produced is contingent on the physiological state of the plant—nutritional status, water availability, temperature—the genetic background of the plant, the nature of the invading microbe, and the time of day. Phytoalexins are eventually catabolized—broken down or detoxified—by both plant tissue and microbes. Thus, the plant, through the use of specific elicitors, is able to rechannel its limited margin of energy away from growth to meet the challenge of an invading microbe, and later channel that energy back into growth again (Darvill 1984).

Albersheim's group has done research indicating that these elicitors are oligosaccharins: polysaccharide fragments of the branched matrix polysaccharide cleaved off the plant or microbial cell wall as part of the molecular warfare involved in this battle of the cell walls. These oligosaccharin fragments activate surrounding plant tissue to synthesize phytoalexins. For example, soybean phytoalexin, synthesized under challenge by a fungus, is elicited by a heptabetaglucoside—a seven glucose unit polysaccharide interconnected by beta-glycosidic bonds—cleaved by a soybean enzyme from the fungal cell wall. When the appropriate active heptaglucoside fragment was isolated from the fungal cell wall, it was found to stimulate phytoalexin production in concentrations of one-billionth (10^{-9}) of a gram. An oligogacturonide—a linear array of galacturonic acid units—cleaved from the soybean cell wall is the elicitor for soybean phytoalexin synthesis in response to challenge by several bacterial species. Oligosaccharides also stimulate phytoalexin when a plant tissue is damaged by bacterial fungal or viral attack without direct exposure to microbial enzymes. Such research has tremendous potential for application in agriculture, as it advances further in delineating the plant's equivalent of an immunological response (Albersheim 1985).

Hence, complex carbohydrates, once thought to be primarily structural polymers and energy reserves, are turning out to be highly chemically differentiated intermediaries for the plant's interaction with its environment.

References

Albersheim, Peter. 1985. "Oligosaccharins," *Scientific American* **253**: 58 (Sept.)

Darvill, Alan. 1984. "Phytoalexins and their Elicitors—A Defense against Microbial Infection in Plants," *Ann. Rev. Plant Physiol* **35**: 243.

Frazer, James. 1985. "New Frontiers in Biophysics." *IJFE* **3**: 63.

Green, Paul B. 1980. "Organogenesis—A Biophysical View," *Ann. Rev. Plant Physiol.*, **31**: 51.

McNeil, Michael. 1984. "Structure and Function of the Primary Cell Walls of Plants," *Ann. Rev. Biochem.* **53**: 625.

Tran Thanh Van, Kiem. 1985 "Manipulation of Morphegenetic Pathways of Tobacco Explants by Oligosaccharins" *Nature* **314**: 615.

How Does Hormesis Work and Is It Necessary for Life?

by Wolfgang Lillge, M.D.

In recent years, significant progress has been made in developing devices that are able to detect the tiniest concentrations of substances in our environment. The sensitivity of these sensors reaches down to the nanogram and terragram regions; that is, they can detect a one-billionth or one-trillionth part of a gram substance in a given volume. While this has led to a remarkable increase in our knowledge of certain processes in nature, the same success has encouraged environmental fanatics to fabricate one horror story after another about how mankind has "poisoned nature" and will thereby destroy itself whenever the existence of traces of certain chemicals have been detected in the air, in the soil, or elsewhere.

Similar scare stories have been spread by the environmentalists that nuclear power plants will pollute nature to a degree that people living near such sites will die like flies after being exposed to even very low doses of radiation.

The reality is quite the opposite. For at least eight decades, scientists have examined the effects of low doses of a wide variety of potentially harmful agents, including ionizing radiation. They employ the concept of *hormesis*, a Greek word that means "stimulation." In other words, toxic substances and radiation that are lethal at high doses demonstrate at low doses *beneficial* effects on plants, animals, and humans.

In fact, every vaccination against an infectious disease is a hormetic effect, stimulating the immune system to produce a sufficient amount of antibodies that can be called into action when the body is exposed to an actual viral or bacteriologic attack.

In the case of ionizing radiation, it has also been established that low doses of X-rays or gamma-rays have beneficial effects for a living organism. In other words, one of the key theories used by antinuclear groups to justify their demand to shut down nuclear power plants—that there is "no safe dose" of radiation—is a lie. The "dose/effect curve" of ionizing radiation, according to the hormesis findings, is not linear. For example, the death rate at an obviously lethal level does not linearly extend back to zero; at a certain point a phase change occurs, transforming deadly radiation into a stimulating effect for life.

Researchers like T.D. Luckey (1980), a pioneer in hormesis work, suggest that such low levels of radiation not only can be tolerated by living organisms, but are, in fact, the precondition for life on this planet. Luckey reports on experiments by other researchers with protozoa cultures shielded from ambient radiation by lead containers that showed a markedly lower cell reproduction rate compared to a control culture. Interestingly, the lowering of cell counts was proportional to the thickness of the lead shielding.

There is an array of other experiments with low doses of ionizing radiation that support the idea of hormesis:

- Animal and plant growth rates were increased in the order of 20 to 150 percent, depending on the experimental procedure. In animals, it was found that a parallel stimulation of neurological functions occurred: increased cerebral blood flow, brain development, excitability of brain and nerves, audio and visual acuity.
- Animal cell cultures showed increased mitosis and cell divisions; animal fecundity was increased.
- Low doses of whole body irradiation may reduce tumor induction and its subsequent growth.
- Preexposure to radiation seems to increase an individual's resistance to subsequent lethal doses of radiation—radioresistance.
- Skin wounds in animals healed faster when the animal was first lightly irradiated with radium.
- Low doses of radiation made animals more disease resistant. Radiation also has an "antitoxin effect"; irradiated rabbits survived longer after injections of diphtheria toxin. And a thymus hormone that controls T-cell maturation was increased in the serum of irradiated mice.
- The average lifespan of lightly irradiated animals and insects was lengthened.

Effects on the Immune System

It seems that one of the primary structures affected by low doses of ionizing radiation is the immune system. This connection is suggested not only by an increase in T-cell counts after low dose irradiation, but also by the universal role the immune system plays in almost all the processes mentioned above: fighting infections and cancer, influencing the central nervous system, and controlling the aging process.

Although it is not yet possible to "radiovaccinate" people against lethal doses of radiation in case of a Soviet nuclear attack, the most interesting application of the hormesis effect today is the stimulation of plant seeds by low doses of ionizing radiation. Many experiments have been conducted showing that after irradiation with a selective low dose air-dried seeds of most investigated plant species demonstrate an increase in the energy of germination, an acceleration of growth and development of the seedlings, an increase in green mass, an enlargement of the shoots bearing the generative organs, an earlier blooming, and an increase in yield. The doses of irradiation differ

for different plant species with different radiosensitivity.

Recently in Canada, more systematic experiments with irradiated seeds were undertaken to determine the initial dose/effect relationship for different kinds of crops. Although it is possible to generate some increase in yield in all cases of irradiated seed, it is currently still a major disadvantage that the results vary too much with different plant species and even within one crop itself, depending on moisture content, age of the seeds, and so forth.

The difficulties in achieving a standardized procedure in seed irradiation largely reflect the problem scientists have in coming up with a coherent explanation about how low doses of ionizing radiation actually affect stimulation of plant and animal growth.

Admittedly, this is a difficult question to answer because, in general, the role of radiation of any kind and intensity in living matter is as yet only poorly understood. The fact that a nonlinear phase change from a lethal to a beneficial effect is involved adds another methodological difficulty, even more so because in the scientific community, the belief in linear processes and relationships is as widespread as among nonscientific environmentalists. Therefore, serious research in what very broadly can be described as hormesis is quite limited, and is viewed by the prevailing scientific schools as insignificant—or even bordering on witchcraft. In fact, many of those working in the field itself are blinded by a mechanistic epistemology that prevents progress in these questions.

The Conference on Radiation Hormesis that took place in Oakland, Calif. Aug. 14-16, 1985 was characteristic of this state of affairs. Participants from around the world exchanged the results of their latest experiments and calculations about effects of low doses of ionizing radiation ranging from cancer to seeds and A-bomb survivors, the immune system, and animal growth. Interesting as all these observations and discussions may have been, the conference organizers did not encourage speakers to go beyond this descriptive level and address the *causal* events behind the growth effects being observed.

Ironically, Russian science, not represented at the Oakland conference, has for quite some time approached the radiation stimulation question from a more rational point of view. It is not surprising, therefore, that many Russian scientific papers deal with basic questions about low levels of radiation in nature.

Electromagnetic Action in Nature

Natural scientists in the tradition of Bernhard Riemann and the Göttingen School in Germany have always viewed processes in nature as coherent events that are of a negentropic, self-organizing character; thus all action in the universe, from astronomical down to submicroscopic levels, must have something basically in common and cannot be interpreted as random, "statistical" events that might or might not have taken place.

The Russian scientist Alexander G. Gurvich, who was educated in Germany around the turn of the century, proposed studying biological growth patterns, especially embryologic growth, using a field conception that would impose a specific geometry on the cell tissue determining its future structure.

Basing his ideas on Plato's demand that geometry is primary, Gurvich states in a book written in the 1930s that any "object of preformation [like an egg or seed] does not appear as a fixed state, but as a process, and since we can subsume under it the whole individual life cycle, we even can talk about a 'life line.'"

Such thoughts are key in studying external influences on biological processes like radiation. Continuing his geometric approach, Gurvich says, "The standard influence on cell trajectories could also be achieved by the circumstance that the field influences the inner condition of the cell, i.e. directly inhibits or stimulates certain system-own factors in their efficiency."

Whatever the external influence on the geometry of life may be, with respect to embryonic development, it will affect the entire "life line" of an individual organism. Such an approach is, of course, very much in opposition to molecular biology today, and Gurvich denies any reality to concepts that are not strictly based on a geometric method: "The conclusion is that the material particles in living systems do not possess degrees of freedom provided to them by laws of diffusion, but are bound to traverse certain trajectories."

Such general considerations are necessary to keep researchers on the path in reviewing hormetic effects in a living organism.

As mentioned above, Russian and East bloc research in this field is very strong, in comparison to work in the United States and Western Europe. The work of A.M. Kuzin from the Institute of Biological Physics, Academy of Sciences of the U.S.S.R., Pushchino, is of some interest (Kuzin 1972). Kuzin, even if he is clearly not in the direct tradition of Gurvich, discusses the mechanisms of radiation stimulation on a higher conceptual level than usually seen in the West.

First, Kuzin describes the effect of stimulation of low doses of X-rays or gamma-rays in plant seeds as a "wave-like manifestation in time," namely, that at different phases of plant development (germination,

formation of the generative organs, blooming, ripening of the fruit) a more rapid growth rate can be observed compared to a control plant. However, in the intermediate phases, the control plant catches up with the irradiated one, and the higher crop yield of the irradiated seed seems only to be the result of the larger number of generative organs and the longer period of ripening of the plants that bloomed earlier.

This important observation, which generally goes unnoticed, suggests a continuous stimulation over the whole "life line" of the plant, but not in the form of a genetic change in the DNA structure. On these grounds, Kuzin dismisses as absurd two of the main hypotheses about hormetic effects:

First, he dismisses the "toxicological hypothesis of radiostimulation," which stipulates that the decomposition products of proteins that result from irradiation are the effective toxic agents involved. An "intoxication," he says at most could explain a very short-term stimulatory effect, but would be entirely inadequate to account for the wave-like manifestation of the effect of stimulation at all stages of development and in the process of formation of the yield.

Second, he dismisses the assumption that when seeds are irradiated at stimulating doses, point somatic mutations occur in a number of cells that lead to the appearance of clones of cells with a somewhat changed metabolism in the tissue during the development of the plant. This theory, Kuzin says, is purely speculative, and does not reveal the actual causes of stimulation. Furthermore, it cannot explain the stimulation of the initial processes of germination of the seeds, nor the phenomenon of stimulation in single-celled organisms.

Before discussing his thoughts about molecular interaction in the cell after weak irradiation, Kuzin poses the important question: are there similar phenomena of stimulation in simpler chemophysical systems with only one or a few molecules involved. His finding is that irradiation of a homogeneous solution of only one molecule may lead merely to a change of the property of this one molecule.

The precondition for a stimulatory effect, Kuzin concludes, is the presence of at least two different molecules, especially systems where one compound influences the properties of another or where a reaction between these molecules is possible.

The simplest model exhibiting stimulation in this sense are substrate/enzyme systems like tyrosine and tyrosinase; in addition, phosphofructokinase—a key enzyme of glycolysis—can be stimulated substantially in vitro by weak irradiation with doses of 0.5-1.0 kR.

In the next step, on the level of the seed, Kuzin was able to demonstrate using the method of electron paramagnetic resonance that, both in the outer membrane and in all the inner structures of the seed, free radicals are formed after irradiation with low doses of X-rays or gamma-rays—that is ionizing radiation—because its high-energy quanta knock out electrons from selected molecules that themselves will transform neighboring molecules into free radicals as well. Thus a chain reaction of events occurs, leading eventually to a stimulation of enzymatic activity.

Another key observation provided by Kuzin is an increase in the permeability of biomembranes after irradiation, that, in the case of a plant seed, would lead to an increased influx of water and oxygen, starting the first stages of germination. The larger the dose of ionizing radiation, the greater the increase of the permeability.

Up to this point, everything that Kuzin says makes sense from an experimental and methodological standpoint. All his subsequent conclusions, however, respecting the formation of "nonspecific and specific trigger-effectors as the basic cause of stimulation at all stages of development" fall back into molecular systems analysis of genetic code models that are not based on causality. As the primary trigger of stimulation is obviously located in the high-energy quanta of ionizing radiation, there is no reason to believe that radiation and its side-effects suddenly cease to play a role in the subsequent growth processes. Quite the contrary, it is only at this point that the actual role of electromagnetic action might start, supporting and accelerating processes in the cell that normally take place there anyway. It seems as if Kuzin stares at the free radical as the one object he was looking for, and forgets about Gurvich's basic concept of the *process* as being primary.

The Role of Laser Light

This leads us to reconsider experimental evidence that demonstrates that laser light of specific frequencies can substantially stimulate enzyme activity. Important work in this respect has been made by J.P. Biscar, who studied "electromagnetic molecular electronic resonance (EMER) frequencies in the chains of the pancreas enzymes α-chymotrypsin (Biscar 1976). The EMER frequencies are collective electronic phenomena along the bonding electrons of large molecules like polypeptides and enzymes. Concerning α-chymotrypsin, he found that the third harmonic of the EMER frequency of one of its side chains, which normally is considered to have no "chemical" function, is transferred to the main chain, providing a critical part of the activation energy to start the enzymatic process.

This coherent action of a specific frequency trans-

ferring energy can be imitated by a laser beam of the same wavelength. When Biscar used a laser of 8,550 Å in the near infrared, exactly the wavelength he previously calculated to be effective to irradiate an enzyme/substrate mixture, he observed a strong increase in enzyme activity. Laser excitation only one-tenth Å away did not show any effect.

Similarly, highly selective excitation processes may occur in all macromolecules, including those Kuzin mentions in the context of radiation stimulation of plants: Gibberellic acid, peroxides, quinones, histones, auxin, and a "flowering factor." In absence of low doses of ionizing radiation, specific excitation energy may be provided by coherent, low-level radiation inside the cell itself with DNA as the most important "light source" (Fraser 1985; Popp 1984). Through the formation of free radicals after hormetic irradiation, harmonic effects of a similar kind as in Biscar's enzyme experiment may occur. It would require only a sufficient down-shifting of the frequency of the free electron created in the cascadic events following the radical formation. These same electron frequencies could couple into the molecular frequencies involved in cellular membranes that are generated by the high charge between inner and outer surface of the membrane. So, the free radical as a molecule might not even be of primary interest as a trigger for stimulatory action, but actually more a destructive force that leads to the death of the cell when generated in too large amounts.

Harmonic mode-coupling may very well explain the increased membrane permeability without resorting to the mechanistic concept of hole-punching by superreactive radicals or pump mechanisms to increase the influx of water, oxygen, proteins, and other substances. There is evidence that the cell membrane is primarily a function of charge distributions and charge redistributions (Fraser 1985).

It is known that glycoproteins and lipoproteins associated with the membrane have a spectral and acoustical wave selectivity, and that charge shifts along large chain molecules can alter potentials at distances long enough to penetrate membranes, and thus induce alterations of intracellular ion dissociation potentials. Oxygen and calcium transport through membranes may take place in this way.

Therefore, irradiation with low doses of ionizing radiation must be explained within the context of coherent electromagnetic action in the cell whose efficiency is being increased by such action. Considering free radicals, enzymes, "factors," and so forth, as mediators for such coherent transformation would open up new insights in biophysics.

Seed irradiation, one of the most obvious applications of hormetic effects, could lead to major improvements in agriculture, including in the Third World. Only recently, spearheaded by the Ionizing Energy Company in Canada, have any efforts been made in the West to develop commercial mobile X-ray seed stimulation systems. In contrast, in Hungary, as reported in 1984, already 10,000 acres had been planted with radiation-stimulated seed. In addition, there is a huge amount of research going on, especially in the Soviet Union. Have the Russians (and their environmentalist fellow-travelers in the West) succeeded here in scaring the West away from using "dangerous" radiation, while they themselves apply it on a broad scale?

References

Biscar, J. 1976. "Photon Enzyme Activation." *Bulletin of Mathematical Biology* **38**: 29.

Frazer, James. 1985. "New Frontiers of Biophysics." *IJFE* **3:** 63.

Gurvich, Alexander G. 1932. "Histological Foundation of Biology." *Die Histologischen Grundlagen der Biologie.*

Luckey, T.D. 1980. *Hormesis with Ionizing Radiation*, CRC Press, 2c. Florida.

Kuzin, A.M. 1972. "Molecular Mechanisms of the Stimulating Effect of Ionizing Radiation on Plant Seeds." *Radiobiology* **12**: 635 (Moscow).

Popp, F.-A. 1984. *Biologie des Lichts: Grundlagen der Ultra-schwachem Zellstrahlung.* Berlin: Verlag Paul Parey.

Research on Cannonball Targets with Carbon Dioxide Lasers

by Charles B. Stevens

Based on: M. Fujita et al, Jpn. J. Appl. Phys., **24:** *737 (1985); H. Azechi et al.,* Jpn. J. Appl. Phys., **20:** *L477 (1981); K. Yamada et al.,* Jpn. J. Appl. Phys., **51:** *280 (1982).*

The two basic approaches to inertial confinement fusion are: direct drive, in which the beam energy is deposited directly upon the target surface leading to an ablative implosion; and indirect drive, in which the beam energy is deposited within a chamber (holhraum) and is converted to other forms of energy, such as X-rays, which then drive the implosion of the fusion fuel target. Although possibly necessitating greater amounts of total beam energy, the indirect-drive approach has been credited with having better characteristics in terms of producing symmetric, isentropic implosions of fusion fuels with greater hydrodynamic efficiencies. The most detailed theoretical and experimental published research on indirect-drive targets

comes from scientists in the Japanese inertial confinement program.

While research in the United States on inertial confinement fusion with the relatively long wavelength carbon dioxide lasers has apparently come to an abrupt halt with the sudden removal of funding for the Los Alamos Antares carbon dioxide laser fusion research facility, many U.S. scientists have suggested that carbon dioxide lasers could overcome the disadvantages that have been experimentally detected with regard to poor coupling characteristics found in long wavelength carbon dioxide irradiation of direct-drive configurations, if innovative indirect-drive targets were developed. In lieu of the recent Los Almos cut-off, the only program apparently carrying such an effort is that of the Institute for Laser Engineering at Osaka University in Japan.

Cannonball Targets

One practical configuration for indirect drive is detailed in Figures 1 and 2—the Osaka cannonball design. Laser beams are directed through small openings in a hollow chamber and the laser light becomes trapped within the chamber. The fusion target to be imploded is placed at the center of the chamber. This configuration has several general advantages over direct drive ablation targets. High absorption and high hydrodynamic efficiency can be achieved because of the confinement of the energy in the cavity. High uniformity in implosion of the fusion fuel is also attained, because the multiple-reflection effect of the trapped laser light between the fuel target surface and the inner wall of the cannonball leads to a smooth distribution of laser energy within the cavity.

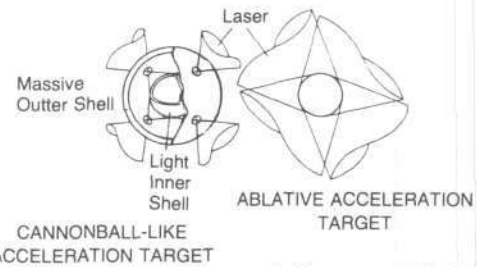

Figure 1. Comparison of cannonball target with direct-drive target.

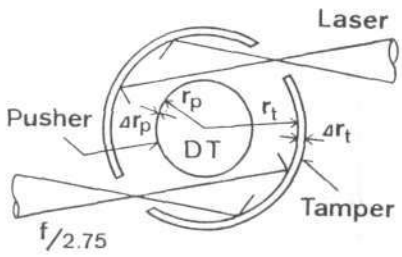

Figure 2. Schematic of cannonball target.

The cannonball is of particular application to carbon dioxide lasers, whose long wavelength leads to the generation of superthermal "hot" electrons that can penetrate to the interior of the fusion fuel in direct-drive targets, thereby causing it to be preheated. This preheating makes it impossible to isentropically compress the fuel to high densities. The cannonball provides the means of controlling the hot electron spectrum by the design of the cavity structure.

Experiments on the Osaka Lekko II carbon dioxide laser utilized planar cannonball targets. Single-sided irradiation of the planar target was effected with 30 to 100 joule nanosecond or less laser pulses. The focal spot size was 180 microns in diameter. The beam was directed at an angle of 27 degrees with respect to the normal of the planar target.

The planar targets, which did not contain fusion fuel pellets, consisted of three parts: (1) a front disk that acts as a tamper; (2) a cavity wall; and (3) a rear foil that corresponds to the pusher on a fusion fuel target, which would otherwise be within the interior of the cannonball. The hole in the front disk had a diameter of 400 microns through which the laser light was directed. A hollow aluminum cylinder formed the cannonball cavity with a volume of $.5 \times \pi \times .5^2$ mm^3. Aluminum was also used for the rear, 2-micron-thick foil. The front disks were varied, as follows: (a) 10-micron-thick gold, (b) 10-micron-thick gold with 2-micron-thick aluminum on its inner surface, and (c) a nickel wire net. The laser intensity was about 10^{14} W/cm^2. A 2-micron single aluminum foil was used as a comparative, conventional ablative target.

The cannonball target was found to have good laser energy absorption above 50 percent and a high hydrodynamic efficiency in the range of 16 percent. The numbers of "hot" electrons emitted from the rear of the type (a) cannonball target were found to be less than those seen in the single foil ablative target. This tendency was even more noticeable for type (b) cannonballs.

Overall the energetic hot electrons are mainly absorbed by the cannonball cavity wall. Their energy is thus converted into plasma generation and heating, which then effectively drives the implosive acceleration of the inner surface representing the fuel target surface in this experiment. Furthermore, low-energy hot electrons in the cavity also become useful in driving the implosion of the inner surface. It was found that the formation of the cavity structure over a plane

foil can modify the energy distribution of the hot electrons. This modification of the hot electron spectrum appears to depend on the cavity materials and geometry. Therefore, proper design of spherical cannonballs can suppress the hot-electron preheating of pellet fusion fuel that is otherwise seen in direct-drive long wavelength laser fusion.

The Los Alamos 'Trailmaster': Explosive Pulsed Power and Energy Compression Program

by Charles B. Stevens

Based on: "System Requirements for the Los Alamos Foil Implosion Project," by J. Brownell et al., presented to Third International Conference on Megagauss Magnetic Field Generation (Novosibirsk, June 12-17, 1983); "A Computational Model of Exploding Metallic Fuses for Multimegajoule Switching," by Irvin R. Lindemuth et al., J. Appl. Phys., **57** *(No. 9): 4447 (May 1, 1985).*

A wide range of frontier scientific and technological developments would derive from an economical and practical source of multimegajoule, high-power-density, 100-terawatt bursts of soft X-rays. The applications range from high-gain nuclear fusion, to materials research and development, weapons testing in a nuclear environment, X-ray laser pumping, X-ray flash radiography diagnostics, and plasma collective particle accelerators. The Los Alamos Trailmaster imploding magnetic foil program is directed at achieving this goal with pulsed power techniques that make single-shot experiments possible at costs several orders of magnitude less than those involved in more conventional approaches like high energy laser, capacitor bank, and particle accelerator facilities.

Trailmaster is based on converting chemical energy into multimegampere currents by explosive compression of magnetic fields. The resulting multimegampere currents are then compressed via electric circuits and transmission lines with fast opening switches. The compressed 50-megampere currents are then passed through thin cylindrical metallic-foil plasmas that undergo implosions in less than .5 microsecond. This would result in the release of more than 10 megajoules of X-rays at power levels approaching 100 terawatts.

These goals impose requirements that switch opening times must be less than .5 microsecond and transmission lines must withstand voltages of about 1 million volts. In order to meet these requirements, the Los Alamos Trailmaster Program has initiated pioneering work on theoretical and computational models for fast-opening plasma switches combined with experimental field tests.

High-explosive electric generators, which function through the implosion of magnetic fields, characteristically require 250-microsecond cycle times. Therefore, to compress the resulting 250-microsecond current pulse down to .5 microsecond, the development of opening switches which operate on .5-microsecond time scales is key. A transmission line utilizing such a switch would achieve a 500-fold compression of current pulses—a 500-fold increase in power.

One of the chief goals of the Trailmaster Program, therefore, is to experimentally and theoretically explore the evolution of plasma flow opening switches. This has involved investigations into the coupling of hydrodynamic, MHD, and atomic processes seen in plasma flow switches.

Force-free Plasmas Prick Big Bang Balloon

by Charles B. Stevens

Based on: A.L. Peratt and J.C. Green, Astrophys. Space Sci.,**91** *(19): 19-33, (1983); A.L. Peratt,* Sky & Telesc., **66:** *19, (1983); A.L. Peratt,* Sky & Telesc., **69:** *389, (1985); A.L. Peratt, J.C. Green, and D.E. Nielsen,* Phys. Rev. Lett., **44:** *1767, (1980); A.L. Peratt,* Sky & Telesc., **68:** *118, (1984); A.L. Peratt and C.M. Snell,* Phys. Rev. Lett., **54:** *1167, (1984).*

The two phenomena upon which empirical evidence for the big-bang cosmological hypothesis have been based are those of the experimentally measured redshift of apparently receding galaxies and the 4-degree K. isotropic microwave background radiation. However, now scientists at Los Alamos National Laboratory who are conducting experimental and computer studies of self-organized magnetic plasmas and relativistic particle beams report that they can calculate the generation of these same effects via plasma processes without need of a cosmological "big bang."

The application of large-scale computer simulations to astrophysics has only recently begun. Los Alamos simulations, in particular, have shown that much of the observed astronomical data could be replicated without need of cosmological interpretations of quasar redshifts and microwave background radiation. Based on observations of the filamentary geometry of the galactic magnetic fields, simulations of filamentary structures have been carried out with galactic-dimensioned current-conducting plasma filaments for all scale

lengths, ranging from kilometers to megaparsecs. Among the phenomena observed were: bursts of synchrotron microwave radiation lasting 10-million to 100-million years at 10^{37} watts output with output configurational contours found in double radio galaxies; compression of intergalactic plasma into a central elliptical separatrix, followed by alternating ejection of quasar-like plasmoids and jets; generation of a range of galactic forms, including spiral and Seyfert geometries, together with characteristic rotational velocities; convection of plasma into radiatively cooled filaments with a redshift; and magnetic repulsion between galaxies, causing their mutual recession.

As noted by Anthony L. Peratt in a recent letter to *Physics Today*, "The statement 'Apostles of the non-cosmological origin of quasar redshifts must now . . . recant, or else maintain that the unknown laws of physics which fix [these] redshifts . . . extend [over] appreciable distances to apparently normal galaxies. . .,' can be taken in good humor but it does preclude the possibility that we live in a plasma universe."

Exploring the Earth's Geotail

by Charles B. Stevens

Prior to making its historic fly through the tail of the Giacobini-Zinner Comet, the International Comet Explorer (ICE) was known as the International Sun-Earth Explorer-3 (ISEE-3) satellite. It had been carrying out studies of the Earth's geomagnetic tail and solar wind "bow shock" and the solar wind itself since it was launched in 1978. Karl F. Gauss was the first to initiate serious studies of the Earth's magnetic field with his founding of the Geomagnetic Union in the 19th century. Gauss directed the Union's observations toward time-varying properties in order to obtain data on the electromagnetic interactions of the Earth with the rest of the solar system. This line of research has been continued by missions such as ISEE-3.

The Earth generates a dipole magnetic field that determines much of the dynamics and configuration of the Earth's ionospheric plasma. In particular, it is the interaction of the magnetosphere with the solar wind, a collisionless plasma that flows outward from the Sun, that could be of great practical significance; it could have crucial effects on the organization of the Earth's atmosphere and definite influence on conditions for shortwave radio communication. The solar wind passage causes a distortion in the dipole magnetosphere such that a long tail is formed on the leeward side of the Earth. The ISEE-3 spent a large part of 1983 exploring this geotail between 60 to 240 Earth radii (Re).

The ISEE-3 instruments found that this geotail was by no means quiescent. Its instruments detected a wide range of phenomena: the generation and acceleration of tailward moving self-organized magnetic plasmoids; traveling compression regions; tailward jetting ions and plasma; field-aligned currents; field-aligned streaming of energetic ions and associated magnetosonic fast mode waves; and flux ropes and plasma vortices. The similarity to plasma phenomena previously detected by ISEE-3 within the bow shock formed on the windward side of the Earth by the interaction of the solar wind with the magnetosphere reveals a possible source of particle acceleration. Drift mirror waves with entrapped energetic ions were observed with scale lengths of 10,000 to 100,000 km. In at least one case, unusual magnetosheath magnetic field conditions led to asymmetric auroral features and an extremely small polar cap.

The ability to obtain these surprising new data over such a great portion of the geotail was made possible by the ingenious orbit configurations devised by Robert Farquhar and his coworkers at Goddard Space Flight Center. NASA took the "risks" of using close lunar encounters to obtain such a wide range of new spacecraft orbits. These deep tail passes have made possible many new findings in a short period of time.

(*See abstracts, p. 77.*)

Abstracts

"Current Rampup by Lower-Hybrid Waves in the PLT Tokamak"
by F.C. Jobes et al.
Plasma Physics Laboratory, Princeton University
***Phys. Rev. Lett.*, Vol. 55, No. 12, pp. 1295-1297 (Sept. 1985)**

Lower-hybrid coupling to tokamak plasmas, which gives a radio frequency (rf) lying between that of the electron and ion cyclotron range of about 1 billion hertz, has been demonstrated. Recent experiments have shown that this rf coupling can be utilized as the sole means, without aide of ohmic-heating current induction, to initiate and maintain electric currents. This report reviews the extension of this rf current-drive regime of such plasmas to include ramping up of the current in order to assist and extend ohmic-heating current induction. In order for lower-hybrid current drive to be useful it is found that high coupling efficiencies are needed. The report finds that at densities of about 2×10^{12} cm^{-3} approximately 20 percent of the launched rf power is converted to plasma current.

"Translation Experiment of a Plasma with Field Reversed Configuration"
by Masayasu Tanjyo et al.
Plasma Physics Laboratory, Osaka University
***Technology Reports of the Osaka University*, Vol. 34, No. 1763, pp. 201-210 (Oct. 1984)**

One type of compact torus, magnetic plasmas in which the confining fields are primarily generated by plasma electric currents, is that of the theta-pinch produced field-reversed configuration. This paper reviews experiments on the Osaka Compact Torus in which field-reversed plasmas are formed and then moved into two kinds of metal containers, magnetic flux conservers; one with a larger radius and one with a smaller radius than the bore of the theta pinch formation coil. It was successfully demonstrated that field-reversed plasmas could be translated into both kinds of containers. The important experimental parameter $x(s)$ [$x(s)$ = the ratio of the radius of the separatrix defining the reversed field configuration to the radius to the conducting wall of the containment chamber] was increased to a value of .6 for the larger vessel and to .7 for the smaller one, while the initial value in the formation chamber was .4. And though this increase in $x(s)$ led to a decrease of plasma beta, it also led to an increase in the plasma particle confinement time, which was the primary objective of the translation experiments. With the increase of $x(s)$ and confinement time, the decay time of the trapped magnetic flux was extended from the range 15-20 microseconds to 50-80 microseconds. The confinement time was found to depend on $x(s)$ more than on the separatrix radius alone. During the translation phase half of the total particle and plasma energy was lost. Therefore, the translated plasma had about half the volume of the original one. As expected, the translation process was nearly isothermal. In conclusion it was found that translation of field-reversed configurations does lead to increases in confinement time due to increases in $x(s)$. From the experiments carried out particle confinement time appears to be proportional to the 5.7 power of $x(s)$.

"Self-Generation of Toroidal Magnetic Flux in a Toroidal Z-Pinch"
by Kiwamu Sugisaki
Electrotechnical Laboratory, Ibaraki, Japan
***Jpn. J. Appl. Phys.*, Vol. 24, No. 3, pp. 328-332 (March 1985)**

Reversed field and compact tori experimental configurations have seen an apparent dynamo effect in which either toroidal magnetic flux has been generated from poloidal magnetic flux or vice versa. In the experiments reported here, a pure toroidal z-pinch is found to self-generate toroidal magnetic flux. The measured toroidal flux is found not to be a product of the plasma current. The greatest toroidal flux self-generation takes place at lower filling pressures. Toroidal flux generation is found to be sufficient for formation of force-free field configurations, though a stationary state has not been reached given the currently short dis-

charge times of less than 120 microseconds. But the magnetic field profiles as measured give a gross force-free field configuration. The actual origin of the generation of the toroidal flux in this experiment is not yet clear, although experimental data suggests that the MHD kink instability provides a source of toroidal flux generation. Generation of the toroidal flux may have some physical mechanisms in common with field-reversal, plasma paramagnetism, and the dynamo effect. However, toroidal flux generation has crucial differences with these in that the initial toroidal field was zero and much more toroidal flux was generated.

"The Dynamo Effect in Fusion Plasmas"
by H.R. Strauss
Courant Institute of Mathematical Sciences, New York University
***Phys. Fluids*, Vol. 28, No. 9, pp. 2786-2792 (Sept. 1985)**

The dynamo effect has now been observed in the Sun, the Earth and reversed field pinch experiments in the laboratory. A dynamo is defined as the generation of electric currents by the motion of an electrical conductor through a magnetic field. The dynamo effect has been invoked in reversed field pinch experiments due to two distinct phenomena: It is observed that given only an applied toroidal electric field, (1) both toroidal and poloidal currents are maintained against resistive decay; (2) the plasma itself generates a sustained reversed toroidal magnetic field.

In this theory paper, a set of MHD equations for mean and fluctuating fields is derived and applied to the dynamo effect for reversed field pinch and tokamak plasmas. It is asserted that there are two dynamo effects: one due to the mean field equilibrium and the other due to fluctuations. Therefore, it is found that the dynamo effect should not drive a net plasma current in steady state. The presence of dynamo effects is ascribed to both growing and stationary tearing modes.

"Generation of Poloidally Rotating Spheromaks by the Conical Theta Pinch"
by K. Kawai et al.
Aerospace and Energetics Research Program and Department of Nuclear Engineering, University of Washington
***University of Washington Report*, PACS numbers: 52,55Ez (1985)**

This report reviews experiments that were designed to simulate those carried out under the Trisops approach previously pursued at the University of Miami (Coral Gables) in which two rotating plasmoids are generated by theta pinch guns and colloided together. The measured fields of the plasma rings were found to have both poloidal and toroidal components like those found in stationary spheromak experiments. The existence of poloidal rotation in these rings was revealed by spatially resolved Doppler broadening measurements. The vortex velocity on axis was estimated to be 10 cm/microsecond in a 5-eV helium plasma. Translational velocities of 5 cm/microsecond were found. A high fusion neutron yield was measured. In this report an attempt is made to explain this yield as the result of the high velocity collision of the two plasma vortices. In general it is found that: "It is truly astonishing that such a simple device produces plasma with very complicated but beautifully organized structure."

"Hall Effect in Plasma Current Sheet Configuration" by Yasuyuki Yagi and Nobuki Kawashima Respectively: Electrotechnical Laboratory, Ibaraki and Institute of Space and Astronautical Science, Tokyo, Japan
***Jpn. J. Appl. Phys.*, Vol. 24, No. 4, pp. L259-L262 (April 1985)**

Both in space plasmas (such as those seen in solar flares and magnetic storms of the Earth's ionosphere) and in laboratory plasmas (such as the disruptive instability of the tokamak), magnetic field line reconnection and the related general properties of plasma current sheets are found to play crucial roles. Experiments are reported here in which a plasma current sheet is generated and magnetic field line reconnection is studied. It is found that fairly intense Hall electric fields and currents exist. The Hall electric field is found to increase as the thickness of the plasma current sheet is decreased. Electrical eddies throughout the plasma current sheet are found. It is also found that the Hall effect affects the equilibrium of the current sheet in a sheared magnetic field configuration and makes the field configuration more complicated.

"Possibility of Ion Beam Pulse Compression by X-Ray Conversion" by Takashi Yabe Osaka University, Osaka, Japan
***Jpn. J. Appl. Phys.*, Vol 24, No. 2, pp. L104-L106 (Feb. 1985)**

In a previous paper the author developed a means for effectively compressing and focusing the energy of ion beam pulses. The scheme consisted of converting the incident ion beam energy into soft X-rays. Within the converter an incident 10^{13} W/cm^2 at 100-nanoseconds pulse length is converted into focusable soft X-rays at 10^{14} W/cm^2 with a 10-nanosecond pulse length. The conversion is accomplished owing to the fact that the ion beam will penetrate high-Z metal layers and deposit its energy into a low-Z foam layer according to the Bragg peak contained within the target. Since the velocity of propagation of the radiation front within the foam is dependent on temperature, the ion beam energy deposited there will be effectively trapped as thermal radiation until the temperature is significantly raised. The amplified thermal radiation is abruptly emitted. In this way the ion beam energy is both compressed and transformed into X-rays.

Criticisms of this concept by Unterseer and Meyer-ter-Vehn (*Jpn. J. Appl. Phys.* **23** (1984) L728) were: (1) The brightness temperature was much smaller than the average interior temperature that the author used to estimate the radiation flux, and therefore the power amplification did not occur even if pulse compression did; (2) the author neglected to take hydrodynamic motion into account. This current paper shows that these criticisms are without basis in the case of realistic targets. In particular, real inertial fusion targets are closed systems unlike those found in astrophysical problems—in which case the system is open and X-rays escape. In realistic spherical geometries, spherical convergence offers possibilities of even greater amplification. In terms of hydrodynamic motion it is found that it is too early to determine if it will degrade the conversion process. The proposal for use of a "supersonic" radiation wave, instead of a "subsonic" wave by Unterseer and Meyer-ter-Vehn should be further examined in detail.

"Stabilization of High Frequency Instability of an Ion Beam in a Plasma by a Low-power Electron Beam"
by Yu. P. Bliokh et al.
Ukranian Academy of Sciences
***Zh. Eksp. Teor. Fiz.*, Vol. 88, pp. 2001-2004 (Aug. 1985)**

This paper reports experimental and theoretical studies of utilizing low-power "hot" electron beams to stabilize monoenergetic ion beams within plasmas. The electron beam has a directed velocity close to that of the ion beam. Given a sufficient high-temperature background plasma and electron beam it should be possible to stabilize ion instabilities without exciting electron beam instabilities. Further, it is shown that at lower electron beam temperatures the kinetic instability of the electron beam that does arise is not sufficient to effect transport of the ion beam within the plasma. Therefore, it is concluded that "hot" electron beams may provide the means to effectively suppress high frequency ion beam instabilities.

"Experimental Evidence of Charge Separation (Double Layer) in Laser-Produced Plasmas"
by A. Ludmirsky et al.
Soreq Nuclear Research Center, Israel
***IEEE Trans. Plasma Sci.*, Vol. PS-13, No. 3, pp. 132-134 (June 1985)**

Double layers consist of two, adjacent, thin plasma regions that possess excesses of opposite electrical charges. These have been observed in a variety of laboratory plasmas and in general are separated by a few Debye lengths and induce large potential drops that can accelerate particles to high engeries, or, vice versa, decelerate incident high energy particles. While such double layers are suspected to exist in laser plasmas, no laboratory measurements of double layers have been made, due to the short lifetime of these plasmas. This paper presents the first experimental data that give evidence for the existence of double layers in laser plasmas. The existence of double layers in laser plasmas should have major effects on acceleration and stopping of high energy ions and electrons within the deposition region. It should also affect density profiles within such regions.

"Light Ion Beam Transport in Plasma Channels"
by T. Ozaki et al.
***Jpn. J. Appl. Phys.*, Vol. 58, No. 6 (Sept. 15, 1985)**

Fusion reactors based on light ion beam diode technology need some means to obtain sufficient standoff between the inertial confinement fusion target and the ion beam generating diodes. Plasma channels have been proposed for beam transport and standoff. This paper reviews experiments on such plasma channeling. Both single and multiple channels are formed by carbon-dioxide laser initiation of plasma within 10-40 torr of ethylene gas with lengths up to 1 meter. Ion beams are generated by a pinch-reflex ion diode on the Reiden IV generator and injected into these channels. Up to 70 percent of the injected beam energy was successfully transported.

"The Galactic Ridge Observed by Exosat"
by R.S. Warwick et al.
University of Leicester, UK
***Nature*, Vol. 317, pp. 218-223 (Sept. 19, 1985)**

This paper reports the observation of a map of X-rays by the Exosat satellite medium-energy proportional X-ray counter array. In addition to numerous point sources, the map reveals a narrow continuous ridge of emission that extends along the whole galactic plane out to 40 degrees longitude on either side of the its center. The existence of this ridge does not fit with any extant astrophysical models, and a major contribution to it from luminous discrete X-ray sources can be excluded.

"X-ray Emission from a Plasma Mirror of a Neodymium Glass Laser"
by M. Kalal et al.
Czech Technical University, Czechoslovakia
Sov. J. Quantum Electron., **Vol. 14, No. 11, pp. 1564-1566, (Nov. 1984)**

It is known that target plasmas can play the role of a laser mirror in mode locking and/or Q switching of lasers. This paper reports experimental investigations of the optical and X-ray characteristics of radiation emitted by a plasma mirror placed within a neodymium glass laser. The optical reflection coefficient of the mirror was found to be nonlinear and the plasma temperature was about 300 eV. It was assumed that stimulated Brillouin scattering was responsible for plasma mirror reflectivity. It was found that the plasma reflectivity was dependent on the incident power density in a manner similar to that of the transmission of a saturable absorber, which is commonly used in passive mode locking of pulsed lasers.

"Absorption Physics at 351 nm in Spherical Geometry"
by M.C. Richardson et al.
University of Rochester
Phys. Rev. Letts., **Vol. 54, No. 15, pp. 1656-1659 (April 15, 1985)**

Although single-beam experiments on planar slab targets at 1054, 526, 351, and 266 nanometer wavelengths have demonstrated higher absorption and lower levels of fast-electron preheat for shorter wavelengths, it is vital to determine how this works for spherical targets, such as those that will be utilized in direct-drive inertial confinement fusion. This paper reports experiments with six beams of the Rochester OMEGA glass laser system irradiating spherical targets at intensities ranging from 10^{13} to 10^{15} W/cm^2. Efficient collisional absorption is found with very low levels of superthermal electron production—less than 10^{-4} of the incident energy going into superthermal "hot" electrons. These results offer considerable encouragement for direct-drive inertial fusion targets.

"Measurement of the Formation and Evolution of a Strange Attractor in a Laser"
by G.P. Puccioni et al.
Istituto Nazionale di Ottica, Italy
Phys. Rev. Lett., **Vol. 55, No. 4, pp. 339-342 (July 22, 1985)**

This paper reports the first experimental measurements of the fractal dimensions and Kolmogorov entropies of periodic and chaotic attractors. A carbon-dioxide laser system with modulated losses was utilized. An increase in the dimension near the accumulation point of the periodic cascade according to the Feigenbaum scaling law was found, together with the expected increase of the attractor dimension in the chaotic region.

"Neutrons, X-Rays, and Charged Particle Beam Emission in a 65 kV Plasma Focus"
by Toshikazu Yamamoto et al.
Gunma University, Japan
Jpn. J. Appl. Phys., **Vol. 24, No. 3, pp. 324-327 (March 1985)**

It has been suggested that increasing the voltage and ringing frequency of the capacitor bank powering a plasma focus will lead to increased neutron yields and particle beam outputs. The experiments on the 65 kV plasma focus were designed to test this through measurements of plasma dynamic behavior, neutron burst output, X-rays, and charged particle beams generated. Increased neutron and particle beam outputs were observed. The neutron yield was found to depend on the generation of anomalous resistivity in the plasma.

"Three-Dimensional Self-Organization of a Magnetohydrodynamic Plasma"
by Ritoku Horiuchi and Tetsuya Sato
Institute for Fusion Theory, Hiroshima University,
***Japan Phys. Rev. Lett.*, Vol. 55, No. 2, pp. 211-213 (July 8, 1985)**

This paper reports theoretical investigations into self-organization of magnetohydrodynamic plasmas. Previous studies have been restricted to two dimensions. The three-dimensional self-organization process investigated here in an incompressible dissipative plasma leads to two distinct phases: (1) an energy-relaxation phase and (2) an inverse-cascade phase. During the relaxation phase, the total magnetic energy rapidly decreases while the magnetic configuration is transformed into a simpler one through magnetic reconnection. The following inverse-cascade phase sees a shift of the magnetic helicity spectrum to longer wavelengths—larger scale organization—while the magnetic energy spectrum shifts toward shorter wavelengths.

In a proposed phenomenological model simulating the process of coalescence of two plasma columns, it is suggested that while large spatial scales are combined by magnetic reconnection, small-spatial-scale modes are excited near the contact region of the two large plasma columns. It is distinctly observed that current peaking occurs locally in the contact region and, therefore, the magnetic field is locally perturbed. Simultaneously, the magnetic helicity was very small in the contact region. The result is that the excited local modes must have relatively small magnetic helicities, in a sense "magnetic bubbles." And because these bubbles do not carry magnetic helicities, their excitation does not lead to the cascade of the helicity toward short wavelengths, while the magnetic energy does so. At the same time, the fusion of the large plasma columns creates longer wavelength helicities and therefore the magnetic helicity cascades inversely as a whole.

"Magnetic Helicity: What Is It and What Is It Good For?"
by John M. Finn and Thomas M. Antonsen, Jr.
University of Maryland
***Comments Plasma Phys. Controlled Fusion*, Vol. 9, No. 3, pp. 111-126 (1985)**

This paper develops a general gauge invariant definition of magnetic helicity in a closed volume and compares it with existing, more restricted ones. It is then applied to four toroidal magnetic trap geometries now being explored by the fusion program: tokamak/reversed field pinch, University of Maryland Spheromak, Los Alamos CTX, and Princeton S-1. Speculations on the ability of helicity injection to generate steady-state current drive are presented. For all the geometries investigated, the helicity injection rate is sufficient for current drive. That is, given the correct phasing of sinusoidal voltages, the time average of injected helicity is positive.

Fundamentally, the reason helicity injection works as a current drive is that the plasma relaxes turbulently on a much faster time scale than that of the oscillating voltages. Therefore, the plasma is continuously in a minimum energy state corresponding to the instantaneous value of the helicity. As a result, the time average of the injected helicity can balance the slow resistive decay of the helicity within the plasma due to plasma resistivity. It is further shown that helicity injection can be accomplished across a resistive plasma or vacuum layer, contrary to previous claims of others.

"Evolution of Self-Focusing Instability in a Semiconfined Plasma"
by L.M. Gorbunov and A.S. Shirokov
P.N. Lebedev Physics Institute, USSR
***Sov. J. Quantum Electron.*, Vol. 15, No. 1, pp. 85-87 (Jan. 1985)**

Self-focusing in the plasma corona of inertial confinement fusion targets leads to the fragmentation of incident laser beams into filaments and to the formation of "hot spots" on the surface of the target. This paper develops a linear approximation to describe the temporal and spatial evolution of electron densities and field pressures due to self-focusing. It is found that filamentation occurs initially far from plasma boundaries and extends to regions increasingly close to such boundaries as a function of time.

"Role of Line and Continuum Opacities in X-Ray Transmission Through a Laser-Heated Au Foil"
by Takashi Yabe et al.
Osaka University, Japan
***Jpn. J. Appl. Phys.*, Vol. 24, No. 6, pp. L439-L441 (June 1985)**

Although considerable theoretical and experimental work has been published on the energy transport and ablation processes in laser-produced low-Z plasmas, very little has appeared with regard to those processes in high-Z plasmas, which have been found to be quite important for the design of indirect drive inertial fusion targets. The complexities involved for the high-Z case prohibits the immediate realization of any simple model. This paper reports theoretical and numerical investigations to clarify the roles of bound-free and bound-bound opacities in the energy transport of laser-irradiated high-Z foils carried out in previous experiments.

Photoionization, that is, the bound-free process, is usually sufficient for describing X-ray transmission through solid materials. This is because the metal is pressure-ionized by changing a highly excited quantum state into a continuum state. Therefore, no vacancies remain in the bound states. Consequently, no bound-bound transitions take place. The situation is altogether different in the case of a thin, highly ionized plasma. Once ionization begins with significant temperature increases, vacancies are created and bound-bound transitions become extremely important in determining X-ray transport. Therefore, if the Rosseland mean-free-path is used for calculating X-ray opacity without taking bound-bound processes into account, there is an overestimation in the mass ablation rate.

The line opacity due to bound-bound states is found to critically determine mass ablation rates, whereas the continuum opacity determines X-ray transmission only in high density regions. X-ray transmission through a .5 micron gold foil, for example, is found to be primarily determined by bound-bound processes. The Bloch-type hydrodynamic model for photoionization is found to be more acceptable than that of the average ion model.

"Dynamic Polarization of Deuterium Nuclei in Completely Deuterated Ethanediol and Propanediol"
by N.C. Borisov et al.
Dubna, USSR
***Zh. Eksp. Teor. Fiz.*, Vol. 97, pp. 2234-2243 (Dec. 1984).**

"Frozen" targets containing polarized hydrogen and deuterium nuclei have found wide experimental use in high-energy and intermediate-energy physics because they can remain unchanged over periods lasting on the order of 100 hours in relatively weak (less than 0.5 tesla) magnetic fields. This paper describes dynamic polarization of approximately .4 for deuterium nuclei in completely deuterated ethanediol and propanediol-1,2 containing a synthesized-in pentavalent chromium complex. The spin-lattice relaxation time is found to be 10 to 15 hours in a .32-tesla magnetic field at a temperature of .054 K. Studies indicate that the dynamic orientation of deuterium nuclei in these materials is chiefly due to dynamic cooling.

"Nuclear Spin Polarization of Solid Deuterium-Tritium" by P.C. Souers et al. UCRL-92700, presented at 32nd National Vacuum Symposium and Topical Conference (Nov. 19-22, 1985)

Parallel alignment of deuteron and triton magnetic moments (spin polarization) increases the cross section for nuclear fusion by 50 percent. This report reviews "brute-force" and dynamic nuclear polarization. Many potential problems with the latter approach are detailed. Significant nuclear polarization utilizing dynamic techniques necessitates small nucleus-to-unpaired electron ratio, a long longitudinal nuclear relaxation time, and a short longitudinal electron relaxation time. Ordinary deuterium-tritium is found to be inadequate. Therefore, pure molecular deuterium-tritium may be essential. Nuclear relaxation time is shown to be the crucial phenomena, which can be determined by either paramagnetic defects deriving from tritium beta radiation or interaction with rotationally excited impurity molecules. It is found that rotational interaction and tritium-radiation-induced decomposition of deuterium-tritium will combat one another to affect deuterium-tritium purity.

"Spin-Polarized Protons and Deuterons in Hydrogen-Isotope Solids" by A. Honig Syracuse University, Presented at Conference on the Intersections between Particle and Nuclear Physics, Steamboat Springs, (May 23-30, 1984)

Given the potential of spin polarization of heavy hydrogen nuclei, new methods for production of highly polarized HD, DD, and DT solids have been developed. For application to high-energy and intermediate-energy physics research, the DD methods are directly applicable to frozen targets and the HD appear to be superior to those previously developed. Relaxation rate switching modes faster than the symmetry species conversion is a crucial feature. Together with epitaxial deposition of molecular isotopic variants on metastably polarized HD or DD blocks, it makes possible operating temperatures of 1 to 4 K. in fractional tesla holding fields. In this case spin diffusion produces high polarization in the deposited layer even in the presence of considerable heat generation from internal radiation or symmetry species conversion.

"Explosive Coalescence of Magnetic Islands and Explosive Particle Acceleration" by T. Tajima and J.-I. Sakai Institute for Fusion Studies at the University of Texas at Austin and Toyama University, Japan DOE/ET-53088-197 and IFSR #197 (July 1985)

Rapid magnetic field line reconnection with resultant rapid conversion of magnetic energy to plasma kinetic energy appears to be a crucial process in both laboratory and space plasmas. Laboratory examples include tokamak disruptive instabilities, field reversal in reversed field pinch configurations, and rapid decay of a plasma following tilting instability. Solar flares and magnetic storms in the Earth's ionosphere represent space plasma examples. Although it is believed that reconnection of field lines takes place because of finite resistivity, even at small levels, in the case of driven reconnection, magnetic reconnection can be viewed as a secondary process triggered by a primary instability.

This paper reviews theoretical and numerical studies of explosive reconnection as a result of MHD instabilities seen in the coalescence of magnetic islands. The explosive coalescense is a process of magnetic collapse in which the magnetic and electrostatic field energies and plasma temperatures explode. The theory developed is macroscopic in nature, without considering the detailed development of the singular layer. Similarities to more general physical processes are reviewed; for example, phase transitions, electrostatic plasma collapse, and fluid turbulence.

"RF Current Drive with Magnetic Helicity Injection"
by D.K. Bhadra and C. Chu
GA Technologies Inc.
***J. Plasma Phys.*, Vol. 33, Part 2, pp. 257-264 (1985)**

This paper reviews the theoretical possibilities of radio frequency (rf) current drive through the external injection of magnetic helicity into magnetically confined plasmas with appropriately polarized electromagnetic waves. Steady-state modes of current drive are projected. The steady-state current is obtained by the conservation of helicity such that injected helicity can compensate for volt-seconds consumed by plasma resistivity. This proposed method of rf current drive differs from those currently being researched in that it appears capable of sustaining currents in much higher density plasmas. The efficiency of the process does not appear to depend on plasma density, as opposed to other rf current drive techniques.

"Solitary Excitations in Muscle Proteins"
by S. Yomosa
Sugiyama Jogakuen University, Japan
***Phys. Rev. A*, Vol. 32, No. 3, pp. 1752-1759, (Sept. 1985).**

Muscle fibers are composed of four major proteins—myosin, actin, tropomyosin, and troponin. Their interactions lead to muscle contraction. Calcium ions in the presence of bioenergetic molecules of adenosine triphosphate (ATP) control these interactions. To understand this molecular process of muscle contraction, it is necessary to know the microstructure of muscle fiber and the molecular functions of muscle proteins. In this paper, a theory of nonlinear lattice solitons in muscle proteins is developed. The superstructure of myosin molecules contains two alpha-helical polypeptides, and in each of these there are three one-dimensional chains of peptide groups joined together by hydrogen bonds, which also stabilize the alpha-helical structure. Hydrogen-bond interactions between peptide groups is highly nonlinear because of charge-transfer interactions. Therefore, the hydrogen-bonded chain of peptide groups can be regarded as a one-dimensional nonlinear lattice. Known solutions of nonlinear lattice solitons are then applied to the initial value problems and the microstructure of muscle contraction can thereby be determined.

"Microwave Generation from Filamentation and Vortex Formation within Magnetically Confined Electron Beams"
by A.L. Peratt and C.M. Snell
Los Alamos National Laboratory
***Phys. Rev. Lett.*, Vol. 54, No. 11, pp. 1167-1170, (March 18, 1985).**

Electron beam propagation studies have revealed the formation of discrete vortex-like current bundles when the beam current or propagation distance exceeds certain values. This process closely resembles that of the Kelvin-Helmholz fluid dynamic shear instability, which occurs when a fluid exceeds a critical velocity and vortices appear throughout it with a large increase in flow resistance. In this paper, microwave generation is investigated experimentally and theoretically for thin magnetized electron beams formed into interacting vortices. Vortex formation is found to occur over a range of electron beam currents that vary by as much as a factor of 1 trillion. Computer simulations demonstrate bursts of microwave radiation because of rapid magnetic line reconnection and breaking between vortices when the vortex structure is well defined.

"Loss of Phase Coherence in the Inversion of Ammonia as a Model for the Racemization of Chiral Molecules"
by James D. Macomber
University of Petroleum and Minerals, Dhahran, Saudi Arabia
***J. Chem. Phys.*, Vol. 82, No. 10, pp. 4551-4556 (May 15, 1985)**

Theory has suggested that time-dependence of optical activity of chiral molecules should be similar to that seen in coherent transient effects found in magnetic resonance and laser spectroscopy, but this has never been observed experimentally. This paper gives detailed calculations needed for observation of these oscillations (sometimes called quantum beams) in optical rotation of freshly prepared samples of a given enantiomer. In particular, it is shown that if an ensemble of ammonia molecules in the gas phase could be prepared with the nitrogen atoms displaced (localized) to one side of the plane of the hydrogen atoms, oscillations with time should occur. The oscillation will be damped. The paper suggests that similar damped oscillations constitute the dominant gas-phase racemization process for disymmetric amines and other chiral molecules, whenever intramolecular pathways dominate the process.

"Fast Euler Solver for Steady One-Dimensional Flows"
by Gino Moretti
GMAF, Inc, Freeport, N.Y.

Although solutions to the Euler equations that include discontinuities should be best for compressible, inviscid flows, when such flows are steady, numerical simulations have focused on solvers of the potential equation that apply relaxation methods.

"Detailed Examination of a Plasmoid in the Distant Magnetotail with ISEE 3"
by E.W. Hones, Jr. et al.
Los Alamos National Laboratory
***Geophys. Res. Lett.*, Vol. 11, No. 10, pp. 1046-1049, (Oct. 1984).**

After Earth stations had detected magnetic storms, the International Sun-Earth Explorer-3 (ISEE-3) satellite observed the passage of closed magnetic plasmoid structures traveling tailward. The plasmoids are large plasma configurations threaded by closed loops of magnetic field. They are produced in regions of the plasma sheet that are severed from the Earth by magnetic reconnection in the range of 15 Earth radii. The plasmoid boundary crossing took on the order of 12 seconds at a speed of 500 to 1000 km/sec, which implies a thickness of about 1 Earth radii for the plasmoid boundary. The uniform plasma temperature and low heat flux is consistent with a magnetically confined system. The plasmoid was found to be between 75 to 100 Earth radii long and was detected by ISEE-3 at 220 Earth radii downtail. This took place 27 minutes after a very strong intensification of auroral electrojet was recorded by ground stations.

"Energetic Ion Observations of a Large Scale Vortex in the Distant Geotail"
by T.R. Sanderson et al.
Los Alamos National Laboratory
***Geophys. Res. Lett.*, Vol. 11, No. 10, pp. 1094-1097, (Oct. 1984)**

This paper presents the first observations of a vortex structure consisting of energetic ions (E >35 keV) and plasma in the deep tail of the magnetosphere at a point 217 Earth radii distance. A vortex period of 15 minutes was observed. Similar events have been observed closer to the Earth. The observations presented here were within the energetic ion boundary layer marking the boundary between the southern lobe of the magnetotail and the plasma sheet, which lies between a region of tailward ion and plasma flow (the plasma sheet) and a region where no tailward flow was observed (the southern lobe).

"Magnetotail Flux Ropes"
by D.G. Sibeck et al.
UCLA
***Geophys. Res. Lett.*, Vol. 11, No. 10, pp. 1090-1093 (Oct. 1984)**

This paper presents International Sun-Earth Explorer-3 (ISEE-3) satellite magnetometer data of apparent instances of flux ropes within the distant magnetotail of the Earth. Correlated wave, high energy particle and electron plasma data are presented. Three cases are reported. The flux ropes are detected with a strong magnetic field in their core, a bipolar magnetic field structure, and a double peaked field that indicates an off-center crossing. The observed flux ropes are aligned parallel to the magnetotail axis. Ground magnetograms near local midnight were highly disturbed during the time that the flux ropes were detected.

These abstracts were written by Charles B. Stevens.